The Role of PGC-1α and PGC-1β in Myotube Protein Synthesis

by

Erin Brown

BAppSci (Exercise and Sport Science) (Hons)

Submitted in fulfilment of the requirements for the degree of

Doctor of Philosophy

Deakin University

July, 2013

DEAKIN UNIVERSITY AUSTRALIA
Worldly

DEAKIN UNIVERSITY
ACCESS TO THESIS - A

I am the author of the thesis entitled:

The Role of PGC-1α and PGC-1β in Myotube Protein Synthesis

submitted for the degree of Doctor of Philosophy

This thesis may be made available for consultation, loan and limited copying in accordance with the Copyright Act 1968.

'I certify that I am the student named below and that the information provided in the form is correct'

Full Name: Erin Louise Brown
(Please Print)

Signed: Signature Redacted by Library

Date: 21/10/2013

DEAKIN UNIVERSITY
CANDIDATE DECLARATION

I certify that the thesis entitled

The role of PGC-1α and PGC-1β in myotube protein synthesis

submitted for the degree of

is the result of my own work and that where reference is made to the work of others, due acknowledgment is given.

I also certify that any material in the thesis which has been accepted for a degree or diploma by any university or institution is identified in the text.

'I certify that I am the student named below and that the information provided in the form is correct'

Full Name: ERIN LOUISE BROWN

(Please Print)

Signed: Signature Redacted by Library

Date: 12/7/13

Acknowledgements

Firstly, I would like to thank my supervisor, Associate Professor Aaron Russell, for his encouragement, guidance and support over my PhD candidature. Without your help and friendship this thesis would never have been possible.

To my co-supervisor, Dr. Torie Foletta, thank you for all your help with the bioinformatics analyses. Your knowledge in this area has been invaluable.

To Professor Rod Snow, thank you for your input with the creatine work.

Thank you to all the members of our research group and within the School of Exercise and Nutrition Sciences who have assisted in various aspects of my research. A special thank you to Craig, who has assisted me with much of the lab work and preparation for this thesis.

Lastly, thank you to my friends and family for all your encouragement and support over the years. And thank you to my parents for letting me live at home during this time.

Erin

Contents

Chapter 3

Identification of Genes and Proteins Regulated by PGC-1α and PGC-1β in C2C12 Myotubes

Chapter 4

PGC-1α and PGC-1β regulate creatine uptake via ERRα/CrT

List of Figures

List of Tables

Abbreviations

10T1/2	Mouse embryonic cell line
36B4	Large ribosomal protein (a.k.a RPLPO)
4E-BP1	4E-binding protein 1
AICAR	5-aminoimidazole-4-carboxamide-1-β-D-ribonucleoside
AIDS	Acquired immuno deficiency syndrome
Akt	Acute Transforming Retrovirus Thymoma
ALS	Amyotrophic lateral sclerosis
AMP	5' Adenosine monophosphate
AMPK	AMP-activated protein kinase
ANOVA	Analysis of variance
ASPRV1	Aspartic peptidase, retroviral-like 1.
ATCC	American type culture collection
ATP	Adenosine triphosphate
β-ATPase	Beta subunit of ATP synthase
β-GPA	β-Guanidinoproprionic acid
BCA	Bicinchoninic acid
Bis-Tris	2-[Bis(2-hydroxyethyl)amino]-2-(hydroxymethyl)propane-1,3-diol
BLAST	Basic Local Alignment Search Tool
Bnip3	BCL2/adenovirus E1B 19 kDa protein-interacting protein 3
BP	Biological processes
BSA	Bovine serum albumin
C2C12	Immortalised mouse myoblast cell line
CACT	Carnitine-acylcarnitine translocase
CaMKIV	Calmodulin-dependent protein kinase IV
CC	Cellular component
CDC14B	Cell division cycle 14 Homolog B
cDNA	Complementary DNA
ChIP	Chromatin Immunoprecipitation
COPD	Chronic obstructive pulmonary disease
COX	Cytochrome c oxidase
COX II	Cytochrome c oxidase subunit II
COX IV	Cytochrome c oxidase subunit IV
COX V	Cytochrome c oxidase subunit V
CPE	Cytopathic effect

CPM	Counts per minute
CPT1	Carnitine palmitoyltransferase I
CRE8	HEK293 cells expressing CRE recombinase
CREB	cAMP response element binding protein
CrT	Creatine transporter
CytC	Cytochrome c
DAVID	Database for Annotation, Visualisation and Integrated Discovery
DEX	Dexamethasone
DLDA	Diagonal Linear Discriminant Analysis
DMD	Duchenne muscular dystrophy
DMEM	Dulbecco's modified eagle medium
DNAse I	Deoxyribonuclease I
EDL	Extensor digitorum longus
eEF1A2	Eukaryotic translation elongation factor 1 alpha 2
eIF2B4	Eukaryotic translation initiation factor 2B, subunit 4
eIF-4E	Eukaryotic-initiation factor 4E
eIF4E3	Eukaryotic translation initiation factor 4E family member 3
ERR	Estrogen related receptor
ERRE	Estrogen-related receptor response element
ERRα	Estrogen-related receptor alpha
ERRβ	Estrogen-related receptor beta
ERRγ	Estrogen-related receptor gamma
ERα	Estrogen receptor-alpha
EXOC1	Exocyst complex component 1
FBS	Foetal bovine serum
FOXO	Forkhead Box O
FOXO1	Forkhead Box protein 1
FOXO3a	Forkhead Box protein 3a
Gabarapl1	GABA receptor-associated protein like-1
GABPα	GA binding protein (a.k.a NRF-2)
GAPDH	Glyceraldehyde 3-phosphate dehydrogenase
GCN5	General control of amino-acid synthesis
GES	Gene expression signature
GFP	Green fluorescent protein
GLUT4	Glucose transporter type 4
GO	Gene Ontology
GR	Glucocorticoid receptor

GSEA	Gene Set Enrichment Analysis
GSK-3β	Glycogen synthase kinase 3-beta
HDAC	Histone deacetylase
HEK293	Human embryonic kindey-293 cells
HNF-4α	Hepatocyte nuclear factor 4 alpha
hPGC-1α	Human PGC-1α
hPGC-1β	Human PGC-1β
HS	Horse serum
IFU	Infectious units
IGF-1	Insulin-like growth factor-1
iTRAQ	Isobaric Tags for Relative and Absolute Quantification
kDa	Kilo-Dalton
KEGG	Kyoto Encyclopaedia of Genes and Genomes
KO	Knock out
L6	Immortalised rat myoblast cell line
LC3	Microtubule-associated protein 1 light chain 3
Lf	Optimal fibre length
L_o	Muscle length
LXRα	Liver X receptor alpha
MAPK	Mitogen-activated protein kinase
MCAD	Medium-chain acyl-coenzyme A dehydrogenase
MCK	Muscle creatine kinase
MEF2	Myocyte enhancer factor 2
MEF2C	Myocyte enhancer factor 2C
MEF2D	Myocyte enhancer factor 2D
MF	Molecular function
MFN1	Mitofusin 1
MFN2	Mitofusin 2
MHC	Myosin heavy chain
MHCIIx	Myosin heavy chain IIx
MOI	Multiplicity of infection
mRNA	Messenger ribonucleic acid
MRPS9	Mitochondrial ribosomal protein subunit 9
mTOR	Mammalian Target of Rapamycin
mtTFA	Mitochondrial transcription factor A
MuRF1	Muscle RING-finger Protein 1
MyoD	Myogenic differentiation 1

NFAT	Nuclear factor of activated T-cell
NFW	Nuclease free water
NRF	Nuclear respiratory factor
NRF-1	Nuclear respiratory factor-1
NRF-2	Nuclear respiratory factor-2 (a.k.a GABP)
NSCLC	Non-small-cell lung carcinoma
Opti-MEM	Optimum Modified Eagle Medium
OXPHOS	Oxidative phosphorylation
p70S6K	p70 ribosomal S6 protein kinase
PBS	Phosphate buffered saline
PCR	Polymerase chain reaction
PDK4	Pyruvate dehydrogenase kinase 4
PGC-1	Peroxisome proliferator-activated receptor-gamma coactivator 1
PGC-1α	Peroxisome proliferator-activated receptor-gamma coactivator 1-alpha
PGC-1β	Peroxisome proliferator-activated receptor-gamma coactivator 1-beta
PI3K	Phosphatidylinositol 3-kinase
P_o	Maximal tetanic force production
PPARα	Peroxisome proliferator-activated receptor alpha
PPARs	Peroxisome proliferator-activated receptors
PPARγ	Peroxisome proliferator-activated receptor gamma
PPARδ	Peroxisome proliferator-activated receptor delta
Ppp1R16a	Protein phosphatase 1, regulatory subunit 16A
PRC	PGC-1 related coactivator
Prnp	Prion Protein
PS	Penicillin streptomycin
P_t	Maximal twitch force
PVDF	Polyvinylidene difluoride
qPCR	Quantitative PCR
rAAv	Recombinant adeno-associated virus
REX	Resistance Exercise
RIPA	Radioimmunoprecipitation
RM	Repetition maximum
RNA	Ribonucleic acid
RNAi	Interference RNA
ROS	Reactive oxygen species
RT	Reverse transcription

RXR	Retinoid X receptor
SAOS2	Sarcoma osteogenic cell line
SDS	Sodium dodecyl sulphate
SDS-PAGE	Sodium dodecyl sulphate polyacrylamide gel electrophoresis
SEM	Standard error of the mean
shERRα	Short Hairpin ERRα
shGFP	Short Hairpin GFP
shRNA	Short Hairpin RNA
siERRα	Small interfering ERRα
siRNA	Small interfering RNA
SIRT1	Sirtuin-1
siSUPER	Small interfering RNA control
SNPs	Single nucleotide polymorphisms
SNR	Signal to noise ratio
SOD1	Superoxide dismutase 1
SPSS	Statistical Package for the Social Sciences
SREBP-1	Sterol regulatory element-binding protein-1
TA	Tibialis anterior
TARBP2	TAR *HIV-1* RNA binding protein 2
TCA	Trichloroacetic acid
TCEAL7	Transcription elongation factor A SII-like 7
TRIM25	Tripartite motif-containing protein 25
TRIM32	Tripartite motif-containing protein 32
TSC1/2	Tuberous sclerosis complex 1 and 2 proteins
TSC22D3	TSC22 domain family protein 3
TX-100	Triton X-100
UCP2	Uncoupling protein 2
UCP3	Uncoupling protein 3
UPP	Ubiquitin proteasome pathway
VEGF/VEGF-A	Vascular endothelial growth factor-A
VP16ERRα	Constitutively active ERRα
WT	Wild type
YY1	Ying Yang-1

Abstract

Skeletal muscle atrophy is a devastating condition, contributing to increased morbidity and mortality during many chronic disease states. Skeletal muscle atrophy is a result of decreased rates of protein synthesis and/or increased rates of protein degradation. Understanding the molecular mechanisms that regulate these processes is therefore a prerequisite to develop therapeutic strategies to target muscle atrophy and improve clinical outcomes. The transcriptional coactivators peroxisome proliferator-activated receptor-gamma coactivator-1alpha (PGC-1α) and PGC-1β are both positive regulators of many functions important for maintaining skeletal muscle health. Notably, many of their actions in skeletal muscle depend on the transcriptional coactivator, estrogen-related receptor alpha (ERRα). Recent evidence suggests that PGC-1α and PGC-1β may be attractive targets to attenuate muscle wasting, as their overexpression attenuates muscle atrophy via decreased activity of signalling pathways involved in protein degradation. As protein synthesis rates are also significantly reduced during many catabolic states, identifying ways to increase protein synthesis is also vital. The role of PGC-1α and PGC-1β in skeletal muscle protein synthesis has not been thoroughly investigated, and therefore further research is required. If PGC-1α and/or PGC-1β can increase protein synthesis in addition to attenuating protein degradation, this may provide a basis for the development of treatment strategies to alleviate the debilitating effects of muscle atrophy.

The aims of the first study were to determine if PGC-1α and/or PGC-1β can increase protein synthesis under basal or catabolic conditions, and if this was dependent on Akt/mTOR signalling or the transcription factor, ERRα. This study showed that overexpression of PGC-1α or PGC-1β increased protein synthesis and myotube diameter in C2C12 myotubes. Secondly, the increase in protein synthesis was independent of Akt and mTOR, members of a signalling pathway known to stimulate protein synthesis in skeletal muscle. Lastly, knockdown of the transcription factor ERRα using siRNA prevented the PGC-1α- and PGC-1β-induced increase in protein synthesis and myotube diameter, while constitutively active ERRα increased protein synthesis and myotube diameter. Like many other important PGC-1α- or PGC-1β-

mediated processes in skeletal muscle, ERRα activity is therefore essential for PGC-1α and PGC-1β to increase protein synthesis in C2C12 myotubes.

The downstream targets that PGC-1α/ERRα and PGC-1β/ERRα regulate to increase protein synthesis are unknown. The primary aims of the second study were to identify global gene and protein expression changes that occur in response PGC-1α and PGC-1β overexpression in C2C12 myotubes, and to create an unbiased gene expression signature (GES) characterising the PGC-1α- and PGC-1β- driven protein synthesis. Gene set enrichment analysis (GSEA) identified several Gene Ontology (GO) terms and Kyoto Encyclopedia of Genes and Genomes (KEGG) pathways differentially regulated in response to PGC-1α or PGC-1β overexpression in C2C12 myotubes, including mitochondrial biology, energy metabolism, nucleotide binding, and the ribosome and ribonucleoprotein complex; the latter supporting the roles of PGC-1α and PGC-1β in protein synthesis. Genes and proteins differentially expressed, specifically by PGC-1β, also clustered significantly with muscle contractile and cytoskeletal related GO terms.

The unbiased GES led to the identification of 7 novel genes regulated by PGC-1α and PGC-β, while 9 other highly regulated genes, which may potentially be involved in muscle growth, were biasedly selected and also explored. Similar to PGC-1α expression, many of the up-regulated genes were increase in human skeletal muscle following resistance exercise, a model of stimulated muscle protein synthesis, suggesting that they may be involved in the positive regulation of protein synthesis. In contrast, many of these genes were decreased in skeletal muscle of amyotrophic lateral sclerosis (ALS) patients, a clinical model of skeletal muscle atrophy, paralleled with reduced PGC-1α and PGC-1β mRNA. Furthermore, genes that were down-regulated by PGC-1α and PGC-1β displayed inverse expression in these models, suggesting that their decreased expression by PGC-1α and PGC-1β may contribute to the attenuation of muscle atrophy. Together these observations provide novel avenues to investigate the effects of PGC-1α and PGC-1β on skeletal muscle protein turnover.

Another mechanism by which PGC-1α and PGC-1β may regulate skeletal muscle mass is via creatine transport into muscle cells. Creatine supplementation increases

strength, fat-free mass, and muscle fibre size when used in combination with resistance training or for the treatment of myopathies presenting with muscle atrophy. However, Creatine transporter (CrT) levels are decreased in many myopathies associated with muscle wasting, suggesting that increasing CrT levels may be an effective strategy to maximise the potential benefits of creatine supplementation. However the molecular mechanisms regulating CrT expression are unknown. As PGC-1α and PGC-1β regulate other important aspects of energy metabolism, it is plausible that they may also regulate creatine uptake via increasing the expression of the CrT. This may also partially explain how PGC-1α and PGC-1β positively influence skeletal muscle mass. The aims of the third study were to determine if PGC-1α and PGC-1β increase CrT mRNA and creatine uptake in L6 myotubes and whether this is via ERRα, and to determine whether PGC-1α and PGC-1β increase protein synthesis via up-regulating CrT expression and creatine uptake. PGC-1α and PGC-1β overexpression increased CrT mRNA and creatine uptake in L6 myotubes. This effect was dependent on ERRα, and PGC-1α and ERRα directly bind to the CrT promoter to induce its expression. Lastly, the PGC-1α- and PGC-1β-induced increase in protein synthesis and myotube diameter was not dependent on the CrT, and therefore other mechanisms may be responsible for the increase in muscle mass seen in response to increasing intracellular creatine. These observations increase the understanding of the molecular mechanisms regulating creatine transport in skeletal muscle, and may provide a basis for a treatment strategy aimed at improving various skeletal muscle diseases characterised by reduced intracellular creatine levels.

The findings of this thesis expand the current knowledge of the PGC-1α- and PGC-1β-regulated functions in skeletal muscle. In addition to their already known attenuation of protein degradation, these observations show that PGC-1α and PGC-1β can also increase protein synthesis and creatine uptake in myotubes. The downstream molecular pathways regulated by PGC-1α and PGC-1β present as attractive targets for the development of treatment strategies to alleviate the debilitating effects of muscle atrophy.

Chapter 1

Literature Review

1.1 Skeletal muscle

Skeletal muscle is the most abundant tissue in the human body, representing about 40% of total body mass and 50-75% of total body protein [1]. It is an essential tissue in the body which controls movement, the maintenance of posture, and occupies a fundamental role in whole body metabolism [2]. Skeletal muscle is a highly adaptable tissue, and can alter its size, structure and function in response to many different stimuli [3, 4]. The most powerful stimulus for skeletal muscle adaptation is physical activity. Endurance exercise increases the oxidative capacity and improves the metabolic profile of skeletal muscle [5-7], while resistance exercise increases the size, strength and function of skeletal muscle [8-10]. In contrast, inactivity, aging, malnutrition, and many chronic diseases result in impairments in skeletal muscle function, metabolism and growth [11-14].

Skeletal muscle atrophy is a devastating condition characterised by a decrease in the size of the muscle fibres and overall muscle mass, resulting in a loss of strength and mobility. Muscle atrophy is a hallmark of many conditions including neuromuscular disorders such as Duchenne muscular dystrophy (DMD) and amyotrophic lateral sclerosis (ALS) [15, 16], as well as sepsis, critical illness myopathy, sarcopenia and immobilisation following acute injuries [17-21]. Muscle atrophy is also common during chronic diseases such as cancer, heart disease, diabetes, chronic obstructive pulmonary disease (COPD), and acquired immuno deficiency syndrome (AIDS), and is a major limiting factor to successful treatment, contributing to increased rates of morbidity and mortality [11, 13, 18, 22-26]. While exercise training can attenuate muscle atrophy and increase strength and functional capacity in conditions such as sarcopenia [27], exercise is often not possible in many of these disease states. Furthermore, the intracellular signalling responses to exercise are often blunted in diseased skeletal muscle [11, 28-30]. Understanding the molecular and physiological mechanisms involved in the regulation of muscle mass is therefore a prerequisite for

developing therapeutic interventions to improve clinical outcomes and reduce the burden on health care systems.

1.1.1 Regulation of skeletal muscle mass

Skeletal muscle mass is regulated by a fine balance between protein synthesis and protein degradation [31]. When the rate of protein synthesis exceeds that of protein degradation, there is a resultant increase in muscle growth, or hypertrophy, which is characterised by an increase in the size of pre-existing muscle fibres. In contrast, decreased rates of protein synthesis compared to protein degradation, results in muscle atrophy, which causes a decrease in muscle fibre size and muscle mass, resulting in a loss of strength and mobility [31]. Skeletal muscle mass can be affected by a variety of factors that result in alterations to the balance between protein synthesis and protein degradation. Stimuli such as resistance exercise [32-35], amino acids [36, 37], and some hormones (insulin, insulin-like growth factor-1 and testosterone) [38-42] are known to increase net skeletal muscle protein content and stimulate hypertrophy, while inactivity, malnutrition, disease and trauma result in decreased skeletal muscle protein and muscle atrophy.

1.1.2 Molecular regulation of protein synthesis and protein degradation

Several signalling pathways involved in skeletal muscle protein synthesis and degradation have been identified. Some of those involved in muscle growth include the calcineurin/nuclear factor of activated T-cells (NFAT) pathway [43, 44], the mitogen-activated protein kinase (MAPK) pathway [45, 46], and the phosphatidylinositol 3-kinase (PI3K)/Acute transforming retrovirus thymoma (Akt)/ mammalian target of rapamycin (mTOR) pathway [31, 47]. Although the role of the calcineurin/NFAT and MAPK pathways in protein synthesis are debateable [47-49], several studies have clearly shown the role of the PI3K/Akt/mTOR in skeletal muscle protein synthesis [39, 47]. Furthermore, this signalling pathway is also linked with protein degradation, as activation of Akt inhibits the forkhead box O (FOXO) transcription factors that are known to increase protein degradation [50, 51].

1.1.3 Protein synthesis

Akt is phosphorylated and activated via upstream signalling involving IGF-1 and PI3K. When active, Akt increases protein synthesis via mTOR and glycogen synthase kinase- 3β (GSK-3β) (Figure 1.01) [47]. Firstly, Akt activates mTOR by direct phosphorylation on its ser2448 site [52], and by removing the inhibitory effect of the tuberous sclerosis complex 1 and 2 proteins (TSC1/2) on mTOR [53, 54]. mTOR phosphorylates p70 ribosomal S6 protein kinase (p70S6k), which increases the activity of ribosomal protein S6, a positive regulator of protein synthesis [55]. mTOR also phosphorylates and inactivates the translation repressor, 4E-BP1, a negative regulator of the eukaryotic initiation factor 4E (eIF-4E) [56]. Secondly, Akt phosphorylates and inactivates GSK-3β, removing its inhibition of translation initiation factor eIF2B, leading to an increase in translation initiation and therefore protein synthesis [57-59].

Compensatory hypertrophy of the plantaris muscle in rats is associated with increased phosphorylation of Akt, GSK-3β and p70S6k, and decreased inhibition of eIF-4E by 4E-BP1 [47]. In contrast, the opposite effects are seen during muscle atrophy induced via hindlimb suspension in rats. Likewise, 8 weeks of resistance training in humans results in muscle hypertrophy and is associated with increases in phosphorylated Akt, GSK-3β, and mTOR, while 8 weeks of detraining results in muscle atrophy and decreased phosphorylation of these proteins [60]. Constitutive activation of Akt in skeletal muscle of mice leads to dramatic hypertrophy, confirming a role for Akt in the positive regulation of muscle mass [47]. This is dependent on mTOR activity, as rapamycin, an mTOR inhibitor, completely blocks this effect. The Akt/mTOR pathway is therefore seen as a major positive regulator of protein synthesis in skeletal muscle.

1.1.4 Protein Degradation

During skeletal muscle atrophy, the majority of protein degradation occurs via two mechanisms, the ubiquitin proteasome pathway (UPP) and the autophagic-lysosomal pathway [61, 62]. In the UPP, proteins targeted for degradation are first tagged with chains of ubiquitin via the activities of three enzymatic components, E1 (ubiquitin activating enzyme), E2 (ubiquitin carrier protein) and E3 (ubiquitin protein ligase)

[63]. This process leads to their recognition by the proteasome, degrading these proteins into small peptides. In skeletal muscle, two muscle-specific E3 ubiquitin ligases, Atrogin-1 and Muscle Ring Finger-1 (MuRF1), have been identified, and their expression is highly induced during skeletal muscle atrophy [64, 65]. Mice deficient in either Atrogin-1 or MuRF1 are resistant to atrophy [66]. The UPP is thought to be responsible for the degradation of most cytosolic and myofibrillar proteins in skeletal muscle [63].

The autophagic-lysosomal pathway also plays a role in the degradative processes during skeletal muscle atrophy [61, 62, 67, 68]. Autophagy involves portions of the cytoplasm and cell organelles being sequestered into autophagosomes, which then fuse with lysosomes and are digested by lysosomal hydrolases [67, 68]. Expression of genes involved in autophagy including microtubule-associated protein 1 light chain 3 (LC3), BCL2/adenovirus E1B 19 kDa protein-interacting protein 3 (Bnip3), GABA receptor-associated protein like-1 (Gabarapl1), and the lysosomal hydrolase cathepsin-L, are also induced during skeletal muscle atrophy, suggesting that a combination of both proteasomal and lysosomal proteolysis contribute to the increased rate of protein degradation.

A characteristic of both of these proteolytic mechanisms is their regulation by the FOXO family of transcription factors (FOXO1 and FOXO3a) (Figure 1.01). When dephosphorylated and active, FOXO transcription factors are located in the nucleus where they regulate the expression of genes involved in the UPP (Atrogin-1 and MuRF1) and autophagy (LC3, Bnip3, Gabarapl1, and cathepsin-L) [61]. These genes have been termed ‘atrogenes’ due to their involvement in skeletal muscle atrophy [64, 65]. Expression of a constitutively active FOXO3a induces both lysosomal and proteasomal proteolysis in muscle cells and in skeletal muscle *in vivo* [61, 62]. In contrast, phosphorylation of FOXOs by Akt reduces FOXO activity, and therefore attenuates protein degradation [51, 69, 70]. Treatment with IGF-1, or activation of Akt, inactivates FOXO transcription factors and consequently antagonises the up-regulation of ubiquitin ligases, Atrogin-1 and MuRF1 [40, 50, 51, 69]. Similarly, Akt may regulate autophagy via FOXOs, as inhibition of Akt results in increased FOXO3a activity and is associated with an increase in lysosomal proteolysis [62].

These findings show that in addition to being a major stimulator of protein synthesis, Akt also regulates muscle mass via the inhibition of protein degradation pathways.

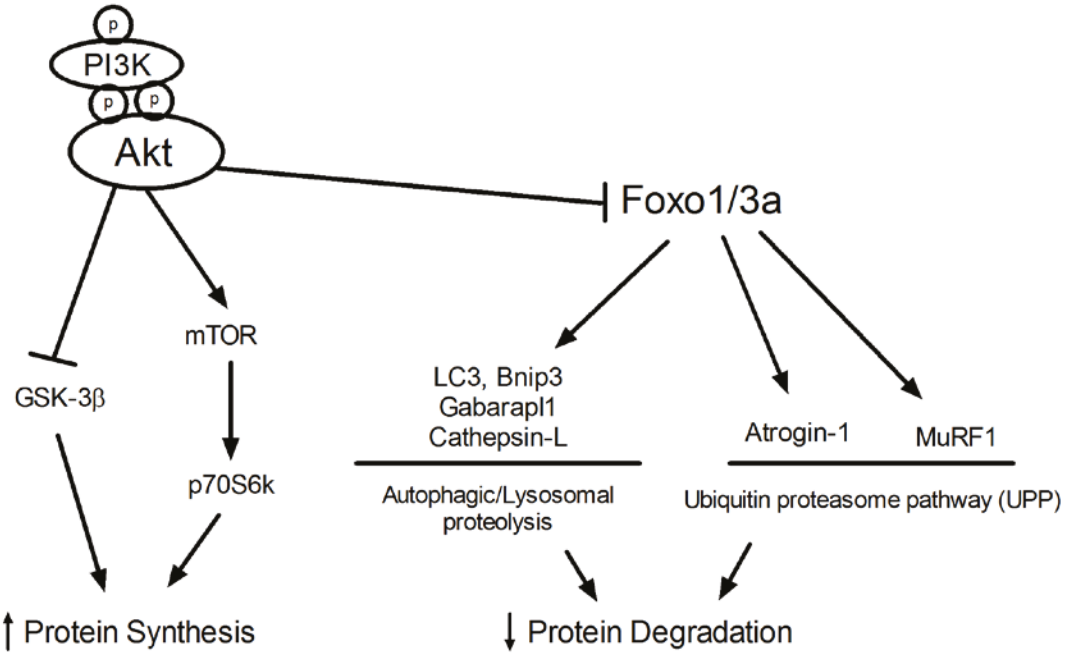

Figure 1.01 Schematic of Akt signalling pathways involved in protein synthesis and degradation. When activated by PI3K, Akt increases protein synthesis by increasing mTOR activity and inhibiting GSK-3β. Akt also phosphorylates and inhibits FOXO1 and 3a, reducing the levels of Atrogin-1 and MuRF1, members of the ubiquitin proteasome pathway. FOXO3a increases lysosomal proteolysis, and inhibition of Akt also causes an increase in FOXO3a phosphorylation and increased expression of lysosomal genes.

1.1.5 Fibre-type specific muscle atrophy

It is worth noting that the atrophy that occurs during many catabolic conditions does not always affect muscle fibres equally. Skeletal muscle is composed of several different fibre types which each have specific metabolic and contractile properties. The three main fibre types in human skeletal muscle are type I (slow-oxidative), type IIa (oxidative-glycolytic) and type IIx (fast glycolytic), while rodents also express another fast-glycolytic fibre, type IIb [71, 72]. The atrophy observed during inactivity and denervation is more profound in type I oxidative muscle fibres [73-76], and causes a shift from oxidative to a higher proportion of glycolytic muscle fibres [73, 74]. In contrast, muscle atrophy seen during ageing [77, 78], COPD [25], heart failure [79, 80], and sepsis [81, 82], is generally more specific to fast-twitch glycolytic muscle fibre types. These findings suggest that intracellular signalling

pathways involved in protein synthesis and protein degradation may be regulated differently among fibre types. However, others have shown that the transcriptional changes induced during muscle atrophy appear to be similar in response to many different stimuli, including denervation/disuse and systemic wasting diseases [64, 65].

1.1.6 Muscle atrophy and mitochondrial dysfunction

Recent evidence suggests that the regulation of skeletal muscle mass may be associated with mitochondrial health. Mitochondrial dysfunction is thought to be involved in the pathogenesis of sarcopenia [83-85], and is observed in most conditions associated with muscle atrophy including chronic disuse [86], diabetes [26], ALS [87], and DMD [88, 89]. The greater sensitivity of type II muscle fibres to systemic muscle wasting may therefore be due to their lower mitochondrial content. However, this does not explain the rapid atrophy seen in type I fibres during disuse and denervation. In fact, disuse atrophy is associated with a decrease in mitochondrial content, alterations in morphology, increased mitochondrial reactive oxygen species (ROS) and mitochondrial dysfunction (reviewed in [90]). Therefore it appears that alterations to the overall mitochondrial network may contribute to muscle atrophy, and mitochondrial impairments have been shown to contribute to both denervation- and fasting-induced atrophy *in vivo* [91]. Key proteins linking mitochondrial function to skeletal muscle mass are the transcriptional coactivators, peroxisome proliferator-activated receptor-gamma coactivator-1alpha (PGC-1α) and PGC-1β. PGC-1α and PGC-1β are well-known regulators of mitochondrial biogenesis and function, and more recently their regulation of skeletal muscle mass has become of interest.

1.2 PGC-1α and PGC-1β transcriptional coactivators

PGC-1α and PGC-1β are part of the PGC-1 family of transcriptional coactivators, which also includes the PGC-1 related coactivator (PRC) [92-94]. Transcriptional coactivators promote gene transcription via their interaction with transcription factors. PGC-1α was first identified in brown adipose tissue as a regulator of adaptive thermogenesis during cold exposure through its interaction with the transcription factor, peroxisome proliferator–activated receptor gamma (PPARγ) [94]. PGC-1β was then identified on the basis of its similarity to PGC-1α [93, 95], although unlike PGC-1α, its expression was not dramatically induced during cold exposure. PGC-1α and PGC-1β are highly expressed in oxidative tissues including skeletal muscle, heart, brown adipose tissue, kidneys and brain [93-99]. Structurally, PGC-1β contains similar domains to PGC-1α along the protein, but with an extended middle region [93, 95, 100]. Both PGC-1α and PGC-1β coactivate a diverse set of transcription factors to coordinate the expression of genes that regulate mitochondrial biogenesis, respiration, oxidative metabolism, and energy homeostasis in many tissues [98, 101]. In addition, they each coactivate their own distinct set of transcription factors in certain tissues, leading to different functional outcomes. For example, in liver, PGC-1α coactivates hepatocyte nuclear factor-4 α (HNF-4α) and FOXO1 to induce gluconeogenesis [102-105], while PGC-1β coactivates the sterol regulatory element-binding protein-1 (SREBP-1) and liver X receptor-α (LXRα) to stimulate hepatic lipogenesis [106, 107]. Moreover, PGC-1α and PGC-1β can modulate different biological programs in a tissue specific manner. For example, in skeletal muscle, both PGC-1α and PGC-1β can improve insulin resistance [100, 108], whereas in liver, they contribute to the induction of insulin resistance [107, 108]. This section will focus only on PGC-1α and PGC-1β in relation to their function and transcriptional activity in skeletal muscle.

1.2.1 Regulation of PGC-1α and PGC-1β in skeletal muscle.

In skeletal muscle, PGC-1α and PGC-1β play similar roles in regulating many processes associated with oxidative energy metabolism; however their regulation differs quite significantly. The expression and/or activity of PGC-1α is induced in response to situations of metabolic stress such as adrenergic stimulation [109, 110],

cold exposure [94, 111], fasting [112], and exercise [113-115]. In fact, the effects of overexpressing PGC-1α in skeletal muscle parallel many of the beneficial adaptations to endurance exercise (reviewed in [7, 116-118]). PGC-1α mRNA and/or protein levels are significantly increased after endurance exercise [113-115, 119] and training [120-122], and high intensity interval exercise [123, 124]. Therefore it is generally viewed that PGC-1α mediates many of the physiological adaptations seen with endurance exercise and training [110, 125, 126]. Furthermore, many of the intracellular signalling pathways activated during exercise regulate PGC-1α activity and expression. Calcineurin and the calmodulin-dependent protein kinase IV (CaMKIV) are activated in response to increased intracellular calcium during exercise [127, 128], and both increase PGC-1α expression *in vivo* [129-132]. The AMP-activated protein kinase (AMPK) is an energy sensor in the cell, and is activated by changes in energy status such as during exercise [115, 123, 133]. Pharmacological activation of AMPK increases PGC-1α expression *in vivo* and *in vitro* [134, 135]. Furthermore, AMPK can directly phosphorylate PGC-1α on its threonine-177 and serine-538 sites, increasing its activity [136]. The p38 mitogen-activated protein kinase (MAPK) is also activated in response to exercise [45, 122, 137], and activation of p38 MAPK increases PGC-1α expression *in vivo* [122]. Finally, PGC-1α is also activated by sirtuin-1 (SIRT1), which acts as a metabolic sensor in the cell [138, 139]. SIRT1 is increased after endurance exercise and fasting in skeletal muscle [112, 140], whereby it deacetylates PGC-1α resulting in increased PGC-1α activity [112]. SIRT1 can also bind to the PGC-1α promoter and enhance the recruitment of PGC-1α to its own promoter region to increase its expression [138].

In contrast to PGC-1α, PGC-1β expression does not increase in response to fasting, cold exposure or adrenergic stimulation [93, 99, 100]. Furthermore, PGC-1β is not elevated following acute endurance exercise [99, 119, 141], and in fact decreases over time post endurance exercise [119], and with endurance exercise training [141]. However, PGC-1β activity can be induced by SIRT1. PGC-1β is acetylated by the acetyl transferase, general control of amino-acid synthesis (GCN5), which inhibits PGC-1β-regulated transcriptional activity [142]. The expression of SIRT1 reverses this acetylation by GCN5, thereby promoting PGC-1β activity. Although PGC-1β expression is not increased in response to the same physical stimuli as SIRT1,

perhaps its deacetylation by SIRT1 may increase its transcriptional activity under such conditions. However, further investigation into this mechanism is required.

Due to differences in their regulation, it has been suggested that PGC-1α and PGC-1β may play complementary roles in regulating energy homeostasis [99, 143]. PGC-1β may play more of a general role, such as maintaining oxidative metabolism for basal energy requirements, while PGC-1α may coordinate the response to acute metabolic stressors such as exercise, cold and fasting. Supporting this, whole body PGC-1β knockout mice show increased expression of PGC-1α in skeletal muscle [144], while muscle specific PGC-1α knockout has no effect on PGC-1β expression [145, 146].

On the other hand, PGC-1β is down-regulated in a similar manner to PGC-1α. Interestingly, skeletal muscle PGC-1α and PGC-1β mRNA and/or protein is reduced in conditions associated with perturbed metabolic function and muscle atrophy, including ageing [147, 148], denervation [65], heart failure [80, 149], sepsis [150], obesity [151], Huntington's disease [152], cancer cachexia, uraemia and diabetes [153] in rodents; and COPD [154], ALS [155], ageing [156], and insulin-resistance and diabetes [156-158] in humans. These observations further link mitochondrial function to the pathogenesis of skeletal muscle atrophy.

1.2.2 Role of PGC-1α and PGC-1β in skeletal muscle

In skeletal muscle, PGC-1α and PGC-1β play similar, but not identical, roles in coactivating a diverse set of transcription factors to coordinate the expression of genes that regulate many functions involved in skeletal muscle health. These functions include, but are not limited to, mitochondrial biogenesis and fusion [159-162], skeletal muscle fibre type [145, 163-165], glucose transport [142, 166], fatty acid oxidation [167, 168], and angiogenesis [110, 169, 170].

Mitochondrial biogenesis and oxidative phosphorylation

PGC-1α and PGC-1β are master regulators of mitochondrial biogenesis and oxidative phosphorylation (OXPHOS) in skeletal muscle. Overexpression of PGC-1α or PGC-1β in rodent myotubes *in vitro,* or skeletal muscle *in vivo,* increases mitochondrial

biogenesis and expression of genes involved in OXPHOS, including several components of the respiratory chain such as the β subunit of ATP synthase (β-ATPase), cytochrome c oxidase subunit II (COX II), IV (COX IV) and V (COX V), cytochrome c (CytC), uncoupling protein 2 (UCP2), and mitochondrial transcription factor A (mtTFA, also known as TFAM), an inducer of mitochondrial DNA replication [162, 171, 172]. PGC-1α and PGC-1β also increase the expression of mitofusin 1 (MFN1) and MFN2 and hence, mitochondrial fusion [155, 159, 161, 173], a critical process required for maintaining mitochondrial function and mitochondrial DNA integrity [174]. In contrast, PGC-1α or PGC-1β knockout or mutant mice show a decrease in mitochondrial OXPHOS gene expression and impaired mitochondrial function, resulting in an impaired exercise performance [144, 145, 175, 176].

Muscle fibre type

PGC-1α is preferentially expressed in type I and type IIa oxidative muscle fibres in mice and humans [120, 126, 163]. Overexpression of PGC-1α in type II glycolytic muscles of transgenic mice causes a fibre-type conversion to types I and IIa oxidative fibres [163]. These fibres are redder due to increased myoglobin, show increased expression of OXPHOS genes, and have greater resistance to fatigue. In contrast, PGC-1α muscle-specific knock-out mice show a decrease in type I and IIa oxidative fibres, and an increase in type IIx and IIb glycolytic fibres [145]. They also show greater susceptibility to fatigue and a reduction in mitochondrial gene expression. Similar to PGC-1α, PGC-1β expression is also positively correlated with mRNA for type I and IIa oxidative fibres in humans [177]. However, PGC-1β expression is highest in type IIx muscle fibres in rodents, which are prevalent in muscles such as the extensor digitorum longus (EDL) [126, 164]. In rodents, type IIx fibres are glycolytic and have faster twitch properties than the oxidative types I and IIa fibres, although they have more mitochondria and oxidative properties than the glycolytic type IIb fibres [178, 179]. Transgenic expression of PGC-1β in glycolytic muscles of mice results in a large increase of these type IIx muscle fibres, and a decrease in types I, IIa and IIb [164]. Interestingly, these mice also have redder muscles, and show an increase in mitochondrial biogenesis and enhanced oxidative capacity during treadmill running; adaptations that would not normally be seen in the presence of decreased type I and IIa fibres. It is therefore unlikely that the increase in

oxidative capacity would be a result of these fibre-type changes. In addition, the full role of PGC-1β on skeletal muscle fibre type remains unknown since it is still highly expressed in the oxidative soleus muscle despite its low proportion of type IIx fibres [164], and infection of PGC-1β in primary rat myotubes results in a contrasting decrease in MHC IIx mRNA expression [180].

Substrate metabolism- Fatty acid and glucose uptake and oxidation

PGC-1α and PGC-1β play a fundamental role in the regulation of glucose and fatty acid uptake and metabolism. Overexpression of PGC-1α or PGC-1β in rodent skeletal muscle *in vivo*, or myotubes *in vitro*, results in increased expression of the glucose transporter type 4 (GLUT4), with parallel increases in insulin-stimulated glucose transport [142, 166, 167]. PGC-1α also increases basal glucose transport [167], although PGC-1β does not have this same effect [142]. Interestingly though, PGC-1α actually decreases glucose oxidation, and increases the expression of pyruvate dehydrogenase kinase 4 (PDK4) in C2C12 mouse myotubes [181]. PGC-1α is therefore thought to increase muscle glycogen stores via increased glucose transport and PDK4 activity, while increasing fatty acid oxidation [181]. Evidently, PGC-1α and PGC-1β increase the expression of the fatty acid transporter, CD36, as well as many genes associated with fat oxidation in skeletal muscle including medium-chain acylcoenzyme A dehydrogenase (MCAD), and carnitine palmitoyltranferase 1 (CPT1) [100, 126, 164, 167, 172, 182]. PGC-1α and PGC-1β also increase fat oxidation in skeletal muscle [167, 182, 183].

Because of their effect on energy metabolism, PGC-1α and PGC-1β are thought to be important targets for opposing insulin resistance and type II diabetes [118, 182, 184], which are characterised by decreased glucose and fatty acid oxidation, as well as impaired mitochondrial function. Indeed, transgenic expression of PGC-1β antagonises insulin resistance caused by a high-fat diet in mice [100]. PGC-1α and PGC-1β are down-regulated in skeletal muscle of type II diabetic patients [156, 158]. Moreover, single nucleotide polymorphisms (SNPs), defective activation, and/or decreased levels of PGC-1α are apparent in insulin resistant and diabetic skeletal muscle, and this has been proposed to contribute to the pathogenesis of these conditions [156-158, 185-188]. Interestingly, insulin stimulation also increases PGC-1α and PGC-1β mRNA expression in human skeletal muscle [156], suggesting that

reduced PGC-1α or PGC-1β levels may contribute to, or be a consequence of, insulin resistance; however this has not been confirmed.

Angiogenesis

An important requirement of increased oxidative metabolism is sufficient blood vessel density within the muscle to match metabolic needs. This is achieved via angiogenesis, or the formation of new blood vessels, which occurs in response to increased metabolic stress such as endurance exercise or ischemia. Transgenic expression of PGC-1α or PGC-β in rodent skeletal muscle stimulates angiogenesis via increased expression of the vascular endothelial growth factor (VEGF) [110, 169, 170]. In contrast, exercise or exposure to hypoxic conditions fail to stimulate angiogenesis in PGC-1α knockout muscle [110, 170], showing that PGC-1α is required for this adaptation in response to metabolic stress.

1.2.3 Transcriptional activity by PGC-1α and PGC-1β in skeletal muscle

PGC-1α and PGC-1β mediate their effects in skeletal muscle via coactivation of several transcription factors. This process consists of docking on transcription factors when bound to their respective response elements on the promoter of target genes, resulting in enhanced gene transcription initiation and/or elongation [101]. Some of the well-known transcription factors regulated by PGC-1α and/or PGC-1β in skeletal muscle include the nuclear respiratory factors (NRFs), peroxisome proliferator-activated receptors (PPARs), myocyte enhancer factor 2s (MEF2s), Ying-Yang 1 (YY1; PGC-1α only), and the estrogen-related receptors (ERRs) [101, 189].

Nuclear Respiratory Factors (NRFs)

Nuclear respiratory factor-1 (NRF-1) and NRF-2 (also known as GA binding protein; GABP) are transcription factors which regulate the expression of genes involved in mitochondrial biogenesis and OXPHOS [101]. In C2C12 myotubes, expression of PGC-1α increases the expression of and coactivates NRF-1 and NRF-2, leading to an increase in mitochondrial biogenesis, oxygen consumption and expression of OXPHOS genes [171, 190]. In particular, PGC-1α coactivates NRF-1 on the promoter for mtTFA, an inducer of mitochondrial DNA replication [171]. PGC-1β also interacts with NRF-1, and NRF-1 is required for the PGC-1β-induced increase

in mitochondrial biogenesis in C2C12 myotubes [172]. More recently, PGC-1α has been shown to stimulate the transcription of genes involved in the neuromuscular junction via coactivation of NRF-2 (GABP), showing that the role of this transcription factor extends beyond the mitochondria [191]. This has implications for neuromuscular diseases such as DMD, which is characterised by skeletal muscle atrophy. In fact, overexpression of PGC-1α ameliorates muscular dystrophy in mdx mice [191], a rodent model for DMD.

Peroxisome Proliferator Activated-Receptors (PPARs)

PGC-1α also coactivates members of the peroxisome proliferator activated-receptor (PPAR) family, a group of nuclear receptors that are known to regulate many genes involved in energy metabolism, and in particular, lipid transport and oxidation [192-196]. Members of the PPAR family include PPARα, PPARδ, and PPARγ. Although PGC-1α was first identified as a coactivator of PPARγ in brown adipose tissue [94], and expression of PPARγ in skeletal muscle protects from insulin resistance [197], its basal expression is relatively low in skeletal muscle [198, 199]. In contrast, PPARδ is highly expressed in skeletal muscle, while PPARα is moderately expressed [194]. Overexpression of PGC-1α in C2C12 myotubes causes a marked increase in PPARα [183] and PPARδ [200], with an associated increase in fatty acid oxidation, and expression of fatty acid transporter CPT1 and MCAD [183, 200]. PPARδ also coactivates and increases the expression of PGC-1α, showing a feed-forward loop regulating PGC-1α expression [200, 201]. Furthermore, transgenic expression of PPARδ in skeletal muscle increases oxidative metabolism and causes a shift towards more oxidative muscle fibres [202, 203], suggesting that PPARδ may be involved in these processes regulated by PGC-1α. However, the direct interaction of PGC-1α or PGC-1β with PPARs in skeletal muscle has not been shown. In fact, as PPARδ can increase PGC-1α expression, it is possible its effect on fibre type switching may actually be via induction of PGC-1α [101].

Myocyte Enhancer Factors-2s (MEF2s)

In skeletal muscle, myocyte enhancer factor-2 (MEF2) transcription factors mediate the expression of genes involved in the determination of slow-twitch fibre types [204, 205], mitochondrial oxidative metabolism [98, 206], glucose transport [207, 208], and muscle differentiation and regeneration [2]. Both PGC-1α and PGC-1β

interact with MEF2 transcription factors in skeletal muscle [163, 164, 166]. In C2C12 myotubes, PGC-1α coactivates MEF2C and MEF2D on type I troponin and myoglobin promoters, which is thought to be responsible for the PGC-1α-induced switch towards slow twitch muscle fibres *in vivo* [163]. The binding and coactivation of MEF2C by PGC-1α also results in increased GLUT4 expression and glucose transport in rodent myotubes [166]. PGC-1α also induces its own expression via MEF2, as the coactivation of MEF2s in C2C12 myotubes results in MEF2 binding and activating the PGC-1α promoter [209]. Lastly, PGC-1β also coactivates MEF2D, which is thought to be responsible for the increase in myosin heavy chain (MHC) IIx in PGC-1β transgenic mice [164]. Supporting this, the activation of the MHC IIx promoter by PGC-1β in 10T1/2 cells is dependent on the coactivation of MEF2D [164].

Ying Yang-1 (YY1)

PGC-1α also coactivates Ying Yang-1 (YY1) to increase the expression of mitochondrial genes in C2C12 myotubes [210]. YY1 also increases the activity of the PGC-1α promoter, showing another mechanism whereby PGC-1α can induce its own expression. Interestingly, the interaction between PGC-1α and YY1 is dependent on the activity of mTOR, a potent regulator of protein synthesis. In addition, treatment with rapamycin, an mTOR inhibitor, decreases the expression of PGC-1α [210].

Estrogen-Related Receptors (ERRs)

Estrogen-related receptor-α (ERRα), ERRβ and ERRγ are orphan nuclear receptors that play a major role in skeletal muscle energy metabolism, but only when partnered by coactivators such as PGC-1α and PGC-1β [211]. ERRs are known to regulate almost all aspects of energy metabolism including substrate uptake and oxidation, mitochondrial biogenesis and function, and oxidative capacity (reviewed in [101, 211]). The best characterised of the three, ERRα, mediates many of the effects of PGC-1α and PGC-1β in skeletal muscle (Figure 1.02).

ERRα is highly expressed in tissues with high energy demand, and its expression in skeletal muscle is induced by physiological stimuli in a similar manner to PGC-1α, such as exposure to cold temperatures [212] and endurance exercise [173]. In fact,

PGC-1α has been shown to regulate ERRα activity via two mechanisms; by increasing ERRα gene expression and by physically interacting with ERRα to regulate its transcriptional activity [190, 212]. It is thought that initially, PGC-1α increases ERRα gene expression via a mechanism involving GABP (NRF-2), and thereafter, the increased levels of ERRα permit increased coactivation by PGC-1α [190]. Interestingly, overexpression of ERRα increases PGC-1α promoter activity, resulting in a feed-forward loop to further increase PGC-1α and ERRα activity [213]. Likewise, PGC-1β increases ERRα gene expression [214], and also coactivates ERRα to increase gene transcription [164]. Furthermore, PGC-1β and ERRα act synergistically to activate the PGC-1β promoter, showing that PGC-1β is also involved in a positive feedback loop to regulate its own activity [164]. Interestingly, PGC-1β in combination with ERRα can also bind to the PGC-1α promoter, showing that PGC-1β may be able to regulate PGC-1α activity [164]. Whether this results in increased PGC-1α activity however is unknown. When co-activated by PGC-1α, or PGC-1β, ERRα induces gene expression by binding to ERR response elements (ERREs) on the promoter region of target genes [212]. ERREs are highly enriched in several OXPHOS related genes, and in particular, those known to be regulated by PGC-1α or PGC-1β [190].

One of the earliest studies showing the involvement of ERRα in PGC-1-mediated mitochondrial biogenesis investigated mitochondrial gene expression in response to PGC-1α overexpression in sarcoma osteogenic (SAOS2) cells [160]. Inhibition of ERRα using siRNA in these cells prevented the PGC-1α-induced increase in the expression of genes involved in mitochondrial DNA replication, mitochondrial transport, fatty acid oxidation and oxidative phosphorylation. Interestingly, inhibition of ERRα had no effect on mitochondrial gene expression in the absence of PGC-1α overexpression, showing that ERRα is required for PGC-1α-induced, but not basal, mitochondrial gene expression. Since then, many experiments using siRNA or pharmacological inhibitors for ERRα have led to the discovery of several genes and functions that require ERRα activity to be induced by PGC-1α or PGC-1β.

ERRα is required for the PGC-1α- and PGC-1β-induced regulation of mitochondrial biogenesis, cellular respiration and induction of several OXPHOS genes in C2C12 myotubes [172, 190]. The PGC-1α/ERRα and PGC-1β/ERRα transcriptional

pathways also regulate the expression of MFN1 and MFN2 [155, 159, 161, 173], and PGC-1α and PGC-1β, in combination with ERRα, directly bind to the ERRE on the MFN1 and MFN2 promoters in C2C12 myotubes [155]. PGC-1α and PGC-1β may also regulate fatty acid oxidation in skeletal muscle via ERRα, as MCAD, a pivotal enzyme involved in fatty acid oxidation, is a known target of ERRα [215]. Indeed, the increase in MCAD by PGC-1α in SAOS2 cells is dependent on ERRα [212], and PGC-1β directly coactivates ERRα on the MCAD promoter in 3T3-L1 cells [100]. PGC-1α also increases PDK4 expression via ERRα in myotubes, resulting in decreased glucose and increased fatty acid oxidation [181]. In addition, PGC-1β coactivates ERRα to increase carnitine/acylcarnitine translocase (CACT) in C2C12 myotubes [214], a protein essential in the oxidation of long-chain fatty acids. The PGC-1α/ERRα transcriptional pathway also increases hypoxia-inducible factor 2α (HIF2α) in primary myotubes, resulting in activation of a slow-twitch gene program [165]. This pathway is therefore thought to be involved in the PGC-1α-induced switch to slow-oxidative muscle fibres *in vivo*. Lastly, PGC-1α and PGC-1β also increase VEGF expression in skeletal muscle via coactivation of ERRα, leading to an increase in angiogenesis [169, 170]. The effects of PGC-1α and PGC-1β are therefore dependent on the coactivation of ERRα for the majority of their roles in skeletal muscle including mitochondrial biogenesis and fusion, substrate oxidation, fibre-type determination and angiogenesis. Further studies will likely identify additional gene targets that are regulated by this transcriptional axis.

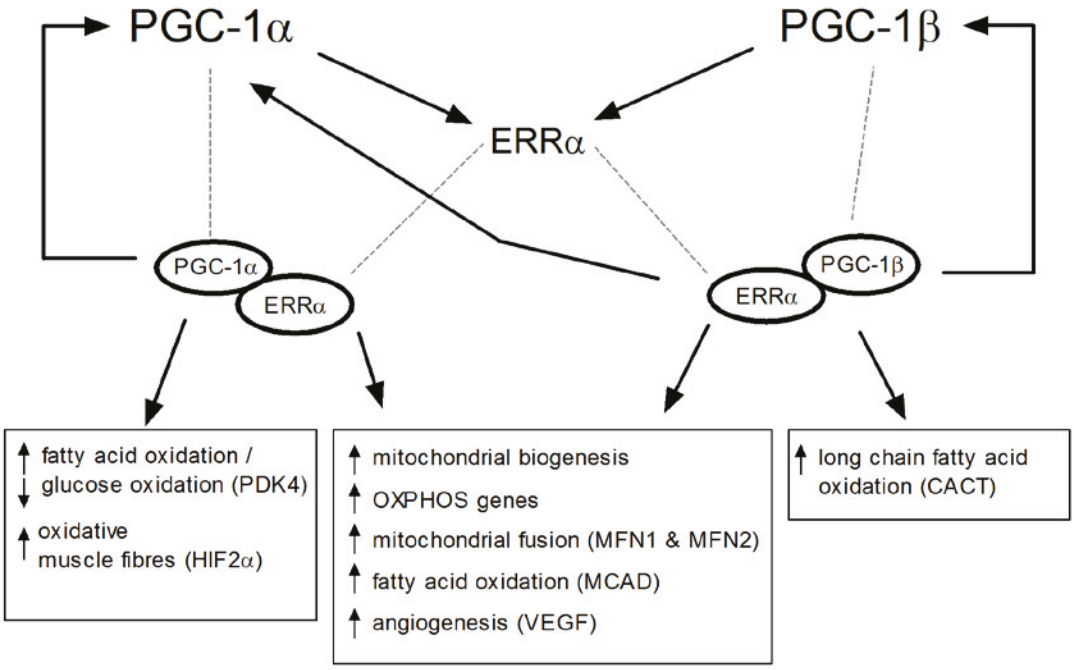

Figure 1.02 Regulation and transcriptional activity of PGC-1α/ERRα and PGC-1β/ERRα. PGC-1α and PGC-1β increase the expression of ERRα and coactivate ERRα on the promoter of several genes to control many functions in skeletal muscle. When partnered with ERRα, PGC-1α and PGC-1β also increase their own expression in a feed-forward manner, resulting in overall increased PGC-1α/ERRα and PGC-1β/ERRα transcriptional activity. PGC-1β also coactivates ERRα on the PGC-1α promoter.

1.3 PGC-1α and PGC-1β in the regulation of skeletal muscle mass

Many conditions characterised by skeletal muscle atrophy are associated with impaired mitochondrial function [84, 86, 91], suggesting that the molecular mechanisms regulating both of these processes may be linked. As mentioned previously, skeletal muscle PGC-1α and PGC-1β mRNA and/or protein is reduced in conditions associated with perturbed metabolic function and muscle atrophy, such as ageing [147, 156], denervation [65, 216], heart failure [80, 149], sepsis [150], COPD [154], ALS [155], ageing [156], cancer cachexia [153], uraemia [153], glucocorticoid treatment [150, 217], Huntington's disease [152], and insulin-resistance and diabetes [26, 157, 158]. Two weeks of hindlimb unloading in rats results in marked atrophy of the soleus with a simultaneous decrease in PGC-1α protein levels [218]. This also coincides with decreased percentage of slow twitch muscle fibres. During reloading and subsequent hypertrophy of the soleus muscle, PGC-1α levels return and further increase above control, suggesting that PGC-1α may be involved in processes regulating both skeletal muscle atrophy and hypertrophy. These observations have led to the investigation of the potential role of PGC-1α and PGC-1β in the regulation of muscle mass. Indeed, many recent studies are starting to reveal a major role for PGC-1α, and potentially PGC-1β, in the protection from muscle atrophy during many catabolic states [150, 153, 191, 219, 220].

Transgenic overexpression of PGC-1α or PGC-1β in mice has been shown to prevent the loss of muscle mass that occurs during catabolic conditions such as denervation and fasting [153, 219]. Using this model, PGC-1α or PGC-1β is overexpressed under the control of a muscle creatine kinase (MCK) promoter which is predominantly active in type IIb glycolytic muscles, and therefore results in greater overexpression in these fibres. Since glycolytic muscle fibres are preferentially targeted for degradation in several systemic catabolic states [81, 82, 221], the PGC-1α-induced increase in oxidative fibres may therefore protect from atrophy by reducing the content of glycolytic fibres. However, this does not explain the protective effect of PGC-1α or PGC-1β during denervation, as the atrophy associated with disuse is predominantly seen in oxidative muscle fibres [73, 222]. Further *in vitro* studies revealed that PGC-1α and PGC-1β protect from atrophy in C2C12 myotubes via the

attenuation of both proteasomal and lysosomal protein degradation [219]; processes known to be regulated by FOXO3a [62]. Furthermore, overexpression of PGC-1α or PGC-1β prevents the FOXO3a-dependent increase in Atrogin-1, MuRF1, and lysosomal hydrolase cathepsin-L expression, and inhibits a constitutively active form of FOXO3a from binding to the Atrogin-1 promoter and causing muscle fibre atrophy *in vivo* [153, 219] (Figure 1.03). Rather than coactivating FOXO3a, PGC-1α and PGC-1β appear to act as transcriptional repressors in this case. Using the same PGC-1α transgenic mouse line, PGC-1α also protects from sarcopenia and prevents a gain in adipose tissue mass in aged mice (22 months) [148]. The reduction in age-related muscle wasting in these mice is also thought to be due to a decrease in proteasomal and lysosomal degradation, as well as apoptosis, as markers of these processes are suppressed in the muscle. More recently, transgenic expression of PGC-1α has been shown to protect from muscle atrophy and improve muscle function in superoxide dismutase 1 (SOD1) mutant mice, a rodent model for ALS [223]. Furthermore, transgenic expression of PGC-1α prevents muscle damage in mdx mice by increasing the expression of several neuromuscular junction genes [191]. These mice show a reduced number of centrally located nuclei, a characteristic of regenerating muscle and a marker for muscle damage. PGC-1α may therefore be an attractive therapeutic target to improve muscle regeneration, reduce muscle atrophy and enhance muscle growth.

The above studies suggest that PGC-1α and PGC-1β can prevent muscle atrophy *in vivo* by attenuating the rate of protein degradation in skeletal muscle. However a decline in protein synthesis is also a major contributor to muscle atrophy during many disease states [224-227], while the stimulation of protein synthesis may even be more important in some cases [12, 227, 228]. In fact, elderly sarcopenic subjects show similar rates of protein degradation compared to younger subjects, and therefore the decline in protein synthesis with age may be a more significant contributor to the cause of muscle loss during aging [228]. An ideal therapeutic strategy to combat muscle wasting would be to target both protein degradation and protein synthesis in skeletal muscle. Although it is thought that PGC-1α and PGC-1β do not regulate protein synthesis [219], their principal role as transcriptional coactivators which results in increased gene and protein expression would suggest otherwise. In fact, aged PGC-1α transgenic mice also exhibit increased

phosphorylation levels of Akt and mTOR in skeletal muscle when compared to age-matched control mice [148], suggesting that PGC-1α may increase protein synthesis via increased Akt/mTOR activity (Figure 1.03). Whether PGC-1α and/or PGC-1β can regulate protein synthesis in healthy or atrophying skeletal muscle has not been thoroughly examined and therefore warrants further investigation.

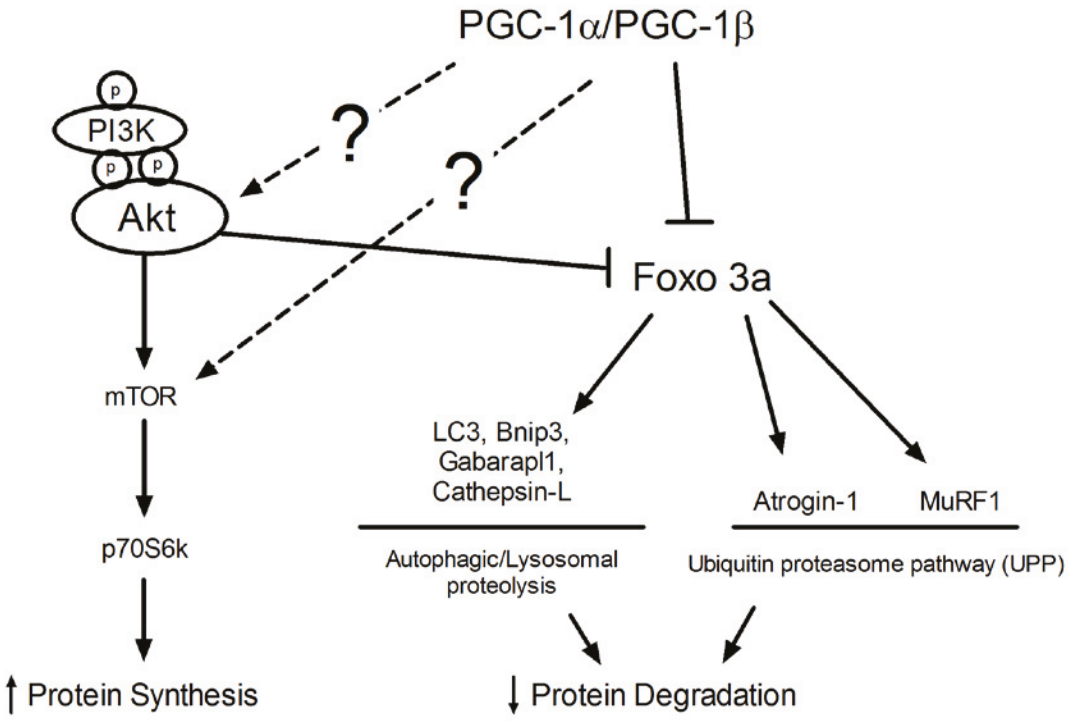

Figure 1.03 The Akt signalling pathway and its potential interaction with PGC-1α and PGC-1β. PGC-1α and PGC-1β inhibit the expression of FOXO3a-dependent genes involved in both proteasomal and lysosomal degradation. Whether PGC-1α and PGC-1β can increase protein synthesis is unknown, however it is hypothesis that they may do so via Akt and mTOR signalling.

1.4 PGC-1α and Creatine in skeletal muscle

In addition to decreased PGC-1α and PGC-1β levels, many conditions associated with skeletal muscle atrophy also display decreased intracellular creatine levels [229]. Creatine is found at high concentrations in highly metabolically active tissues such as skeletal muscle, heart and brain [230]. In addition to glucose and fatty acids, creatine is also an essential fuel source within skeletal muscle, where it plays an important role in maintaining cellular energy homeostasis by resynthesising ATP when in its phosphorylated form, phosphocreatine. Traditionally, creatine supplementation, in combination with resistance training, has been used to assist with skeletal muscle growth [231-233]. More recently, its use in the clinical setting has become of interest. Skeletal muscle creatine levels are reduced in many conditions associated with skeletal muscle atrophy, such as in patients with muscular dystrophy, and inflammatory, congenital and mitochondrial myopathies [229]. Supplementation with creatine monohydrate in these patients leads to gains in muscular strength and total body weight [234]. Creatine supplementation also stimulates muscle hypertrophy during rehabilitative strength training following limb immobilisation [235], attenuates corticosteroid-induced muscle wasting in rats [236], and reduces muscular degeneration in mdx mice [237]. Interestingly, these effects are comparable to when PGC-1α or PGC-1β are overexpressed in skeletal muscle under similar conditions [150, 153, 191, 219]. However, creatine supplementation does not always increase intracellular creatine content, which is controlled via the Na^+/Cl^- dependent Creatine transporter (CrT) [238]. Long-term creatine supplementation decreases CrT expression in rat skeletal muscle [238], and may therefore not be effective for longer term use. Furthermore, CrT mRNA is significantly reduced in skeletal muscle of patients with various myopathies, suggesting that CrT levels may be the limiting factor to increase intracellular creatine content in response to creatine supplementation [239, 240]. Understanding the molecular mechanisms regulating the expression and/or activity of the CrT is therefore important to maximise the efficiency and benefits of creatine supplementation in skeletal muscle.

Currently, little is known about how the CrT is regulated. In healthy rodent skeletal muscle, high-dose creatine supplementation (initially increasing intracellular

creatine) decreases CrT expression [238], while depletion of intracellular creatine by β-Guanidinoproprionic acid (β-GPA), a competitive inhibitor of the CrT, increases sarcolemmal CrT expression [241, 242]. Similar to PGC-1α and PGC-1β, the CrT is more abundant in slow-oxidative muscle fibres, resulting in increased rates of creatine uptake when compared to fast-glycolytic fibres [243, 244]. However the molecular mechanisms regulating these changes in CrT and therefore creatine uptake in skeletal muscle are unknown. It is noteworthy that many conditions associated with decreased CrT levels and reduced muscle mass [234, 239], also show reduced levels of PGC-1α or PGC-1β [65, 245]. As PGC-1α and PGC-1β play a major role in energy metabolism and regulate the expression of glucose and fatty acid transporters in skeletal muscle [142, 164, 167], it would be interesting to determine if they also regulate expression of the CrT, and therefore creatine uptake, in skeletal muscle. Furthermore, as many of the metabolic effects that PGC-1α and/or PGC-1β have on skeletal muscle health involve the coactivation and regulation of ERRα, it is possible that PGC-1α and PGC-1β may regulate the CrT and creatine uptake in an ERRα-dependent manner.

Lastly, while creatine supplementation *in vivo* increases muscle growth, the molecular mechanisms regulating this occurrence remain elusive. Studies that have investigated the effect of creatine supplementation on protein synthesis have shown varying results [246, 247], although creatine has been shown to increase the synthesis of contractile proteins in differentiating myotubes *in vitro* [248, 249]. Therefore it is possible that PGC-1α and PGC-1β may increase protein synthesis by regulating CrT levels and increasing intracellular creatine content, however further investigation is required to test this hypothesis.

1.5 Summary and significance of research

Skeletal muscle atrophy is a devastating condition, contributing to increased morbidity and mortality during many chronic disease states. Skeletal muscle atrophy is a result of decreased rates of protein synthesis in combination with increased rates of protein degradation. Understanding the molecular mechanisms that regulate these processes is therefore a prerequisite to developing therapeutic strategies to target muscle atrophy and improve clinical outcomes. The transcriptional coactivators PGC-1α and PGC-1β are both positive regulators of many functions important for maintaining skeletal muscle health. Notably, many of their actions in skeletal muscle depend on the transcriptional coactivator, ERRα. Recent evidence suggests that PGC-1α and PGC-1β may be attractive targets to attenuate muscle wasting, and they have been shown to reduce protein degradation via decreased activity of signalling pathways involved in muscle atrophy. As protein synthesis rates are also significantly reduced during many catabolic states, identifying ways to increase protein synthesis is equally as important. The role of PGC-1α and PGC-1β in skeletal muscle protein synthesis has not been thoroughly investigated, and therefore further research is required. If PGC-1α and/or PGC-1β can increase protein synthesis in addition to attenuating protein degradation, this may provide a basis for the development of treatment strategies to alleviate the debilitating effects of muscle atrophy.

Another mechanism by which PGC-1α and PGC-1β may regulate skeletal muscle mass is via the CrT. Creatine supplementation is known for its ability to stimulate muscle growth *in vivo*. However, CrT levels are significantly decreased in many myopathies associated with muscle wasting, suggesting that increasing CrT levels may be an effective strategy to maximise the potential benefits of creatine supplementation. However the molecular mechanisms regulating CrT expression are unknown. As PGC-1α and PGC-1β regulate other important aspects of energy metabolism, it is plausible that they may also regulate creatine uptake via increasing the expression of the CrT. This may partially explain how PGC-1α and PGC-1β positively influence skeletal muscle mass. Furthermore, as the role of creatine on protein synthesis is ambiguous, it would be interesting to determine if increased CrT

expression, potentially via PGC-1α and PGC-1β, can affect protein synthesis in skeletal muscle. Understanding the regulation of the CrT, and how CrT levels affect muscle growth, may provide a basis to improve the efficiency of creatine supplementation in the clinical setting.

1.6 Aims and Hypothesis

This PhD thesis will investigate the roles of both PGC-1α and PGC-1β in the regulation of C2C12 myotube protein synthesis. The general working hypothesis is that PGC-1α and PGC-1β can positively regulate skeletal muscle protein turnover by increasing the rates of protein synthesis, and therefore maintaining or increasing their levels will protect against skeletal muscle atrophy.

1.6.1 Specific Aims:

1. To determine if overexpressing PGC-1α and/or PGC-1β in C2C12 myotubes can increase myotube diameter and protein synthesis under basal and catabolic conditions, and to determine if this is dependent on Akt/mTOR signalling or ERRα.

2. **a.** To identify global gene and protein expression changes that occur in response PGC-1α and PGC-1β overexpression in C2C12 myotubes and create an unbiased gene expression signature (GES) characterising PGC-1α- and PGC-1β- driven protein synthesis.

   b. To measure the expression of the unbiased GES selected genes in human models of increased and decreased muscle protein synthesis.

3. **a.** To determine if PGC-1α and PGC-1β increase the expression of the CrT and creatine uptake in L6 myotubes and whether this is via ERRα.

   b. To determine whether PGC-1α and PGC-1β increase protein synthesis by increasing CrT expression and creatine uptake.

1.6.2 Specific Hypotheses:

1. Overexpression of PGC-1α and/or PGC-1β will increase protein synthesis in C2C12 myotubes under basal and catabolic conditions, and this will be via increased Akt/mTOR signalling, and dependent on the transcription factor, ERRα.

2. Global gene and protein expression changes that occur in response PGC-1α and PGC-1β overexpression in C2C12 myotubes will represent signalling pathways involved in protein synthesis and growth, and lead to the identification of new PGC-1α/PGC-1β gene targets that may be involved in protein synthesis. These targets will be up- and down-regulated in models of increased and decreased protein synthesis, respectively.

3. Overexpression of PGC-1α and PGC-1β will increase CrT mRNA and creatine uptake in L6 myotubes, and this will be via the coactivation of ERRα. Furthermore, PGC-1α and PGC-1β will increase protein synthesis via their increased expression of CrT mRNA and creatine uptake.

Chapter 2

The Role of PGC-1α and PGC-1β in C2C12 Myotube Protein Synthesis

2.1 Introduction

Skeletal muscle mass is regulated by a fine balance between protein synthesis and protein degradation [31]. Decreased rates of protein synthesis and increased rates of protein degradation result in skeletal muscle atrophy, a devastating condition and a hallmark of neuromuscular disorders such as Duchenne muscular dystrophy (DMD) and amyotrophic lateral sclerosis (ALS) [15, 16]. Muscle atrophy is also a consequence of many chronic diseases including cancer, heart disease, chronic obstructive pulmonary disease (COPD), and AIDS, as well as sepsis, critical illness myopathy, sarcopenia and immobilisation following acute injuries [13, 17-20, 22]. Muscle atrophy secondary to these conditions is a major limiting factor to successful treatment and recovery, and contributes to an increase in morbidity and mortality [11, 23, 24]. Understanding the molecular and physiological mechanisms involved in the regulation of muscle mass is essential for developing therapeutic interventions to improve clinical outcomes and reduce the burden on health care systems.

The transcriptional coactivators, peroxisome proliferator-activated receptor-γ coactivator-1α (PGC-1α) and its much less studied homologue, PGC-1β, have been identified as potential molecular targets that contribute to the positive regulation of skeletal muscle mass. In skeletal muscle, PGC-1α and PGC-1β coactivate a diverse set of transcription factors to coordinate the expression of genes that regulate mitochondrial biogenesis and fusion [159-162], skeletal muscle fibre type [145, 163, 164], glucose transport [142, 166], lipid oxidation [167, 168], and angiogenesis [110, 169]. These transcription factors include, but are not limited to, peroxisome proliferator-activated receptors (PPARs), nuclear respiratory factors (NRFs), myocyte enhancer factor 2 (MEF2), and the estrogen-related receptors (ERRs) [101, 189].

The expression of PGC-1α and/or PGC-1β is reduced in conditions associated with muscle atrophy and perturbed metabolic function, such as ageing [147], denervation [65], heart failure [80, 149], sepsis [150], Huntington's disease [152], cancer cachexia, uraemia and diabetes [153] in rodents, and chronic obstructive pulmonary disease (COPD) [154], ALS [155], ageing [156], insulin-resistance and diabetes [157, 158] in humans. Recently, transgenic overexpression of PGC-1α or PGC-1β in mice has been shown to prevent the loss of muscle mass that occurs during catabolic conditions such as denervation, fasting or sarcopenia [148, 153, 219]. This is thought to be via a decrease in protein degradation, as overexpression of PGC-1α or PGC-1β in C2C12 myotubes inhibits both proteasomal and lysosomal protein degradation; processes known to be regulated by the transcriptional activity of forkhead box O protein 3a (FOXO3a) [62, 219]. However, a decline in protein synthesis is also a major contributor to muscle atrophy during many disease states [224-227], and therefore an effective therapeutic strategy would target both protein degradation and protein synthesis. While it is thought that PGC-1α and PGC-1β do not regulate protein synthesis [219], their principal role as transcriptional coactivators which results in increased gene and protein expression would suggest otherwise. Whether PGC-1α and/or PGC-1β regulate protein synthesis in healthy or atrophying skeletal muscle has not been thoroughly examined and therefore warrants further investigation.

The Akt/mTOR signalling pathway is a major intracellular signalling pathway known to regulate protein synthesis in skeletal muscle [39, 47]. The activation of Akt by PI3K leads to the phosphorylation of mTOR and its downstream substrates p70S6k and 4E-BP1, resulting in translation initiation and elongation [39]. The activation of mTOR/p70S6k and protein synthesis can also be induced by mechanical stimulation independently of Akt [250]. PGC-1α transgenic mice that are protected from sarcopenia show increased phosphorylation of Akt and mTOR compared to their control littermates [148], suggesting that PGC-1α may in fact regulate this signalling pathway and consequently protein synthesis. Supporting this, PGC-1α has been shown to activate the Akt pathway in non-small cell lung carcinoma (NSCLC) cells [251]. Furthermore, mTOR is required for PGC-1α to coactivate YY1 and induce the expression of many mitochondrial genes in C2C12 myotubes [210]. Akt also inhibits protein degradation by decreasing FOXO activity and the expression of

genes involved in the ubiquitin proteasome pathway [50, 51]; a role similar to that of PGC-1α and PGC-1β [153, 219]. Whether PGC-1α or PGC-1β can regulate the activity of the Akt/mTOR signalling pathway to regulate protein synthesis is unknown.

Lastly, many of the effects that PGC-1α and/or PGC-1β have on skeletal muscle health involve the coactivation of the orphan nuclear receptor, ERRα. When activated by PGC-1α or PGC-1β, ERRα increases the transcription of its target genes by binding to the ERR response element (ERRE) in their promoter regions [101]. ERRα is required for the PGC-1α- and PGC-1β-induced regulation of mitochondrial biogenesis and induction of several OXPHOS genes [172, 190], mitochondrial fusion [155], angiogenesis [169, 170] and substrate oxidation [181, 214] in skeletal muscle. It may therefore be possible that any effect PGC-1α or PGC-1β may have on protein synthesis, may involve ERRα.

The primary aim of this study was to determine if PGC-1α and/or PGC-1β can regulate protein synthesis in mouse C2C12 myotubes under basal or catabolic conditions. A secondary aim was to determine if PGC-1α or PGC-1β act via the Akt/mTOR signalling pathway to regulate protein synthesis. Finally, it was of interest to determine whether PGC-1α or PGC-1β can regulate protein synthesis via their coactivation of ERRα.

2.2 Methods

2.2.1 Cell culture

C2C12

Mouse C2C12 myoblasts (American type culture collection; ATCC, Manassas, VA) were incubated at 37°C with 5% CO_2, in high-glucose Dulbecco's Modified Eagle Medium (DMEM) supplemented with 10% foetal bovine serum (FBS), 100 U/ml penicillin and 100 µg/ml streptomycin (Invitrogen, Carlsbad, CA). Myoblasts were plated at a density of 1.5 x $10^4/cm^2$ in 6 and 12-well plates. Upon confluence (~48 hrs), medium was changed to high-glucose DMEM supplemented with 2% horse serum (HS; Invitrogen), 100 U/ml penicillin and 100 µg/ml streptomycin for 4-5 days until multinucleated myotubes had formed. Medium was changed every 48 hours.

CRE8- used for adenovirus amplification

Human embryonic kidney cells (HEK293) expressing CRE recombinase (CRE8) were a donation from Natasha Kralli (Scripps Research Institute, La Jolla, CA). CRE8s were incubated at 37°C and 5% CO_2, in high-glucose DMEM supplemented with 10% FBS, and 200µg/mL of geneticin (G418; Sigma-Aldrich, St Louis, MO), an antibiotic used for selection.

2.2.2 Adenovirus amplification, purification and titration

Amplification

Adenoviruses expressing human PGC-1α (hPGC-1α), human PGC-1β (hPGC-1β), siERRα, siSUPER, VP16-ERRα and VP16-control were a gift from Natasha Kralli (Scripps Research Institute, La Jolla, CA). Green fluorescent protein (GFP) adenovirus was a donation from the metabolic research unit (Deakin University, Geelong, Vic). All adenoviruses were under the control of the cytomegalovirus promoter as described previously [212, 252]. To amplify each adenovirus, 3 µL of adenovirus stock was added to 7.32 x 10^7 CRE8 cells in suspension. After mixing, cells were split and plated into 5 x 150 mm dishes and the adenovirus was taken up and amplified in these cells. Cells were incubated for 3-5 days, until 50% of the cytopathic effect (CPE) was complete. The CPE refers to the morphological changes

that the cells undergo after infection. Cells typically round up and detach, and 50% CPE represents 50% of these cells being detached. Cells were then harvested and centrifuged for 10 min at 1,500 rpm, and the pellet was resuspended in 5 mL fresh DMEM.

Purification

Cells were lysed by 3 consecutive freeze/thaw cycles in a dry ice/ethanol bath and 37°C water bath respectively. Each adenovirus was then purified using the Adeno-X Maxi Purification Kit (Clontech, Mountain View, CA), according to manufacturer's protocol.

Titration

Adenoviruses were titrated using the Adeno-X qPCR Titration Kit (Clontech). Briefly, the viral genomic DNA was purified using NucleoSpin Virus spin columns. Viral DNA was then amplified using real-time quantitative PCR (qPCR), and the DNA copy number was determined from a standard curve generated by serial dilutions of the Adeno-X DNA control template. The amount of virus to use for experiments was calculated using the multiplicity of infection (MOI), which is the desired amount of viral copies per cell:

Amount of virus per well = (no. of cells to infect) x (desired MOI) / (copy number/mL).

Adenovirus optimisation

To determine the optimal MOI to use for each adenovirus, C2C12 myotubes were infected using an MOI of 50, 100 and 200. To infect cells, the required amount of adenovirus was added to fresh cell culture medium and then added to each well. Cells were harvested after 48 hours of infection and mRNA expression was determined via real-time qPCR.

Adenoviral Infections

GFP, PGC-1α and PGC-1β experiments

Myotubes were infected with adenoviruses expressing GFP, hPGC-1α or hPGC-1β using an MOI 100. Cells were harvested after 72 hours for RNA, protein and protein synthesis assays.

siERRa combined with PGC-1 experiments

Myotubes were infected with an adenovirus expressing short interfering RNA (siRNA) for ERRα (siERRα) or its control, siSUPER, using an MOI 200, as described previously [155, 172, 253]. After 24 hours, myotubes were infected with an additional dose of siERRα (or its control vector), as well as GFP, hPGC-1α or hPGC-1β at an MOI of 100. Cells were harvested after 96 hours for RNA, protein and protein synthesis assays.

VP16-ERRα experiments

Myotubes were infected with an adenovirus expressing ERRα with a heterogeneous strong transcriptional activation domain, VP16-ERRα, or its control VP16-control, using an MOI of 100. Cells were harvested after 72 hours for RNA, protein and protein synthesis assays.

2.2.3 Cell culture treatments

Following 48 hours infection with PGC-1α or PGC-1β adenoviruses, myotubes were treated with or without 10 μM LY-294002 (Sigma-Aldrich, St Louis, MO) or 20 ng/mL rapamycin (Sigma-Aldrich), for 24 hours to inhibit PI3K and mTOR respectively [39, 50].

2.2.4 Messenger RNA (mRNA) expression

RNA extraction

RNA was extracted using Tri-Reagent solution (Ambion Inc., Austin, TX) according to manufacturer's protocol. RNA concentrations were determined using the NanoDrop 2000 (NanoDrop products, Wilmington, DE). RNA (1 μg) was reverse transcribed to complementary DNA (cDNA) using a High Capacity cDNA reverse

transcription kit (Applied Biosystems, Forster City, CA) according to manufacturer's protocol.

Real-time polymerase chain reaction

Real-time qPCR was performed using a Stratagene Mx3000P QPCR System and the MxPro qPCR software (Stratagene, La Jolla, CA). Cycling conditions for the qPCR consisted of one denaturing cycle at 95°C for 2 minutes, followed by 40 cycles of denaturing at 95°C for 5 seconds and annealing at 60°C for 20 seconds, and elongation at 72°C for 60 seconds. A dissociation curve was generated to show that only one product had been amplified during the PCR. Each 20 µL reaction contained 0.5 x Power SYBR Green PCR Master Mix (Applied Biosystems), 25 ng of cDNA, and the forward and reverse primers for the gene of interest. Primers were designed across exons using Primer 3 (www.primer3.sourceforge.net) and the sequences cross checked for gene specificity using a BLAST search (www.ncbi.nlm.gov/BLAST). Primers were synthesised by Gene Works (Adelaide, SA). Genes amplified in the qPCR are shown in Table 2.1. To compensate for variations in input RNA amounts and efficiency of the reverse transcription, data was normalised to ribosomal protein, 36B4 (also known as RPLPO) mRNA.

Table 2.01 Primers used in the real-time qPCR.

Primer	GenBank accession no.	Forward Primer (5'-3')	Reverse Primer (5'-3')
Human-PGC-1α	NM_013261.3	TCAGTCCTCACTGGTGGACA	TGCTTCGTCGTCAAAAACAG
Human-PGC-1β	NM_133263.3	CTGCTGGCCCAGATACACTGA	ATCCATGGCTTCATACTTGCT
Mouse COX IV	NM_009941.2	ACTACCCCTTGCCTGATGTG	GCCCACAACGTCTTCCATT
Mouse ERRα	NM_007953.2	TTGAAGATGCTGAGGCTGTG	CCAGCTTCACCCCATAGAAA
Mouse 36B4	NM_007475.5	TTGTGGGAGCAGACAATGTG	AGTCCTCCTTGGTGAACACG

2.2.5 Protein expression

Protein extraction

Myotubes were lysed in RIPA buffer (Merck-Millipore, Kilsyth, VIC) with 1 µL/mL protease inhibitor cocktail (Sigma-Aldrich) and 10 µL/mL Halt Phosphatase Inhibitor Single-Use Cocktail (Thermo Scientific, Rockford, IL). Protein concentrations were determined using the bicinchoninic acid (BCA) Protein Assay Kit (Thermo Scientific) according to the manufacturer's protocol, and absorbance

was measured at 562 nm on a Synergy 2 Microplate Reader (BioTek, Winooski, VT).

Western Blotting

Electrophoresis was performed using a 4-12% NuPAGE® Novex Bis-Tris Gel (Invitrogen) in NuPAGE® SDS MOPS Running Buffer (Invitrogen). Twenty micrograms of protein was loaded into each well of a 10-well gel. Protein transfer was performed in a Bjerrum buffer containing 50 mM Tris, 17 mM glycine and 10 % methanol using polyvinylidene difluoride (PVDF) membranes (Merck-Millipore). The membranes were blocked with 5 % bovine serum albumin (BSA; Sigma-Aldrich) in PBS for one hour, and incubated overnight at 4ºC with the following primary antibodies diluted in 5% BSA in PBS: PGC-1α (Merck-Millipore); PGC-1β (Novus Biologicals, Littleton, CO); ERRα (Epitomics, Burlingame, CA); Glyceraldehyde 3-phosphate dehydrogenase (GAPDH; Sigma-Aldrich); Phospho-Akt (ser473), Akt, Phospho-p70S6k (thr389), and p70S6k (Cell Signalling Technology, Danvers, MA). All primary antibodies were diluted 1:1,000, except for GAPDH which was diluted 1:10,000. Antibodies for PGC-1α and PGC-1β were sensitive to both human and mouse, and therefore showed endogenous as well as overexpressed levels of these proteins. Following washing, the membranes were incubated for 1 hour with either IRDye® 800CW Goat Anti-Rabbit IgG (H+L) (LI-COR Biosciences, Lincoln NE), or Alexa Fluor® 680 Rabbit Anti-Mouse IgG (H+L) (Invitrogen), diluted 1:5,000 in PBS containing 50% Odyssey Blocking Buffer (LI-COR Biosciences). Proteins were visualised on an Odyssey Infrared Imaging System (LI-COR Biosciences) and densitometry was achieved using Odyssey Application Software 3.0 (LI-COR Biosciences). All blots were normalised to GAPDH protein.

2.2.6 Protein synthesis

Protein synthesis was determined by measuring the incorporation of radio-labelled [^{3}H]-tyrosine (Perkin Elmer, Boston, MA) into the myotubes (modified from [254]). After adenoviral infections, myotubes were treated for 24 hours with or without 10 μM dexamethasone (DEX; Sigma-Aldrich) to induce catabolic stress [224]. During this time, myotubes were incubated in 1 μCi/ml of radio-labelled [^{3}H]-tyrosine and 2 mM L-tyrosine (Sigma-Aldrich). The use of excess non-radioactive tyrosine in the

medium gives an accurate indication of protein synthesis rates without alterations in the free intracellular tyrosine pool [255]. The reaction was stopped by washing the cells with cold phosphate buffered saline (PBS), and then 0.5 ml of cold 10% trichloroacetic acid (TCA; Sigma-Aldrich) was added to each well. After scraping, myotubes sat on ice for 1 hour to precipitate the protein, followed by centrifugation at 20,000 x g for 10 minutes. The supernatant was removed, and the precipitates were dissolved in 0.1 M NaOH/1% Triton X-100 (Sigma-Aldrich) overnight at room temperature. The samples were mixed with Ultima Gold scintillation liquid (Perkin Elmer) and myotube protein radioactivity was measured using a Wallac 1409 DSA liquid scintillation counter (Perkin Elmer) and expressed as counts per minute (CPM). Counts were normalised to total genomic DNA which was extracted using the Allprep DNA/RNA mini kit (Qiagen, Clifton Hill, VIC) as per the manufacturer's protocol. DNA was quantified using the NanoDrop 2000.

2.2.7 Myotube Diameter

Myotubes were visualised using an Olympus IX70 microscope (Olympus, Mt Waverly, VIC), and digital images were obtained using a DS-U3 microscope camera and NIS-Elements imaging software (Nikon Instruments Inc., Melville, NY). Approximately 10 myotubes from 10 different fields of view were analysed for myotube diameter from each of the different adenoviral infections. Three measurements along each myotube were made to allow for differences in diameter across the length of the myotube.

2.2.8 Statistics

Statistical analyses were performed using either a t-test or a two-way analysis of variance (ANOVA) (Prism, GraphPad Software, La Jolla, CA). Multiple t-tests were used for post-hoc analysis to determine differences between groups if significant interactions were found. The level of significance was set at $P < 0.05$ for paired t-test analysis, while a Bonferroni adjustment was used for the two-way ANOVA reducing the level of significance to $P < 0.0125$. All data is presented as mean ± standard error of the mean (SEM) and as fold-change relative to GFP control, unless otherwise stated.

2.3 Results

2.3.1 PGC-1α and PGC-1β adenovirus optimisation

To overexpress PGC-1α and PGC-1β in C2C12 myotubes, adenoviruses expressing the human PGC-1α (hPGC-1α) and PGC-1β (hPGC-1β) were used. A GFP adenovirus was used as the infection control. To determine the efficiency of the hPGC-1α and hPGC-1β adenoviruses, C2C12 myotubes were infected using a multiplicity of infection (MOI) of 50, 100 and 200. PGC-1α and PGC-1β mRNA levels increased as the MOI was increased from between MOI 50 to MOI 100; no further increase in mRNA levels was observed when increasing the MOI from 100 to 200 (Figure 2.01A&B). PGC-1α and PGC-1β mRNA expression levels could not be compared to the GFP infected group as the adenovirus encoded the human PGC-1α and PGC-1β, which is not endogenously expressed in mouse cell lines. Therefore, the expression of COX IV mRNA was measured as it is known to be induced by both PGC-1α and PGC-1β [159, 171]. Figure 2.01C shows that hPGC-1α and hPGC-1β infection led to increases in COX IV mRNA expression, with no differences between MOIs for each virus. An MOI of 100 was therefore chosen to be used for all remaining experiments. Using an MOI of 100, PGC-1α and PGC-1β overexpression lead to a 2.2-fold and 2.6-fold increase in PGC-1α (Figure 2.01D) and PGC-1β (Figure 2.01E) protein levels, respectively.

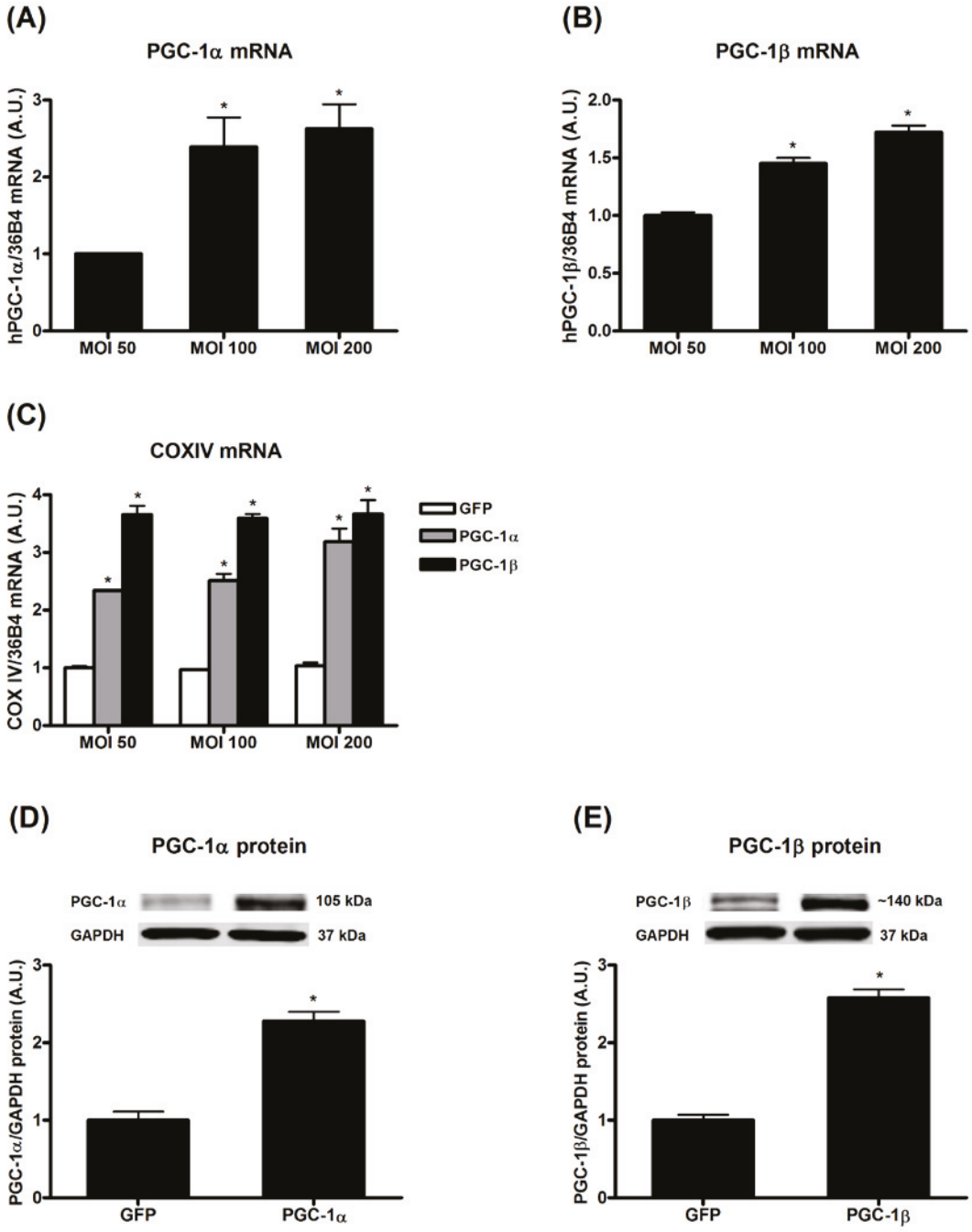

Figure 2.01 PGC-1α and PGC-1β overexpression in C2C12 myotubes. (A) Human PGC-1α and (B) human PGC-1β expression when measured 48 hours after infection, using a multiplicity of infection (MOI) of 50, 100 and 200. Values were normalised to 36B4 mRNA expression. $n = 3$ per group. *$P <$ 0.01 compared to MOI 50. (C) COX IV mRNA expression in GFP, PGC-1α and PGC-1β infected C2C12 myotubes using an MOI of 50, 100 and 200 for 48 hours. Values were normalised to 36B4 mRNA expression. $n = 4$ per group. *$P < 0.0125$ compared to GFP for each MOI. (D) PGC-1α and (E) PGC-1β protein levels when measured 48 hours after infection, using an MOI of 100. Bands were normalised to GAPDH protein. $n = 4$ per group. *$P < 0.01$, compared to GFP.

2.3.2 PGC-1α and PGC-β increase protein synthesis and myotube diameter in C2C12 myotubes.

To investigate the effect of PGC-1α and PGC-1β overexpression on protein synthesis, the incorporation of [^{3}H]-tyrosine was measured over 24 hours following adenovirus infections. Protein synthesis was measured under basal conditions, or with dexamethasone (DEX) to induce catabolic stress [224]. Overexpression of PGC-1α and PGC-1β increased the basal rate of protein synthesis by 21% and 23% respectively when compared to GFP (Figure 2.02). DEX treatment decreased basal protein synthesis by 14% (Figure 2.02). DEX decreased protein synthesis in the myotubes overexpressed with PGC-1α and PGC-1β. However, PGC-1α or PGC-1β still increased protein synthesis when compared to GFP-DEX, and therefore PGC-1α and PGC-1β can increase protein synthesis under catabolic conditions.

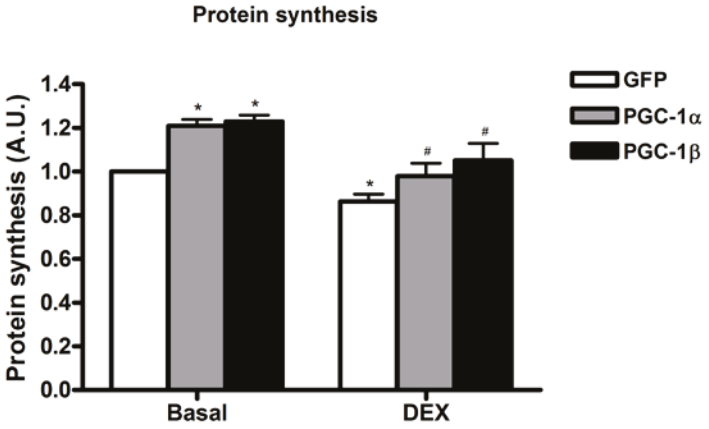

Figure 2.02 Protein synthesis in GFP, PGC-1α and PGC-1β infected myotubes. Shows protein synthesis rates under basal and DEX-treated conditions, when measured for 24 hours following 48 hours of infection with GFP, hPGC-1α and hPGC-1β adenoviruses. n = 5-10 per group, repeated in 3 experiments. *$P < 0.0125$, compared to GFP-Basal; $^{\#}P < 0.0125$, compared to GFP-DEX.

Overexpression of PGC-1α and PGC-1β increased myotube diameter by 38% and 52% respectively (Figure 2.03A).

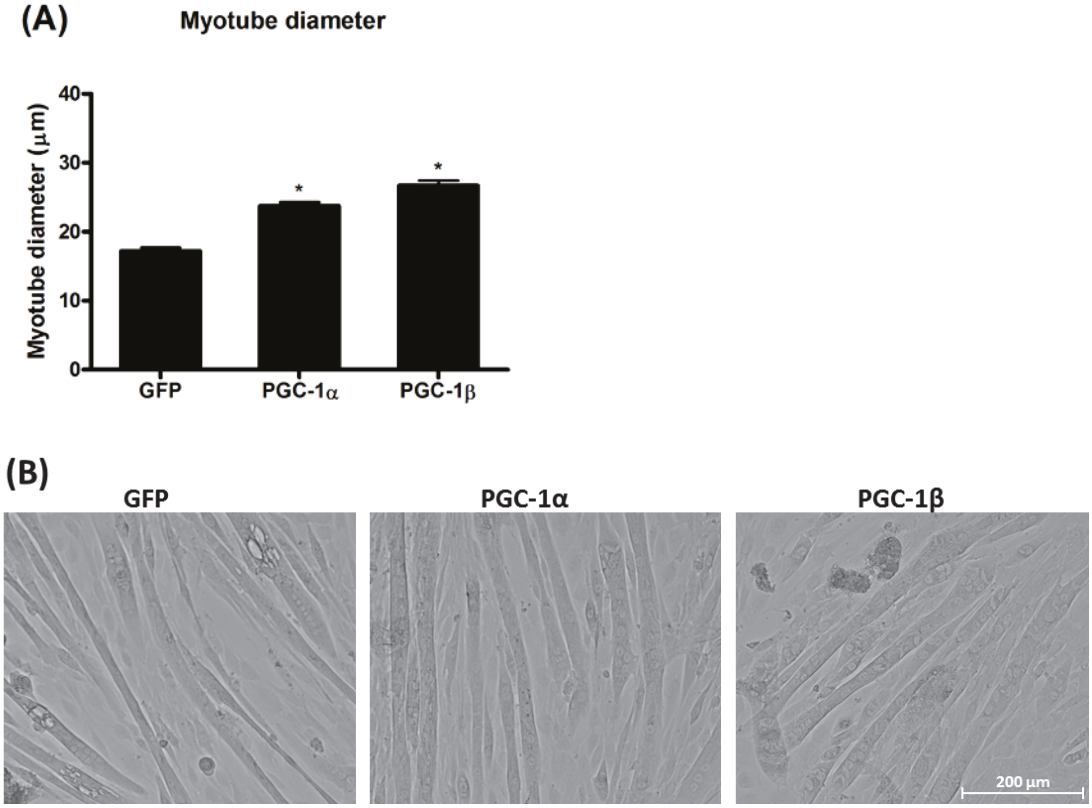

Figure 2.03 Myotube diameter in GFP, PGC-1α and PGC-1β infected myotubes. (A) Average myotube diameter from 10 myotubes per visual field (10 visual fields for each group). (B) Representative images of myotubes infected with GFP, hPGC-1α and hPGC-1β adenoviruses for 72 hours. **P* < 0.0125, compared to GFP.

2.3.3 PGC-1α and PGC-1β regulate protein synthesis independently of Akt/mTOR signalling.

To investigate whether the Akt/mTOR pathway is regulated by PGC-1α or PGC-1β, the expression of key proteins in this pathway were measured via Western blot analysis. Figure 2.04 shows the protein expression of phosphorylated-Akt (ser473), total Akt protein, phosphorylated-p70S6k (thr389), and total p70S6k protein. Overexpression of PGC-1α and PGC-1β led to a decrease in the phosphorylation of Akt (Figure 2.04A) and p70S6k (Figure 2.04C). There was also a small decrease in total Akt protein with PGC-1α overexpression (Figure 2.04B), and p70S6k protein with PGC-1β overexpression (Figure 2.04D).

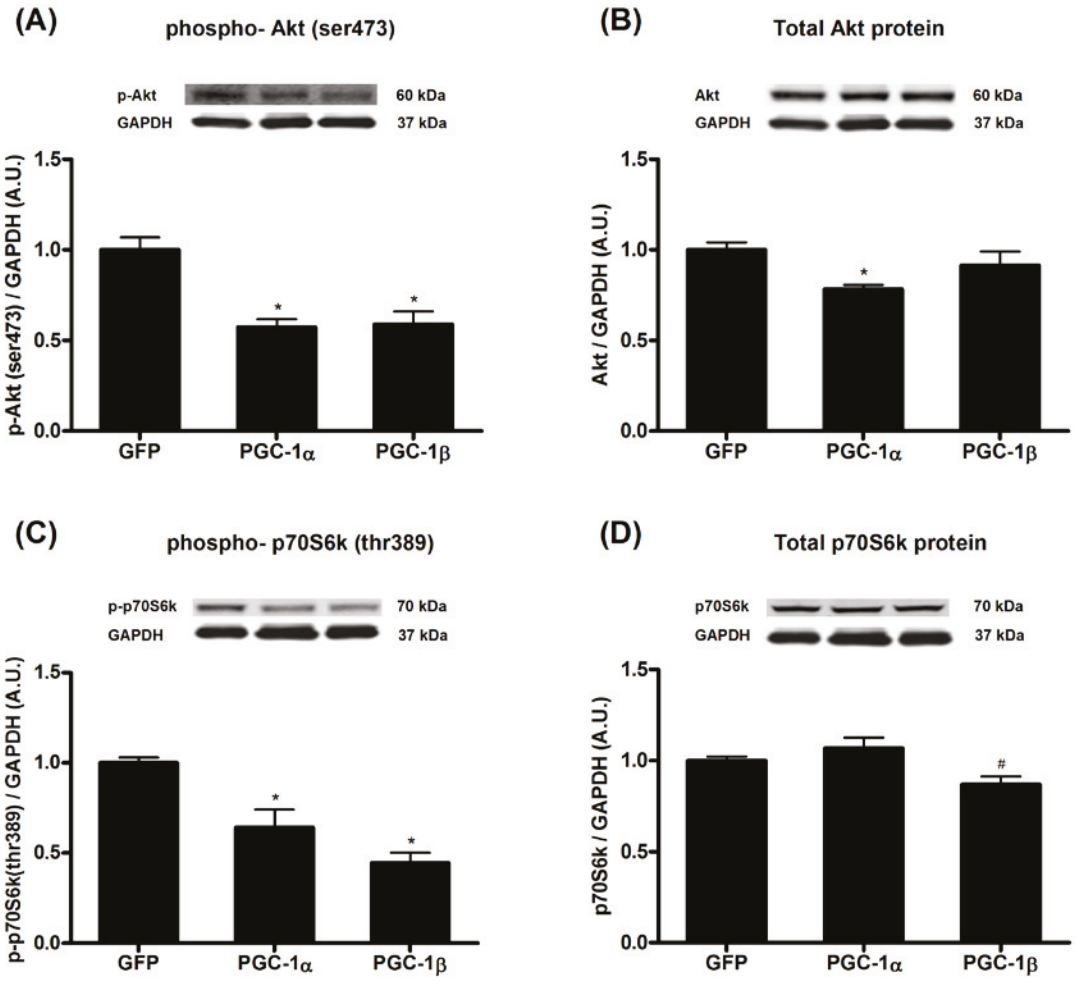

Figure 2.04 Western blot analysis of Akt/mTOR pathway proteins in GFP, PGC-1α and PGC-1β infected C2C12 myotubes. (A) phospho-Akt (ser473), (B) total Akt protein, (C) phospho-p70S6k (thr389), and (D) total p70S6k protein expression. Samples were harvested after 72 hours of infection. Bands were normalised to GAPDH protein. $n = 5$ per group. $^{*}P < 0.01$, $^{\#}P < 0.05$, compared to GFP.

To further investigate whether Akt/mTOR signalling is involved in the PGC-1α- and PGC-1β-induced stimulation of protein synthesis, myotubes were treated with a PI3K inhibitor, LY294002, or an mTOR inhibitor, rapamycin. Figure 2.05 shows that when compared to the basal group, treatment with LY294002 and rapamycin decreased protein synthesis by 18-20 % and 35-43 % respectively, in the GFP, PGC-1α- and PGC-1β-infected myotubes. The per cent increase due to PGC-1α and PGC-1β was not changed. These results show that both PGC-1α and PGC-1β increase protein synthesis independently of Akt/mTOR signalling.

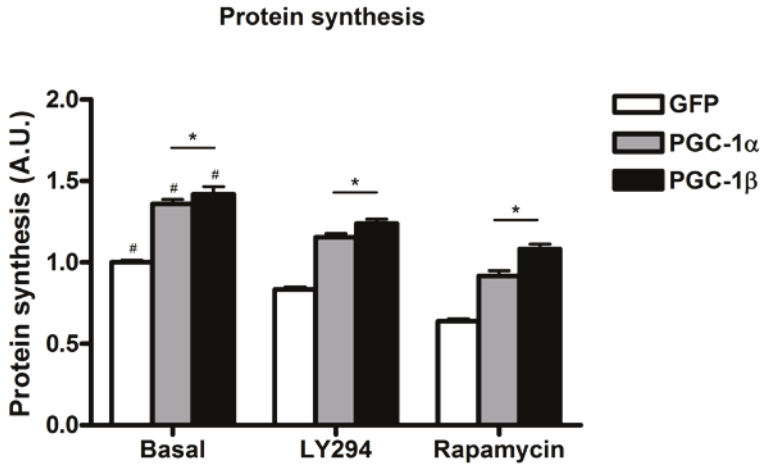

Figure 2.05. Protein synthesis in GFP, PGC-1α and PGC-1β infected C2C12 myotubes. Myotubes were treated with LY294002 (LY294) or Rapamycin and compared to basal conditions. n = 10, repeated in 3 experiments. $^{\#}P < 0.0125$ when compared to LY294 or Rapamycin treatment for the same infection group. $*P < 0.0125$ when compared to GFP within each treatment group.

2.3.4 ERRα is involved in the PGC-1α- and PGC-1β-induced increase in protein synthesis.

To determine if ERRα is involved in the PGC-1α- and PGC-1β-induced increase in protein synthesis, C2C12 myotubes were infected with an adenovirus expressing siRNA for ERRα (siERRα) or a control siRNA vector (siSUPER). To determine the efficiency of siERRα infection, myotubes were infected using a multiplicity of infection (MOI) of 50, 100 and 200. Figure 2.06 shows that infection with siERRα lead to a 51%, 62%, and 72% decrease in ERRα mRNA expression for MOIs of 50, 100 and 200 respectively, when compared to siSUPER. An MOI of 200 was used for all remaining experiments as described previously [155, 172, 253].

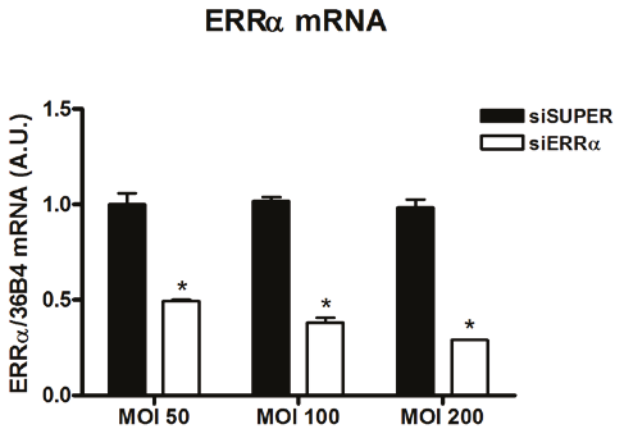

Figure 2.06 ERRα mRNA in C2C12 myotubes infected with siERRα. mRNA was measured 48 hours after infection, using a multiplicity of infection (MOI) of 50, 100 and 200. siSUPER was used as a control. Values were normalised to 36B4 mRNA expression. $n = 3$ per group. $*P < 0.01$ compared to siSUPER for each MOI.

Next, myotubes were infected with either siERRα or siSUPER, followed by infection with GFP, PGC-1α or PGC-1β adenoviruses. As expected [100, 190], PGC-1α and PGC-1β overexpression lead to a significant increase in ERRα mRNA (Figure 2.07A) and protein expression (Figure 2.07B). Infection with siERRα decreased ERRα mRNA and protein by 70% and 87% respectively, when compared to siSUPER. Furthermore, knockdown of ERRα prevented the increase in ERRα mRNA expression that was seen with PGC-1α and PGC-1β overexpression. Figures 2.08A and B show protein expression for PGC-1α and PGC-1β respectively, to confirm their overexpression in these samples. PGC-1α expression was increased in

both the siSUPER and siERRα groups when compared to GFP (Figure 2.08A). PGC-1β expression was also increased in both groups, however it was lower in the PGC-1β-siERRα group when compared to the PGC-1β-siSUPER group (Figure 2.08B).

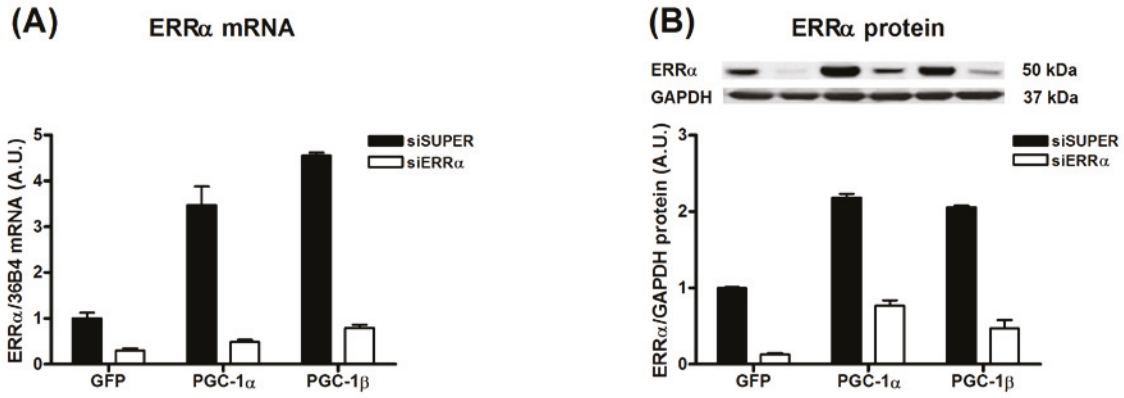

Figure 2.07 ERRα expression in C2C12 myotubes infected with siERRα and PGC-1 adenoviruses. Myotubes were infected with either siSUPER or siERRα at an MOI of 200, followed by infection with GFP, hPGC-1α or hPGC-1β. Samples were harvested after 72 hours. (A) ERRα mRNA expression, normalised to 36B4. (B) ERRα protein expression, normalised to GAPDH. $n = 4$ per group.

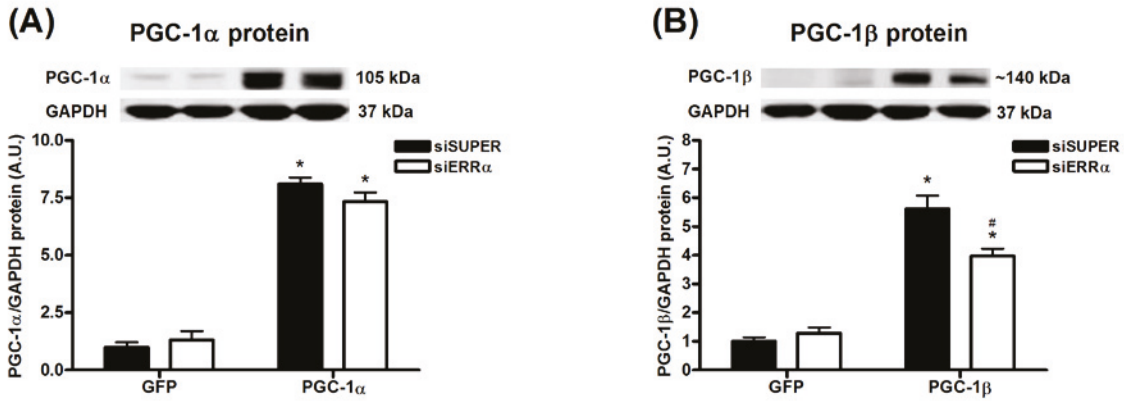

Figure 2.08 PGC-1α and PGC-1β protein expression in C2C12 myotubes infected with siERRα and PGC-1 adenoviruses. Myotubes were infected with either siSUPER or siERRα, followed by infection with GFP, hPGC-1α or hPGC-1β. Samples were harvested after 72 hours. (A) PGC-1α protein, and (B) PGC-1β protein. Bands were normalised to GAPDH protein. $n = 4$ per group. $^{*}P < 0.0125$ compared to GFP-siSUPER; $^{\#}P < 0.0125$ compared to PGC-1β-siSUPER.

Overexpression of PGC-1α and PGC-1β increased protein synthesis under basal conditions (Figure 2.09A). Knockdown of ERRα had no effect on protein synthesis in the GFP-infected group. However, when overexpressed with PGC-1α or PGC-1β, knockdown of ERRα attenuated the PGC-1α- and PGC-1β-induced increase in protein synthesis. Similarly, knockdown of ERRα did not affect myotube diameter in the GFP-infected myotubes but reduced the PGC-1α- and PGC-1β-induced increase in myotube diameter (Figure 2.09B & C).

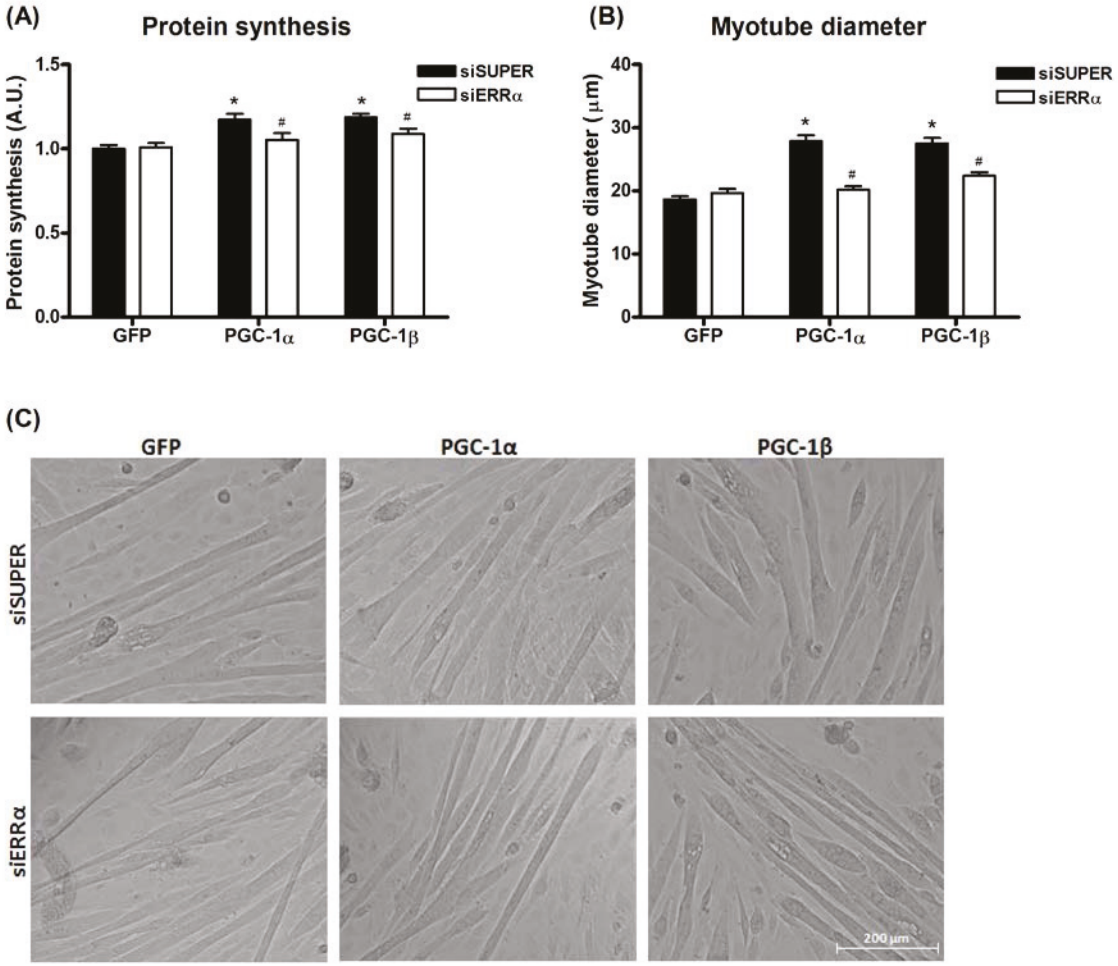

Figure 2.09 Protein synthesis and myotube diameter in C2C12 myotubes infected with siERRα and PGC-1 adenoviruses. Myotubes were infected with either siSUPER or siERRα, followed by infection with GFP, hPGC-1α or hPGC-1β. (A) Protein synthesis, measured via [^{3}H]-tyrosine incorporation during the 24 hours after infections. n = 6 per group, repeated in 3 experiments. (B) Average myotube diameter from 10 myotubes per visual field (10 visual fields for each group). (C) Representative images of GFP-, PGC-1α- and PGC-1β-infected myotubes, with siSUPER or siERRα. *P < 0.0125 compared to GFP-siSUPER. $^{\#}P$ < 0.0125 compared to siSUPER for each group.

As it was shown that PGC-1α and PGC-1β reduce the activity of the Akt/mTOR signalling pathway, Akt and p70S6k were also measured in these samples to see if knockdown of ERRα affected these results. Figure 2.10A shows that knockdown of ERRα increased the phosphorylation of Akt in the GFP and PGC-1α, but not the PGC-1β-infected myotubes when compared to the siSUPER control. There were no significant changes in the total Akt protein (Figure 2.10B), phosphorylated p70S6k (Figure 2.10C), or total p70S6k protein (Figure 2.10D).

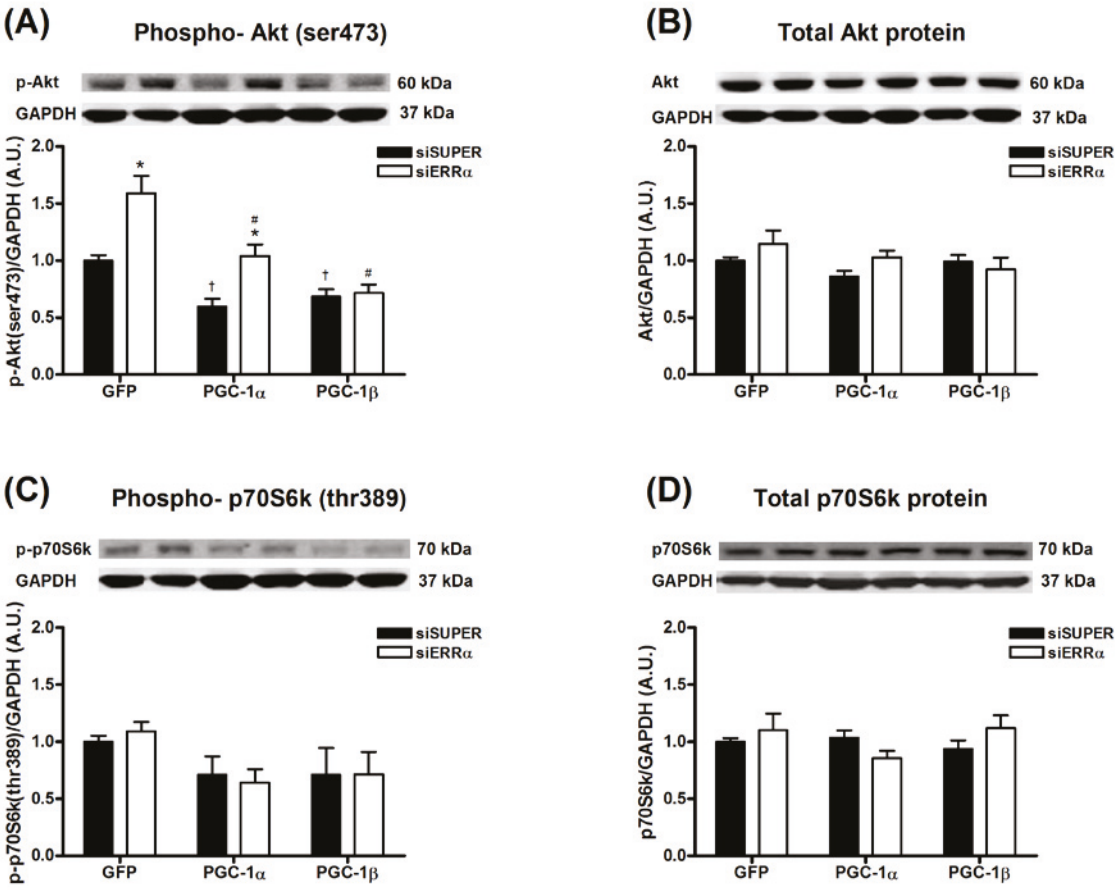

Figure 2.10 Western blot analysis of Akt/mTOR pathway proteins in C2C12 myotubes infected with siERRα and PGC-1 adenoviruses. Myotubes were infected with either siSUPER or siERRα, and after 24 hours infected with GFP, hPGC-1α or hPGC-1β. (A) phospho-Akt (ser473), (B) total Akt protein, (C) phospho-p70S6k (thr389), and (D) total p70S6k protein expression. Bands were normalised to GAPDH protein. n = 6 per group. *$P < 0.0125$ compared to siSUPER for each group; $^{\#}P < 0.0125$ compared to GFP-siERRα; † $P < 0.05$ when compared to GFP-siSUPER.

2.3.5 Constitutively active ERRα increases protein synthesis and myotube diameter.

The previous results show that ERRα may regulate protein synthesis when activated by PGC-1α or PGC-1β, but had no effect under basal conditions. To further support the role ERRα in increasing protein synthesis, C2C12 myotubes were expressed with a constitutively active form of ERRα (VP16-ERRα), or its control (VP16-control) [160]. Figure 2.11A shows ERRα mRNA levels after infection with VP16-ERRα using an MOI of 50, 100 and 200. ERRα mRNA was increased by approximately 53-, 91- and 103- fold respectively. An MOI of 100 was chosen for remaining experiments. Figure 2.11B shows that infection with VP16-ERRα at an MOI of 100 increased ERRα protein levels by approximately 4.5-fold.

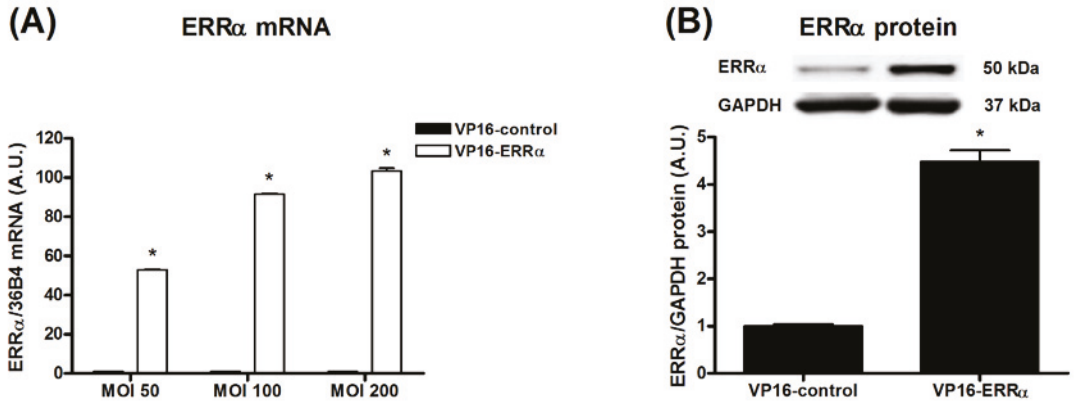

Figure 2.11 ERRα mRNA and protein in C2C12 myotubes infected with VP16-ERRα and VP16-control adenoviruses. (A) ERRα mRNA levels after infection with VP16-ERRα adenovirus using MOIs of 50, 100 and 200. VP16-control was used as the control adenovirus. Samples were harvested after 48 hours. Values were normalised to 36B4 expression. $n = 3$ per group.*$P < 0.0125$ compared to VP16-control. (B) ERRα protein expression using an MOI of 100 for 48 hours. Bands were normalised to GAPDH protein. $n = 3$ per group. *$P < 0.01$ compared to VP16-control.

VP16-ERRα infection increased the rate of protein synthesis by 52% compared to the VP16-control (Figure 2.12A), which also resulted in an increase in myotube diameter (Figure 2.12B & C).

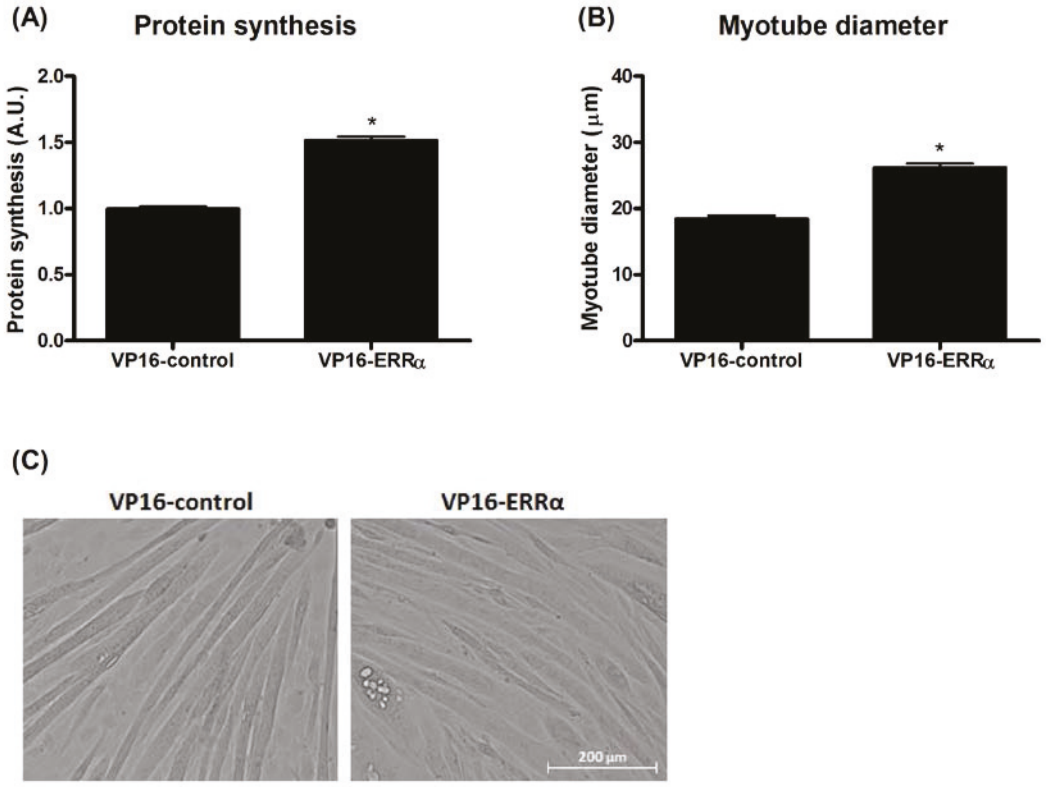

Figure 2.12 Protein synthesis and myotube diameter in C2C12 myotubes infected with VP16-ERRα and VP16-control adenovirus. (A) Protein synthesis, measured by [^{3}H]-tyrosine incorporation for 24 hours following adenovirus infection. n = 6 per group, repeated in 3 experiments. (B) Average myotube diameter from 10 myotubes per visual field (10 visual fields for each group). (C) Representative images of myotubes infected with VP16-control or VP16-ERRα for 72 hours. *P < 0.01 compared to VP16-control.

Lastly, as it was shown that PGC-1α and PGC-1β overexpression reduces the activity of the Akt/mTOR signalling pathway, these proteins were also measured in samples infected with VP16-ERRα. Figure 2.13 shows that expression of a constitutively active ERRα decreased phosphorylated Akt (Figure 2.13A) and p70S6k (Figure 2.13C) in C2C12 myotubes by 78% and 82% respectively. Furthermore, total Akt (Figure 2.13B) and p70S6k (Figure 2.13D) protein levels were reduced by 42% and 47% respectively.

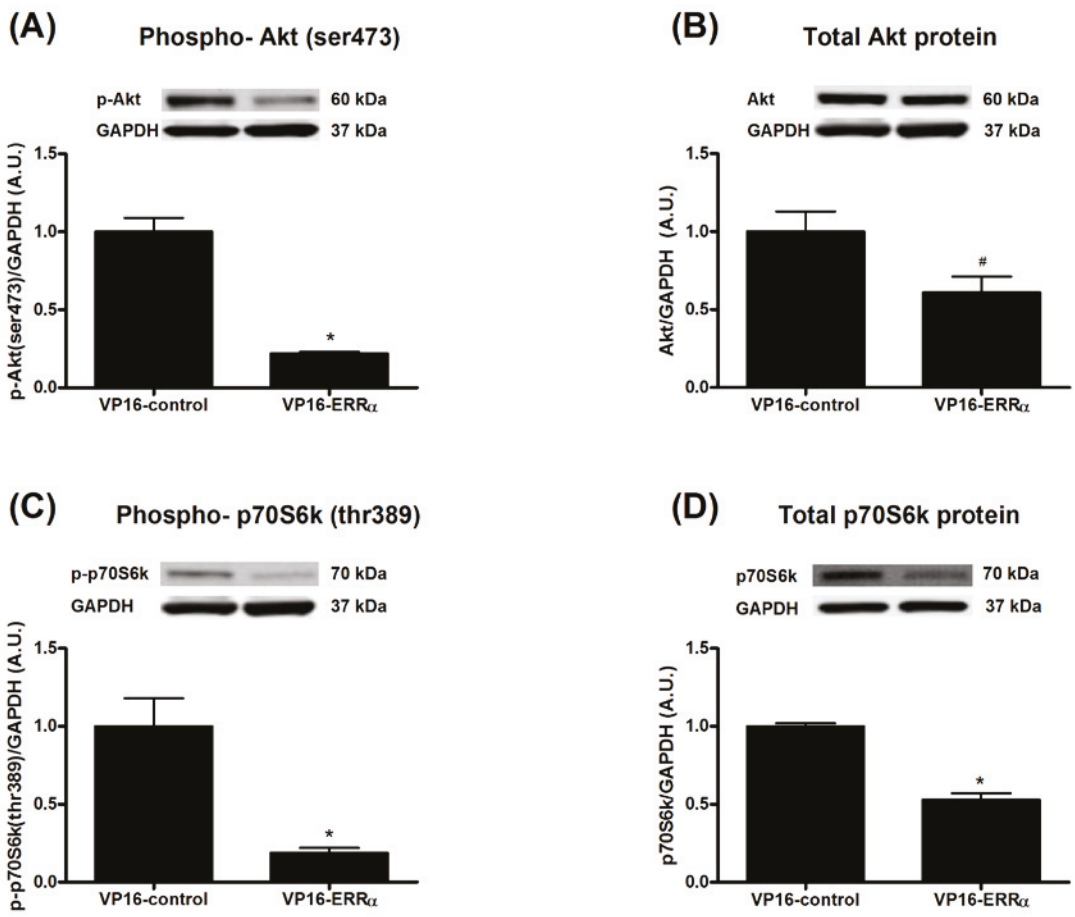

Figure 2.13 Western blot analysis of Akt/mTOR pathway proteins in C2C12 myotubes infected with VP16-ERRα. (A) phospho-Akt (ser473), (B) total Akt protein, (C) phospho-p70S6k (thr389), and (D) total p70S6k protein expression. Bands were normalised to GAPDH protein. n = 6 per group. *P < 0.01, #P < 0.05, compared to VP16-control.

2.4 Discussion

Understanding the molecular mechanisms that regulate protein synthesis in skeletal muscle is essential for developing therapeutic interventions to combat muscle atrophy during diseases characterised by perturbed skeletal muscle growth. The transcriptional coactivators, PGC-1α and PGC-1β, regulate the expression of a wide range of genes in skeletal muscle including those involved in oxidative metabolism and protein degradation [96, 219]. This study aimed to determine whether PGC-1α and PGC-1β can regulate protein synthesis in mouse C2C12 myotubes. Several novel observations were made. Firstly, it was shown that overexpression of PGC-1α or PGC-1β led to an increase in the rate of protein synthesis and myotube hypertrophy. Secondly, this increase in protein synthesis was independent of Akt and mTOR signalling. And lastly, the PGC-1α- and PGC-1β-induced increase in protein synthesis and myotube hypertrophy was dependent on ERRα.

PGC-1α and PGC-1β are down-regulated in many models of muscle atrophy; a process characterised by increased protein degradation and decreased protein synthesis. Several studies have shown that overexpression of PGC-1α and/or PGC-1β in rodents can protect from muscle atrophy in many catabolic states including sarcopenia [148], DMD [191, 256], denervation and fasting-induced atrophy [153, 219]. Using a similar cell culture model to the current study, Brault *et al*. observed that this protective effect of PGC-1α and PGC-1β is via a decrease in protein degradation, with no effect on protein synthesis [219]. However the results from the present study show that overexpression of PGC-1α and PGC-1β can increase the rate of protein synthesis under basal and catabolic conditions induced by dexamethasone treatment; the latter suggesting that PGC-1α and PGC-1β may be attractive targets to increase protein synthesis during systemic wasting diseases. Several methodological differences may have contributed to these different observations between studies. Firstly, Brault *et al*. measured protein synthesis after 24 and 48 hours infection with PGC-1α- and PGC-1β- overexpressing adenoviruses for two hours only, while the present study measured protein synthesis over a 24 hour period from 48-72 hours after infection. The effect of PGC-1α and PGC-1β overexpression on protein synthesis may therefore be time-dependent. Furthermore, Brault et al. measured

citrate synthase activity, a marker of mitochondrial content, as a measure of PGC-1α and PGC-1β activity. The greatest increase in citrate synthase activity occurred from 48-62 hours post-infection and it is therefore likely that a PGC-1α and PGC-1β effect on protein synthesis would have also occurred during this time. Another difference between the studies was the methodology used to measure protein synthesis. Brault *et al.* normalised [^{3}H]-tyrosine incorporation to protein content in the myotubes. As an increase in protein synthesis would be expected to increase total protein content, normalising to protein content would potentially negate the increase in protein synthesis. The present study normalised protein synthesis levels to DNA content which was unchanged in mature myotubes, a method previously used by Quinn *et al*. [257]. Therefore using the current methodology, this study has clearly shown that overexpression of PGC-1α or PGC-1β leads to an increase in protein synthesis and myotube diameter in C2C12 myotubes, when measured 48-72 hours post adenoviral infection.

The Akt and mTOR signalling pathways are well known regulators of protein synthesis in skeletal muscle [31]. It was therefore of interest to determine if the effect of PGC-1α and PGC-1β on protein synthesis was via the Akt and/or mTOR signalling pathways. After 72 hours, overexpression of PGC-1α and PGC-1β decreased the phosphorylation of Akt and p70S6k, the latter phosphorylated and activated by mTOR. This is in contrast to findings by Wende *et al*., whereby the transgenic expression of PGC-1α increased the phosphorylation of Akt and mTOR and protected from skeletal muscle atrophy of aged mice [148]. Whether this was associated with an increase in protein synthesis however, was not determined. As Akt and p70S6k phosphorylation was only measured after 72 hours, it may be possible that their phosphorylation was increased at an earlier time point following PGC-1α or PGC-1β overexpression. In fact, the phosphorylation of Akt and p70S6k are increased acutely following resistance exercise in trained subjects, but return to baseline within 4 hours although protein synthesis rates remain elevated [258]. The effect of PGC-1α and PGC-1β on protein synthesis in the present study may therefore be due to the long-lasting effects of the acute activation of these signalling pathways. To test this hypothesis, myotubes were treated with LY294002 and rapamycin to inhibit PI3K (Akt) and mTOR respectively. Although these inhibitors

decreased the overall rate of protein synthesis in all adenovirus treatment groups (GFP, PGC-1α and PGC-1β), overexpression of PGC-1α or PGC-1β still increased protein synthesis rates above the GFP-infected myotubes. These findings show that PGC-1α and PGC-1β regulate protein synthesis in C2C12 myotubes independently of Akt and mTOR signalling pathways.

As many of the effects of PGC-1α and PGC-1β in skeletal muscle involved the orphan nuclear receptor, ERRα, it was of interest to determine if PGC-1α and PGC-1β regulate protein synthesis via ERRα. This study shows that knockdown of ERRα using siRNA prevents the PGC-1α- and PGC-1β-induced increase in protein synthesis and myotube hypertrophy. However, there was no effect on the basal rate of protein synthesis, and therefore ERRα may only be involved in the regulation of protein synthesis when stimulated by PGC-1α or PGC-1β. While ERRα plays an important role in the regulation of mitochondrial gene expression in response to cues such as exposure to cold or exercise, it has been suggested that it may not be essential for mitochondrial function under basal conditions [101]. This also appears to be the case for protein synthesis. Further supporting the role of ERRα, overexpression of a constitutively active ERRα (VP16-ERRα) increased protein synthesis by over 50%. These results show that when activated, ERRα itself can increase protein synthesis and myotube hypertrophy, suggesting that the transcription of genes by ERRα may be crucial for PGC-1α and PGC-1β to increase protein synthesis. The identification of new genes regulated by PGC-1α/ERRα and PGC-1β/ERRα may therefore elucidate potential mechanisms by which PGC-1α and PGC-1β regulate protein synthesis. Lastly, this study also shows that PGC-1α/ERRα and PGC-1β/ERRα may negatively regulate the Akt and mTOR signalling pathways. While the functional significance of this is unknown, these observations demonstrate that the PGC-1α- and PGC-1β-induced increase in protein synthesis is independent from Akt/mTOR signalling.

Recent work published during the preparation of this thesis has shown that a specific isoform of PGC-1α, PGC-1α4, leads to muscle hypertrophy via the induction of insulin-like growth factor-1 (IGF-1) and repression of myostatin [259], which are positive and negative regulators of protein synthesis respectively [260, 261]. These observations support the present findings that, at least for the alpha isoform, PGC-1

can regulate protein synthesis and therefore skeletal muscle growth. However, the induction of IGF-1 would suggest increased Akt activity, which is the opposite of what was observed in this study. PGC-1α4 also did not regulate many mitochondrial genes that are known to be regulated by PGC-1α, and its effect on muscle hypertrophy was actually independent of ERRα activity. Therefore, although PGC-1α4 also appears to have positive effects on skeletal muscle growth, it is likely that these effects are via a distinct mechanism to which PGC-1α regulates protein synthesis in the current study.

Lastly, it is important to note that while myotube diameter was increased in the current study, there are several limitations to this method which cannot be overlooked. Although myotube diameter was assessed from multiple measurements along the length of the myotube, this technique assumes that all myotubes are cylindrical, which is often not the case when these cells are grown *in vitro* [262]. Many myotubes are also branched and there is a large variability in myotube sizes, even within the same field of view. Furthermore, myotubes often extend in length beyond the field of view, and therefore only a segment of the myotube is measured. These factors need to be taken into consideration when interpreting this data. The increase in myotube diameter seen in the current study can also not be solely attributed to the increase in protein synthesis. As PGC-1α and PGC-1β also attenuate protein degradation in C2C12 myotubes [219], an increase in myotube diameter could be a result of both increased protein synthesis and reduced protein degradation.

In conclusion, this study has shown for the first time that the transcriptional coactivators, PGC-1α and PGC-1β, can increase protein synthesis and myotube hypertrophy in C2C12 myotubes. This effect was independent from the Akt and mTOR signalling pathways, but dependent on ERRα. Therefore PGC-1α and PGC-1β, in conjunction with ERRα, may increase protein synthesis by regulating the expression of one or several genes/proteins in skeletal muscle. These genes and proteins are yet to be identified, and future studies identifying further downstream transcriptional targets of PGC-1α/ERRα and PGC-1β/ERRα will improve the current knowledge of how PGC-1α and PGC-1β increase protein synthesis in C2C12 myotubes and potentially mature skeletal muscle.

Chapter 3

Identification of Genes and Proteins Regulated by PGC-1α and PGC-1β in C2C12 Myotubes

3.1 Introduction

Understanding the molecular regulation of protein synthesis in skeletal muscle is essential for developing therapeutic interventions aimed at increasing muscle growth, or preventing skeletal muscle atrophy, during conditions characterised by perturbed skeletal muscle function. In Chapter two, it was established that the transcriptional coactivators, PGC-1α and PGC-1β, can increase protein synthesis in mouse C2C12 myotubes. This effect was independent from the well-known positive regulators of skeletal muscle protein synthesis, Akt and mTOR [39, 47], but was dependent on the transcription factor ERRα. The PGC-1α/ERRα and PGC-1β/ERRα transcriptional pathways are known to regulate the expression of many genes and proteins involved in skeletal muscle mitochondrial biogenesis and oxidative phosphorylation [160, 172, 190]. However, the downstream targets that are regulated by PGC-1α and PGC-1β that may be involved in protein synthesis have not been identified.

High throughput gene and protein screening using microarray and iTRAQ (Isobaric Tags for Relative and Absolute Quantification) techniques respectively, are appropriate tools to detect differentially expressed genes and proteins in response to disease or following experimental manipulation [85, 263, 264]. Bioinformatics analysis of this data, such as Gene Set Enrichment Analysis (GSEA), ranks gene and protein expression data into pathways of biological significance. This method focuses on groups of genes that share a common biological function, rather than single gene analysis, and is considered a powerful method to interpret global gene and protein expression data [265]. GSEA involves the identification of Gene Ontology (GO) terms to categorise gene targets based on their cellular component, molecular function or biological process; and pathway mapping (Kyoto Encyclopaedia of Genes and Genomes; KEGG) to identify biological pathways that may be differentially regulated [266]. GSEA has previously identified several genes

that are down-regulated in diabetic skeletal muscle, are up-regulated following PGC-1α overexpression in C2C12 myotubes [157]. Using this technique may provide insight into the PGC-1α- and PGC-1β-controlled biological functions that increase protein synthesis in C2C12 myotubes.

Data generated from microarray analysis can also be used to create novel gene expression signatures (GES). A GES generally represents a small subset of genes, identified via non-biased statistical analysis, that are most consistently regulated in a microarray. Application of a GES has identified a set of genes that best predict survival in breast cancer [264], as well as a set of genes related to reduced mitochondrial content and neuromuscular junctions in sarcopenic rat skeletal muscle [85]. Combining analytical and bioinformatics approaches such as a GES and GSEA may be an effective strategy to identify genes and proteins regulated by PGC-1α and PGC-1β, which regulate protein turnover in C2C12 myotubes.

The primary aim of this study was to identify the global gene and protein expression changes that occur in response to PGC-1α and PGC-1β overexpression in C2C12 myotubes, and identify the potential functional and biological significance of these changes by GSEA. A secondary aim was to create a GES to represent the most consistent transcriptional changes in response to PGC-1α and PGC-1β overexpression. Lastly, it was of interest to measure the genes identified in the GES, as well as other highly regulated genes, in human models known to show increased or decreased rates of protein synthesis. Together, these experimental approaches will significantly add to the understanding of the gene transcription and protein signalling pathways that are regulated by PGC-1α and PGC-1β in skeletal muscle.

3.2 Methods

3.2.1 Cell Culture

C2C12

Mouse C2C12 myoblasts (American type culture collection; ATCC, Manassas, VA) were incubated at 37°C with 5% CO_2, in high-glucose Dulbecco's Modified Eagle Medium (DMEM) supplemented with 10% FBS, 100 U/ml penicillin and 100 µg/ml streptomycin (Invitrogen, Carlsbad, CA). Myoblasts were plated at a density of 1.5 x $10^4/cm^2$ in 6 and 12-well plates. Upon confluence (~48 hrs), medium was changed to high-glucose DMEM supplemented with 2% HS (Invitrogen), 100 U/ml penicillin and 100 µg/ml streptomycin for 4-5 days until multinucleated myotubes had formed. Medium was changed every 48 hours.

Adenoviral Infections

Myotubes were infected with adenoviruses expressing GFP, hPGC-1α or hPGC-1β using an MOI 100. Medium was changed after 48 hours and cells were harvested after 72 hours for RNA and protein.

3.2.2 RNA extraction

RNA was extracted using Tri-Reagent solution (Ambion Inc., Austin, TX) according to manufacturer's protocol. RNA concentrations were determined using the NanoDrop 2000 (NanoDrop products, Wilmington, DE). Following extraction, RNA was treated with 1 unit/µg of DNase I (Invitrogen) and incubated at 37ºC for 30 min to remove any DNA contamination of the samples. For the microarray, 2 µg of RNA was sent to the Australian Genomic Research Facility (AGRF; Parkville, VIC) for further analysis. For qPCR, 1 µg of RNA was reverse transcribed to complementary DNA (cDNA) using a High Capacity cDNA reverse transcription kit (Applied Biosystems, Forster City, CA) according to manufacturer's protocol. The cDNA was diluted to 5 ng/µl in nuclease free water (NFW).

3.2.3 Protein extraction

Myotubes were lysed in RIPA buffer (Merck-Millipore, Kilsyth, VIC) with 1 µL/mL protease inhibitor cocktail (Sigma-Aldrich) and 10 µL/mL Halt Phosphatase

Inhibitor Single-Use Cocktail (Thermo scientific, Rockford, IL). Protein concentrations were determined using the bicinchoninic acid (BCA) Protein Assay Kit (Pierce Biotechnology, Rockford, IL) according to the manufacturer's protocol, and absorbance was measured at 562 nm on a Synergy 2 Microplate Reader (BioTek, Winooski, VT). Approximately 100 μg of protein for each sample was sent to Proteomics International (Nedlands, WA) for analysis.

3.2.4 DNA microarray

The DNA microarray, data transformation and ANOVA analyses were performed by the AGRF (Parkville, VIC). The quality and quantity of the RNA extracted from the C2C12 myotubes overexpressed with GFP, PGC-1α and PGC-1β (a total of 6 samples per treatment) were determined initially with the Agilent Bioanalyzer and RNA 600 Nano Assay kit (Agilent Technologies, Paolo Alto, CA). A total of 500 ng of RNA was labelled using the Total Prep RNA amplification kit (Ambion). Labelled cRNA (0.05 μg/μl) was then combined with the GEX-HYB Hybridisation Buffer in a 30 μl final volume and hybridized to the Illumina Mouse-6v2 Expression Beadchip (Illumina Inc., San Diego, CA) overnight at 58^{o}C for 16 hours. The chips were washed as outlined in the Illumina manual, coupled with Cy3, and scanned in the Illumina iScan Reader using GenomeStudio software (Illumina Inc.). Raw signal intensity values were subjected to variance stabilisation transformation including background correction, log2 transformation and variance stabilisation using the lumiR package of R Bioconductor (www.Bioconductor.org) [267, 268]. ANOVA of normalised Illumina probe intensity values was performed using Partek® Genomic SuiteTM software, version 6.6 (Partek Inc., St. Louis, MO). Pairwise comparison of sample groups was performed using ANOVA. Differentially expressed genes were selected by a change in expression level over 50% (fold-change > ± 1.5) in compared groups, and "nominal" ANOVA p-value < 0.05.

3.2.5 Isobaric Tags for Relative and Absolute Quantification (iTRAQ)

Sample preparation and Isobaric Tags for Relative and Absolute Quantification (iTRAQ) labelling and analyses were performed as described previously [269] by Proteomics International (Nedlands, WA). Briefly, protein samples were precipitated individually with acetone and resuspended in 0.5 M triethylammonium bicarbonate,

pH 8.5. Samples were then reduced, alkylated and trypsin-digested according to the iTRAQ protocol (Applied Biosystems). Peptides from uninfected myotubes as well as GFP-, PGC-1α- or PGC-1β- infected myotubes were labelled with iTRAQ reagents 114 (uninfected samples), 115 (GFP), 116 (PGC-1α) and 117 (PGC-1β). Labelled peptides were combined, desalted on a Strata-X 33µm polymeric reversed phase column (Phenomenex, Torrance, CA) and dissolved in 10% acetonitrile with 10 mM KH_2PO_4, pH 3.0. Samples were then separated by strong cation exchange liquid chromatography on a PolySulfoethyl column (4.6 x 100 mm, 5 µm, 300 Å) using an Agilent 1100 HPLC system (Agilent Technologies, Paolo Alto, CA). A 0-400 mM KCl gradient was used to elute fractions, which were desalted again before separation on a C18 PepMap100, 3 mm column (LC Packings-Dionex, Sunnyvale, CA) using an Ultimate 3000 nano HPLC system (Dionex). Peptide fractions were resolved on a 10-40% acetonitrile/0.1% trifluoroacetic acid gradient, spotted onto an AnchorChip MALDI plate using a ProBot robotic spotter (Dionex), and analysed on a 5800 MALDI TOF/TOD Analyser (AB Sciex, Foster City, CA). Peptide samples were identified and quantitated using ProteinPilot 4.0.8085 software (AB Sciex), and false discovery rate was estimated using reversed sequences. Sequences were searched against the Swissprot database (taxonomy = *mus musculus*). For each protein ratio (116 or 117 relative to 115), a p-value of < 0.05 was considered significant.

3.2.6 Analysis of microarray and iTRAQ data

Gene Set Enrichment Analysis (GSEA) of microarray and iTRAQ data

Following the identification of genes and proteins that were differentially regulated with overexpression of PGC-1α and PGC-1β, gene-set enrichment analyses (GSEA) was performed using Database for Annotation, Visualisation and Integrated Discovery (DAVID) v6.7 (http://david.abcc.ncifcrf.gov) [270, 271]. DAVID provides an unbiased approach to rank gene and protein expression data into pathways of biological significance by identifying groups of genes or proteins that are enriched and functionally related. Using DAVID, Gene Ontology (GO) and Kyoto Encyclopedia of Genes and Genomes (KEGG) pathway mapping was performed. GO categorisation uses a selection of defined terms representing gene product properties to group genes and/or proteins with their possible roles or

functions. These GO terms describe either a cellular component (CC), molecular function (MF) or a biological process (BP). KEGG pathway mapping uses molecular pathway maps for biological interpretation of higher-level systemic functions of large-scale data sets [266]. These include pathways involved in metabolism, genetic and environmental information processing, cellular processes, organisation systems and human diseases. From these analyses, GO terms and KEGG pathways were identified for PGC-1α and PGC-1β from both the microarray and iTRAQ data.

Gene expression signature (GES) from microarray data

To identify an optimal set of genes, called a gene expression signature (GES) [264], that reflects the overall state of the C2C12 myotubes following the overexpression of PGC-1α and PGC-1β, a combination of Diagonal Linear Discriminant Analysis (DLDA) and the Signal to Noise Ratio (SNR) statistics were used [272]. DLDA algorithm was used to generate gene sets that classified arrays into each treatment group. Using a Forward Step-Wise Variable Selection, sets of genes from the dataset with optimal predictive power were identified and ranked according to their SNR statistic. To eliminate genes that were co-regulated, SPSS software version 14.1 was used to reduce signature genes to a small subset that were discriminating and displayed divergent expression profiles that were not highly correlated to each other. The result of these analyses was the identification of a subset of transcripts, the GES, which exhibit the best predictive performance to discriminate between the different groups.

Biased selection of genes from the microarray

To elucidate possible mechanisms by which PGC-1α and PGC-1β regulate protein synthesis, genes that were highly regulated by PGC-1α and PGC-1β were selected based on their gene ontology functions and processes. Nine genes were biasedly selected that had GO terms linked to growth and protein synthesis. The expression of these genes was then measured via real-time qPCR.

3.2.7 Gene validation: Real-time polymerase chain reaction

To confirm the gene expression profile of the GES and the selected genes potentially involved in muscle growth, gene expression was analysed using real-time qPCR. These genes were also measured in skeletal muscle samples from subjects before and after an acute bout of resistance exercise (REX), and in muscle samples from patients with amyotrophic lateral sclerosis (ALS), and healthy age/sex matched controls. Real-time qPCR was performed using a Stratagene Mx3000P qPCR System and the MxPro qPCR software (Stratagene, La Jolla, CA). Cycling conditions for the PCR consisted of one denaturing cycle at 95°C for 2 minutes, followed by 40 cycles of denaturing at 95°C for 5 seconds and annealing at 60°C for 20 seconds, and elongation at 72°C for 60 seconds. A dissociation curve was generated to show that only one product had been amplified during the PCR. Each 20 µL reaction contained 0.5 x Power SYBR Green PCR Master Mix (Applied Biosystems), 25 ng of cDNA, and the forward and reverse primers for the gene of interest. Primers were designed using Primer 3 (www.primer3.sourceforge.net) and the sequences cross checked for gene specificity using a BLAST search (www.ncbi.nlm.gov/BLAST). Primers were synthesised by Gene Works (Adelaide, SA). Genes amplified in the PCR are shown in Tables 3.01 and 3.02. All samples were measured in triplicate. To compensate for variations in input RNA amounts and efficiency of the reverse transcription, data was normalised ribosomal protein, 36B4 (also known as RPLPO) mRNA.

Table 3.01 Mouse Primers used in the real-time qPCR

Primer	GenBank accession no.	Forward Primer (5'-3')	Reverse Primer (5'-3')
Ppp1R16a	NM_033371.2	GCTGCACATCGCCGCTGCTA	GGCCCGCAGGAGTGCATCTT
MRPS9	NM_023514.3	CACGGCACAGGCGGTCGTTT	CAAGCGTATGGCGCCTGCCT
TARBP2	NM_009319.1	CAGCTGCACTGGTCAGGGCC	GTGCAGCCTGGCCCACGATT
CDC14B	NM_172587.2	GCGTGAAGAAGAGCCGCAGC	ACCATGGCCAGATTGAGTGGTCC
EXOC1	NM_027270.1	CACCACGTGTGGACCGCACA	TCGCCACGGCGTTCAGCATT
TRIM25	NM_009546.2	CCCGAGCATGGCGAGTGCAT	GCTGGTCTCTGCTGCGTCGA
TRIM32	NM_053084.1	GTGGACTCGCGTCGGAGCTG	GGGCAGCGGACGCCATTGAT
eEF1A2	NM_007906.2	CAGTTCACCTCTCAGGTTATCATCCT	GCCGTGTGACAGTCGATGAC
eIF2B4	NM_001127356.1	CTTCTCCCACCTGCCTCAGTA	CAGAGGATGGGATGCTCATGTA
eIF4E3	NM_025829.4	ACCATTGGAGAGCAGTTCACAGA	TCACGCTGACTCCGATGATC
VEGF-A	NM_001025250.3	AAGCCAGCACATAGGAGAGATGA	TCTTTCTTTGGTCTGCATTCACA
Caspase1	NM_009807.2	AAAAGCCCAGAAGTTATGGAAAGA	GACGTGTACGAGTGGTTGTATTCAT
TCEAL7	NM_001127169.1	AACCCTGCGGAGCACTTG	TGAAGCAACCTCTGTCTGAAATTG
TSC22D3	NM_001077364.1	TTCTCCATCTCCTTCTTTTCTTCTCT	CTCCGGAGGCACTGTTATCC
ASPRV1	NM_026414.2	TTGGCACAGACGTCTTGCA	GCAGGTGCGGTGTTCGA
Prnp	NM_011170.2	CACCGAGACCGATGTGAAGA	GGTACTGGGTGACGCACATCT
36B4	NM_007475.5	TTGTGGGAGCAGACAATGTG	AGTCCTCCTTGGTGAACACG

Table 3.02 Human Primers used in the real-time qPCR

Primer	GenBank accession no.	Forward Primer (5'-3')	Reverse Primer (5'-3')
Ppp1R16a	NM_032902.5	ACGCCCCTTGATGTGTGCGG	GAGGGCGTCGTGCTTGTGCT
MRPS9	NM_182640.2	GCCCTGTGTGTCCTACGGCG	CAGAGGCCTTGCTTCCGGGC
TARBP2	NM_134323.1	TCAGCAGTCTGAGTGCAACC	GTGCCACTCCCAATCTCAAT
CDC14B	NM_003671.3	TCGACCTCGCCGGGTGTGAA	ACACGTCGTCCTGGGGGTCC
EXOC1	NM_018261.3	AGGCCTGCACCAATGCTGCT	CTGGCCAGTCTCCGGGCAAA
TRIM25	NM_005082.4	CGACCTGGAGGCCACCCTGA	CCGCACATCCTGCTGCCTGT
TRIM32	NM_012210.3	GGAGGCCACAGCGTCTGCTG	GGCAACCACTTCCTCCGGGC
eEF1A2	NM_001958.3	CGTGGGCGTGAACAAAATG	TCGTAGCGCTTCTCGCTGTA
eIF2B4	NM_172195.3	CCGGTGTATTGCCCTGCTT	CATTAGGCGGTGTTGTGTAATCC
eIF4E3	NM_001134651.1	GCAGCAGATGATGAAGTAATAGGAGTT	AGTGCCCATCTGTTCTGTAGGGA
VEGF-A	NM_001171623.1	CCCACTGAGGAGTCCAACATC	GGCCTTGGTGAGGTTTGATC
Caspase1	NM_001223.4	CTGCTCTTCCACACCAGATAATGT	TCCAATAAAAACAGAGCCCATTG
TCEAL7	NM_152278.3	CGCCCGTATGGAGAATTTGA	GAAGCAGCCTCTGTCTAAAATTCC
TSC22D3	NM_198057.2	TGGCCATAGACAACAAGATCGA	TCACAGCATACATCAGATGATTCTTC
ASPRV1	NM_152792.2	GAGGTCACTGATGGCGATCTG	GGCCACCTTTACCACATTCTCA
Prnp	NM_000311.3	ATGGAGCGCGTGGTTGA	GGCCTGAGATTCCCTCTCGTA
36B4	NM_001002	GTGATGTGCAGCTGATCAAGACT	GATGACCAGCCCAAAGGAGA

3.2.8 Human skeletal muscle samples

Resistance Exercise (REX) Methods

The skeletal muscle samples were a gift from Dr Paul Della Gatta, Deakin University.

Subjects

Eight untrained, but recreationally active Australian individuals volunteered to take part in the exercise component of the study (mean ± SD age 22.0 ± 0.5 yrs, height 1.79 ± 0.05 m, body mass 83.3 ± 19.1 kg and BMI 24.1 ± 0.1 $kg.m^{-2}$). Exclusion criteria included resistance training within the past six months, medication, or a history of a condition or illness that would present as a health risk during strenuous resistance exercise. Before participating in the study, the nature, purpose and risks of the study were explained to the subjects. They then provided informed written consent. All experimental procedures involved in this study were formally approved by the Deakin University Human Research Ethics Committee (EC 18-2004).

Experimental design

Each subject in the exercise group completed a familiarisation session prior to the experimental protocol to learn how to perform each exercise, and to determine their individual 1 repetition maximum (1 RM). During the session, a 5 RM test was performed for each subject for the leg press, squat (assisted by the Smith machine) and leg extension. 1 RM was then calculated using the Brzycki equation (1 RM = weight lifted (kg)/1.0278–[reps to fatigue x 0.0278]). The familiarisation session took place at least 7 days prior to allow sufficient recovery time before the experimental trial commenced.

For the 24 h preceding exercise, and the day of the trial, the subjects consumed a standard diet (20% fat, 14% protein and 66% carbohydrate) and abstained from alcohol, caffeine, tobacco and additional exercise. On the morning of the trial, subjects presented to the laboratory in a fasted state. Following 30 min of supine resting, a muscle sample was collected from the *vastus lateralis* under local anaesthesia (Xylocaine 1%) by percutaneous needle biopsy technique modified to include suction. Excised muscle tissue from each biopsy was immediately frozen and

stored in liquid nitrogen for later analysis. Subjects then completed a single bout of resistance exercise, specifically targeting muscles of the leg. Following 5 min of light cycling for warm-up, subjects completed two sets of eight to twelve repetitions of bilateral leg press, squat and leg extension at 80% 1-RM. This was followed by a third set to voluntary fatigue, also at 80% 1-RM. Subjects were allowed 1 min rest between exercises and 3 min rest between sets. The entire exercise protocol lasted 20–25 min. This intensity of this exercise protocol was similar to other studies on resistance exercise [273-275], but lower than other studies involving purely eccentric exercise that caused severe muscle damage [276, 277].

Additional muscle samples were collected at 2 h and 4 h after the exercise. The following morning, subjects again reported to the laboratory in a fasted state for the collection of a muscle sample 24 h post-exercise. To minimise the potential for inflammation arising from the biopsy procedure itself, biopsies were collected from separate incisions at least 2 cm distal from previous sites.

RNA extraction

Total cellular RNA was extracted using the TōTALLY RNA™ Kit (Ambion Inc.) according to the manufacturer's protocol. RNA quality and concentration were determined using the Agilent 2100 Bioanalyzer (Agilent Technologies, Palo Alto, CA). RNA (1 μg) was reverse transcribed to complementary DNA (cDNA) using a High Capacity cDNA reverse transcription kit (Applied Biosystems).

Statistics

A one-way repeat measures ANOVA with a Bonferroni adjustment was to investigate the effect of exercise on the genes of interest.

Amyotrophic Lateral Sclerosis (ALS) methods

Skeletal muscle samples from were provided by the Eurobiobank and Telethon (GUP 07001) [155].

Subjects

Skeletal muscle biopsies were obtained from fourteen patients diagnosed with ALS [278] and 10 age-matched healthy control subjects (Table 3.03). At the time of the biopsy, the duration of illness was 3-48 months. The research protocol was approved by the institutional ethics committees and informed consent was obtained from all participants according to the Declaration of Helsinki (BMJ 1991; 302:1194) [279].

Table 3.03 Characteristics of subjects included in the study

	Control	**ALS**
Patients (n)	10	14
Male/Female	7/3	10/4
Age (years)		
Mean ± SD	53 ± 17	59 ± 9
Range	25-73	33-79

Muscle biopsies

For the ALS patients biopsies were taken from the vastus lateralis muscle using either Bergstrom or open biopsy procedures. For the healthy control subjects biopsies were taken from the vastus lateralis muscle using the Bergstrom technique. All biopsies were immediately frozen in liquid nitrogen and stored at -80°C until analysed.

RNA Extraction

Total RNA was extracted from 5-20 mg skeletal muscle samples using Tri-Reagent® Solution (Ambion Inc.) according to the manufacturer's protocol. First-strand cDNA was generated from 1µg RNA in 20µL reaction buffer using the AMV reverse transcriptase (RT) kit and random hexomer primers (500ng) according to manufacturer's protocol (Promega, Madison WI).

Statistics

A one-way ANOVA with a Dunnett C post-hoc test was used for all analyses when comparing control and ALS subjects.

3.3 Results

3.3.1 Microarray and iTRAQ analyses

To investigate the transcriptional and translational effects following PGC-1α and PGC-1β overexpression in C2C12 myotubes, both microarray genomic and iTRAQ proteomic analyses were performed. In the microarray analyses, PGC-1α and PGC-1β were found to significantly regulate 1019 and 3054 genes respectively, with a greater than 1.5-fold increase or decrease in expression levels when compared to the GFP control group. Using iTRAQ quantification, PGC-1α and PGC-1β regulated 166 and 68 proteins, respectively.

3.3.2 Gene Ontology (GO) terms

The genes and proteins significantly regulated by PGC-1α or PGC-1β overexpression identified by microarray and iTRAQ analyses, respectively, were next submitted to GSEA through DAVID bioinformatics platform (http://david.abcc.ncifcrf.gov). GSEA revealed genes clustered significantly with a range of mitochondrial and metabolic related GO terms. Genes and proteins differentially expressed specifically by PGC-1β also clustered significantly with muscle contractile and cytoskeletal related GO terms. An overview of these GO terms is represented in Figure 3.01 for both genes and proteins, where overlapping terms have been grouped together. The full lists of GO terms are in Appendix 1 (Tables S1-4). The majority of GO terms for both PGC-1α and PGC-1β belonged to mitochondrial biology, nucleotide binding, the ribosome and ribonucleoprotein complex, oxidative metabolism and energy production. These GO terms were generally reflected in the iTRAQ analyses, despite fewer proteins being identified compared to microarray expression profiling.

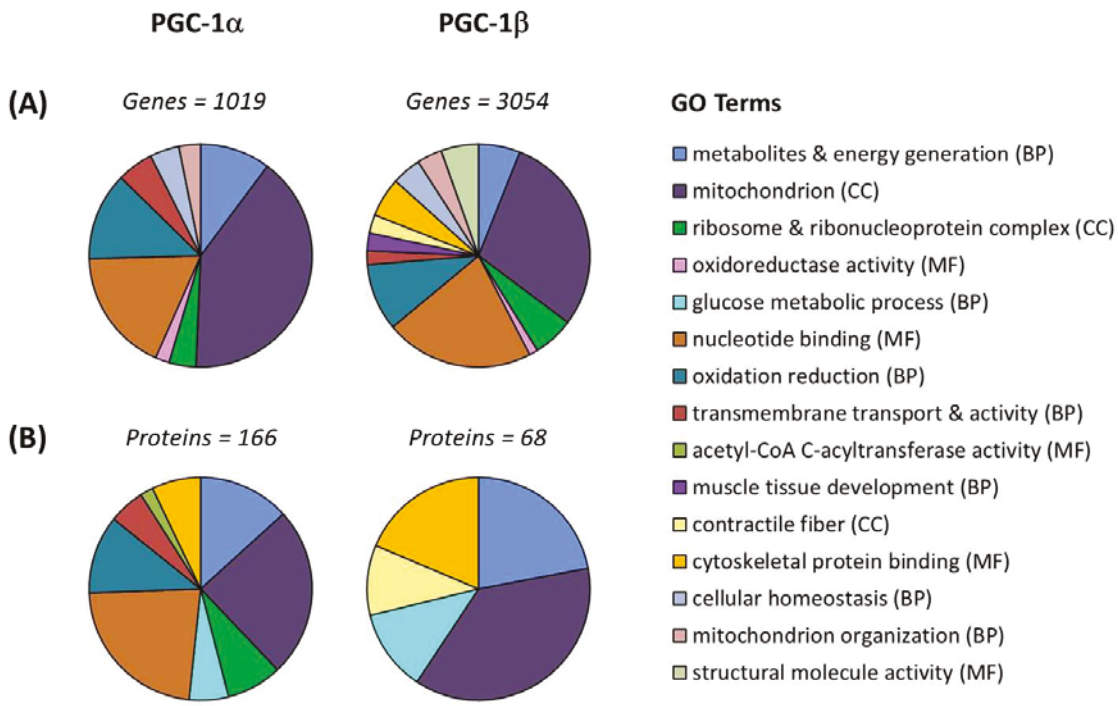

Figure 3.01 Pie charts representing the major gene ontology (GO) terms used to group genes and proteins regulated by PGC-1α and PGC-1β. (A) GO terms identified from microarray analyses of genes regulated by PGC-1α and PGC-1β overexpression in C2C12 myotubes. (B) GO terms identified from iTRAQ analyses of proteins regulated by PGC-1α and PGC-1β overexpression. The total number of genes and proteins analysed are shown above each pie chart. Genes and proteins were selected based on $P < 0.05$ Bonferroni's multiple comparison test, and on a $\geq$ 1.5-fold change for microarray genes. CC = cellular component, MF = molecular function, BP = biological process.

3.3.3 KEGG pathway mapping

KEGG pathway mapping (http://www.genome.jp/kegg/) of the genes regulated by PGC-1α and PGC-1β identified signalling pathways significantly associated with oxidative phosphorylation (OXPHOS) in both normal and disease states, and in the citrate cycle associated with carbohydrate and fatty acid metabolism (Tables 3.04 and 3.05). These pathways were essentially confirmed at the protein level using iTRAQ quantification, although fewer pathways were listed for PGC-1β due to fewer proteins being identified by the iTRAQ analyses. Furthermore, a significant association of proteins involved in glycolysis and gluconeogenesis pathways were identified in PGC-1α and PGC-1β expressed lysates, but not at the gene expression level. Overall, the effects of PGC-1α and PGC-1β overexpression generated similar profiles at both the transcriptional and translational level.

Table 3.04 KEGG pathway analyses of PGC-1α-regulated genes and proteins

Analysis	Term	Count	Fold Enrichment	P-Value
Microarray	Oxidative phosphorylation	62	8.0	2.80E-39
	Parkinson's Disease	62	7.8	1.55E-38
	Huntington's disease	64	5.9	6.31E-31
	Alzheimer's disease	61	5.6	3.92E-28
	Citrate cycle (TCA cycle)	18	9.7	2.05E-11
	Cardiac muscle contraction	25	5.4	1.20E-09
	Pyruvate metabolism	12	4.9	0.003
	Fatty acid metabolism	11	4.1	0.039
	Alanine, aspartate & glutamate metabolism	9	5.0	0.044
iTRAQ	Citrate cycle (TCA cycle)	9	16.7	3.5E-06
	Ribosome	12	7.7	2.9E-05
	Oxidative phosphorylation	13	5.7	2.0E-04
	Parkinson's disease	13	5.6	2.5E-04
	Alzheimer's disease	14	4.4	0.001
	Glycolysis/Gluconeogenesis	9	7.6	0.002
	Huntington's disease	13	4.1	0.007
	Fatty acid metabolism	7	8.9	0.011

Table 3.05 KEGG pathway analyses of PGC-1β-regulated genes and proteins

Analysis	Term	Count	Fold Enrichment	P-Value
Microarray	Oxidative phosphorylation	72	3.5	6.41E-23
	Parkinson's Disease	66	3.2	1.85E-17
	Alzheimer's disease	78	2.7	3.28E-16
	Huntington's disease	73	2.5	6.29E-13
	Citrate cycle (TCA cycle)	18	3.7	1.05E-04
	Cardiac muscle contraction	31	2.5	1.53E-04
	Hypertrophic cardiomyopathy	30	2.3	0.003
	Sugar metabolism	18	2.6	0.035
iTRAQ	Citrate cycle (TCA cycle)	5	23.7	0.002
	Glycolysis/Gluconeogenesis	5	10.8	0.050

3.3.4 GES of microarray data

Analysis was performed to identify the genes that were highly regulated by PGC-1α and PGC-1β, developing a non-biased gene expression signature (GES). The top 33 genes regulated by PGC-1α and PGC-1β are listed in Appendix 2 (Table S5). The top 7 genes that were highly regulated by PGC-1α and PGC-1β were selected for further analysis and are shown in Table 3.06. The expression of these targets was validated via real-time qPCR (Figure 3.02). Overexpression of PGC-1α and PGC-1β increased the expression of protein phosphatase 1, regulatory subunit 16A (Ppp1R16a), mitochondrial ribosomal protein sub-unit 9 (MRPS9), TAR *HIV-1* RNA binding protein 2 (TARBP2), and cell division cycle 14 homolog B (CDC14B) (Figure 3.02A). In contrast, exocyst complex component 1 (EXOC1), Tripartite motif-containing protein 25 (TRIM25), and Tripartite motif-containing protein 32 (TRIM32) were down-regulated (Figure 3.02B). Although the GES identified TRIM25 to be regulated by PGC-1β only, and TRIM32 to be regulated by PGC-1α only, the expression of these genes was reduced in response to both PGC-1α and PGC-1β overexpression when measured via real-time qPCR.

Table 3.06 Microarray profile of genes chosen from the GES regulated by both PGC-1α and PGC-1β.

Primer	GenBank accession no.	Direction vs. GFP	PGC-1α P-value	PGC-1β P-value
Ppp1R16a	NM_033371.2	Up	0.001	5.77E-11
MRPS9	NM_023514.3	Up	6.61E-06	4.35E-12
TARBP2	NM_009319.1	Up	9.03E-04	3.30E-11
CDC14B	NM_172587.2	Up	0.018	2.76E-10
EXOC1	NM_027270.1	Down	8.04E-05	6.35E-12
TRIM25*	NM_009546.2	Down		5.15E-09
TRIM32**	NM_053084.1	Down	0.001	

* PGC-1β only; ** PGC-1α only.

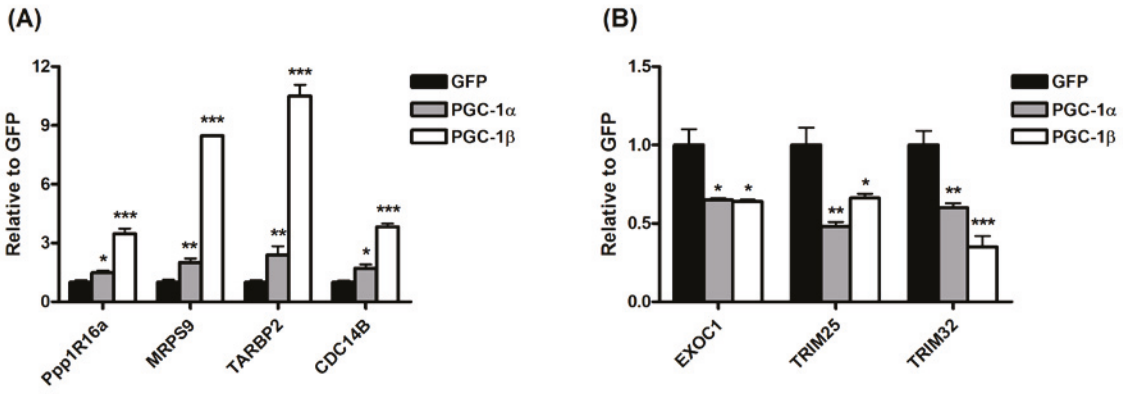

Figure 3.02 mRNA levels of genes highly regulated by PGC-1α and PGC-1β from the GES, validated by qPCR. (A) Genes up-regulated by PGC-1α and PGC-β from the GES. (B) Genes down-regulated by PGC-1α and/or PGC-1β from the GES. Values were normalised to 36B4 mRNA expression. * $P < 0.05$, ** $P < 0.01$, *** $P < 0.001$ compared to GFP.

3.3.5 Biased selection of genes from the microarray

To elucidate possible mechanisms by which PGC-1α and PGC-1β regulate protein synthesis, the top regulated genes that may potentially be involved in skeletal muscle development and growth were explored. The genes that were highly regulated by PGC-1α and PGC-1β are shown in Table 3.07. The expression of these genes was validated via qPCR (Figure 3.03). Overexpression of PGC-1α or PGC-1β led to a large increase in mRNA for eukaryotic translation elongation factor 1 alpha 2 (eEF1A2), eukaryotic translation initiation factor 2B, subunit 4 (eIF2B4), eukaryotic translation initiation factor 4E family member 3 (eIF4E3), and vascular endothelial growth factor-A (VEGF-A) (Figure 3.03A). In contrast, Caspase1, transcription elongation factor A SII-like 7 (TCEAL7), TSC22 domain family protein 3 (TSC22D3), aspartic peptidase retroviral-like 1 (Asprv1) and Prion Protein (Prnp) were all decreased in response to PGC-1α and PGC-1β overexpression (Figure 3.03B).

Table 3.07 PGC-1α and PGC-1β regulated genes obtained from microarray and selected for validation based on their potential roles in protein turnover.

Primer	GenBank accession no.	Direction vs. GFP	PGC-1α P-value	PGC-1β P-value
eEF1A2	NM_007906.2	Up	5.42E-16	3.46E-18
eIF2B4	NM_001127356.1	Up	5.12E-07	3.49E-11
eIF4E3	NM_025829.4	Up	1.97E-06	1.30E-08
VEGF-A	NM_001025250.3	Up	1.81E-05	4.49E-07
Caspase1	NM_009807.2	Down	2.02E-09	4.11E-12
TCEAL7	NM_001127169.1	Down	3.51E-12	5.78E-15
TSC22D3	NM_001077364.1	Down	5.62E-07	1.11E-11
ASPRV1	NM_026414.2	Down	7.26E-09	4.63E-10
Prion protein	NM_011170.2	Down	2.65E-07	9.91E-12

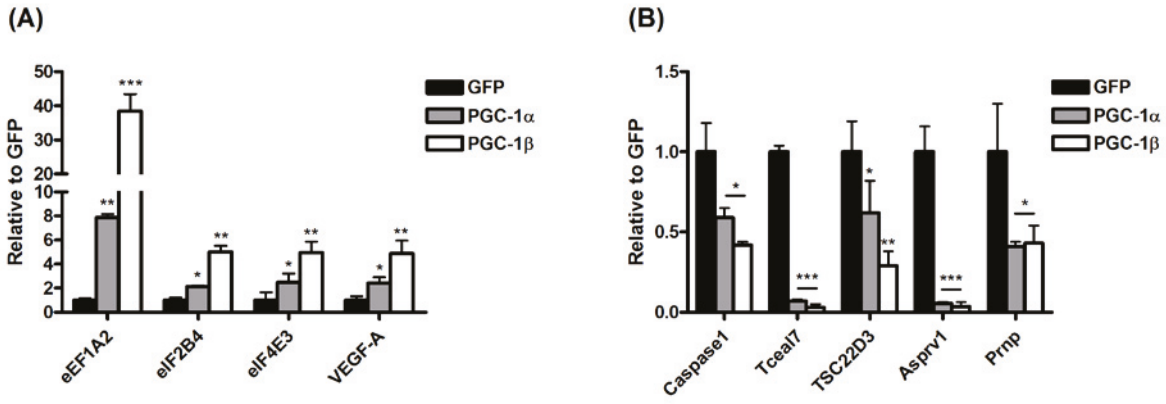

Figure 3.03 mRNA levels of genes selected biasedly from the microarray, validated by qPCR. (A) Genes up-regulated by PGC-1α and PGC-β from the microarray. (B) Genes down-regulated by PGC-1α and PGC-1β from the microarray. * $P < 0.05$, ** $P < 0.01$, *** $P < 0.001$ compared to GFP.

3.3.6 Regulation of genes in models of muscle hypertrophy and atrophy

It was of interest to establish the potential clinical relevance of these observations. To do so, the expression levels of the genes from the non-biased and biased approaches were measured in a human model of stimulated muscle protein synthesis, acute resistance exercise (REX), and in a model of severe muscle atrophy, amyotrophic lateral sclerosis (ALS).

Resistance exercise

In response to resistance exercise, PGC-1α mRNA increased acutely at 2 and 4 hours post-exercise, but was then reduced after 24 hours (Figure 3.04A). In contrast PGC-1β mRNA was decreased at 4 and 24 hours post exercise (Figure 3.04B). This was associated with significant increases in Ppp1R16a and CDC14B (Figure 3.05A), and decreases in EXOC1 and TRIM32 (Figure 3.05B), genes selected from the non-biased GES. Additionally, resistance exercise led to significant increases in genes selected from the biased approach, including eEF1A2, eIF2B4, eIF4E3 and VEGF-A at 2 hours post-exercise (Figure 3.06A). After 24 hours, the expression of eIF2B4 increased further, while VEGF-A, eEF1A2 and eIF4E3 expression returned to, or was slightly below, pre-exercise levels. From the selected genes that were down-regulated in the microarray, only TSC22D3 was decreased following resistance exercise, while Caspase1 and Prnp were increased 24 hours post-exercise (Figure 3.06B). Out of all genes investigated, VEGF-A, a known target of PGC-1α and PGC-1β, mirrored PGC-1α expression very closely.

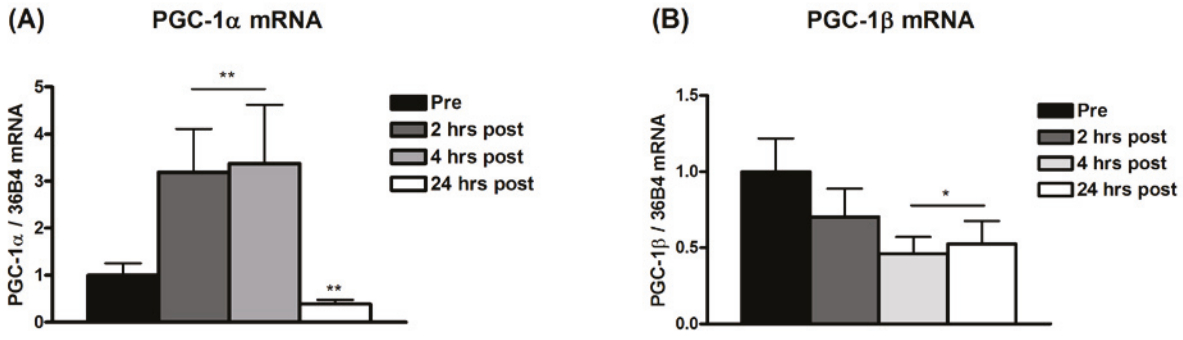

Figure 3.04 PGC-1α and PGC-1β mRNA expression in skeletal muscle after an acute bout of resistance exercise in humans. (A) PGC-1α mRNA, and (B) PGC-1β mRNA when measured 2, 4 and 24 hours after resistance exercise. Values were normalised to 36B4 mRNA expression. * $P < 0.05$, ** $P < 0.01$ compared to Pre-exercise.

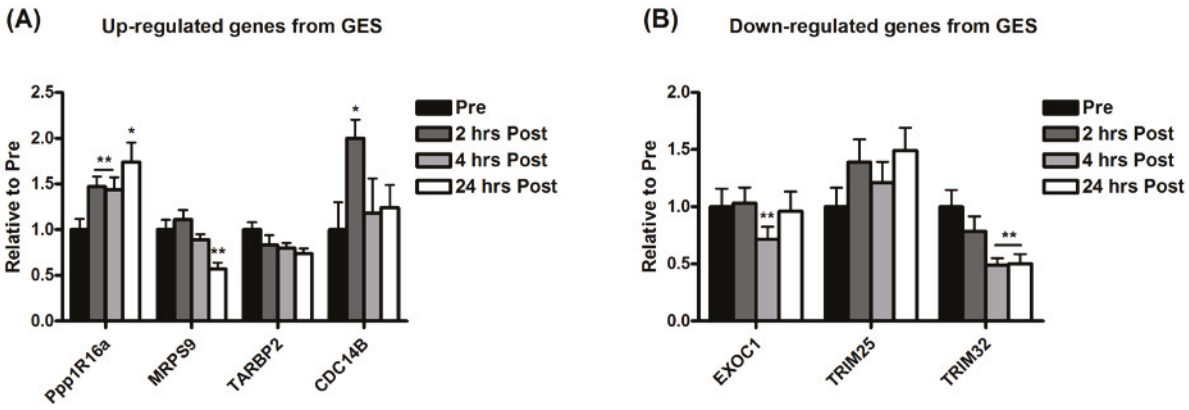

Figure 3.05 mRNA expression of the gene expression signature (GES) genes that are regulated by PGC-1α and PGC-1β, in skeletal muscle after an acute bout of resistance exercise in humans. (A) Genes that were up-regulated in the GES, and (B) genes that were down-regulated in the GES, when measured 2, 4 and 24 hours after resistance exercise. Values were normalised to 36B4 mRNA expression. * $P < 0.05$, ** $P < 0.01$ compared to pre-exercise (Pre).

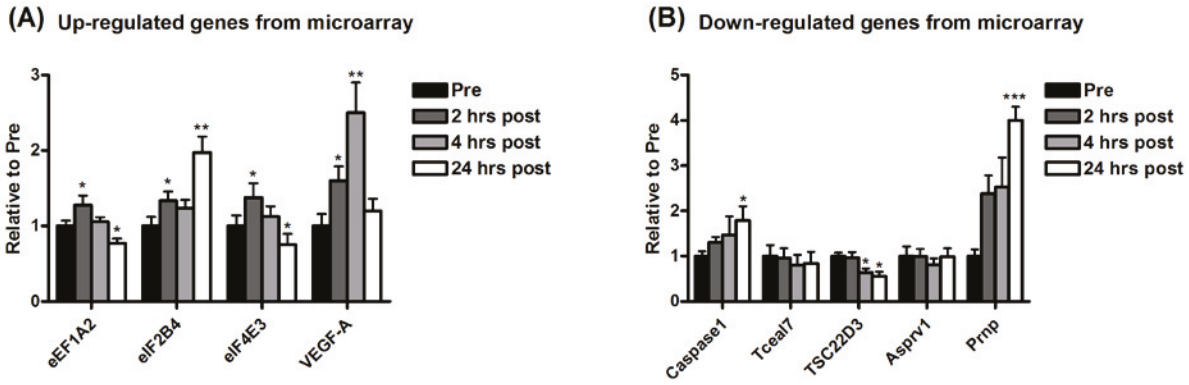

Figure 3.06 mRNA expression of biasedly-selected genes that are regulated by PGC-1α and PGC-1β, in skeletal muscle after an acute bout of resistance exercise in humans. (A) Genes that were up-regulated in the microarray, and (B) genes that were down-regulated in the microarray, when measured 2, 4 and 24 hours after resistance exercise. Values were normalised to 36B4 mRNA expression. * $P < 0.05$, ** $P < 0.01$, *** $P < 0.001$ compared to pre-exercise (Pre).

ALS patients

Our group has previously shown that PGC-1α and PGC-1β mRNA levels are decreased in atrophied skeletal muscle from patients with ALS [155]. Figure 3.07 shows that PGC-1α (A) and PGC-1β (B) mRNA were decreased by 52% and 63%, respectively. Of the genes selected from the GES, MRPS9 was decreased (Figure 3.08A), and TRIM25 and TRIM32 were increased (Figure 3.08B), showing inverse regulation when compared to PGC-1α and PGC-1β overexpression. However, TARBP2 expression was also increased, which is similar to what was observed from the microarray. ALS skeletal muscle also displayed inverse regulation of genes selected from the biased approach, including decreases in eEF1A2 and VEGF-A (Figure 3.09A), and increases in TSC22D3, Asprv1 and Prnp (Figure 3.09B).

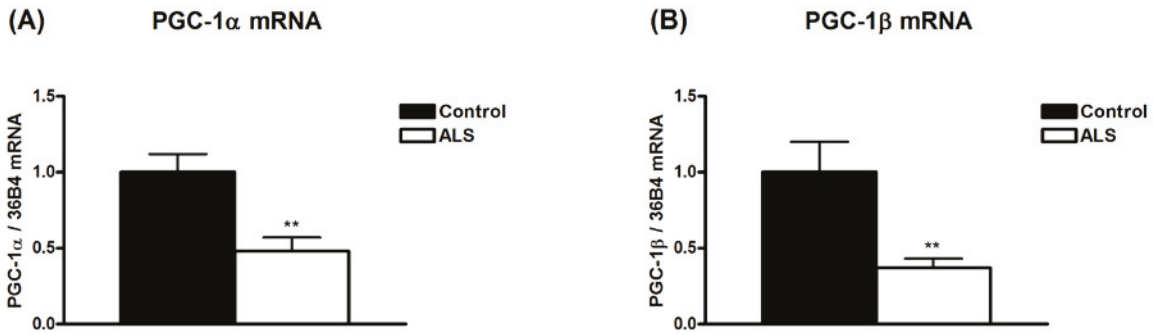

Figure 3.07 PGC-1α and PGC-1β mRNA expression in skeletal muscle of ALS (amyotrophic lateral sclerosis) and control patients. (A) PGC-1α mRNA, and (B) PGC-1β mRNA. Values were normalised to 36B4 mRNA expression. ** $P < 0.01$ compared to Control.

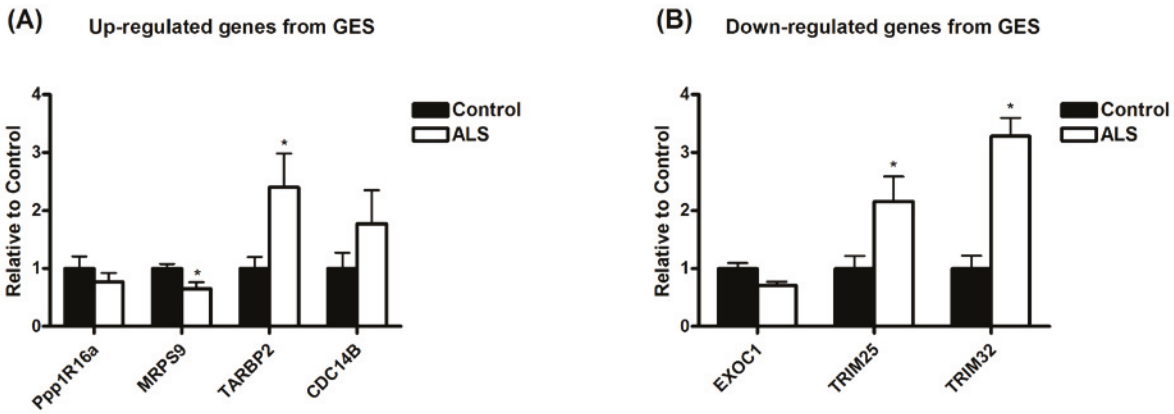

Figure 3.08 mRNA expression of gene expression signature (GES) genes that are regulated by PGC-1α and PGC-1β, in skeletal muscle of ALS (amyotrophic lateral sclerosis) and control patients. (A) Genes that were up-regulated in the GES, and (B) genes that were down-regulated in the GES. Values were normalised to 36B4 mRNA expression. * $P < 0.05$ compared to Control.

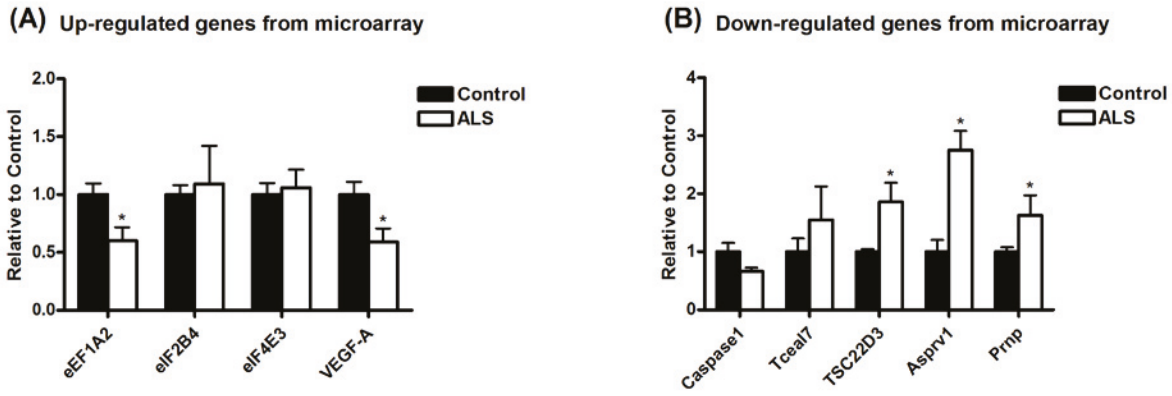

Figure 3.09 mRNA expression of biasedly-selected genes that are regulated by PGC-1α and PGC-1β, in skeletal muscle of ALS (amyotrophic lateral sclerosis) and control patients. (A) Genes that were up-regulated in the microarray, and (B) genes that were down-regulated in the microarray. Values were normalised to 36B4 mRNA expression. * $P < 0.05$ compared to Control.

3.4 Discussion

Understanding the downstream PGC-1α- and PGC-1β-regulated targets increasing protein synthesis will aid in developing targeted therapeutic approaches to increase skeletal muscle mass during catabolic wasting conditions. This study aimed to identify global gene and protein expression changes that occur in response to PGC-1α and PGC-1β overexpression in C2C12 myotubes, and create an unbiased GES characterising the PGC-1α- and PGC-1β-regulated targets that may be involved in increasing protein synthesis. Several observations were made. Firstly, GSEA revealed that many genes differentially expressed by PGC-1α and PGC-1β overexpression clustered significantly with a range of GO terms related to mitochondrial biology, oxidative metabolism, nucleotide binding, and the ribosome and ribonucleoprotein complex. These findings were generally reflected at the protein level via iTRAQ analysis. Genes and proteins differentially regulated by PGC-1β also clustered with muscle contractile and cytoskeletal related GO terms. KEGG pathway mapping of the genes and proteins regulated by PGC-1α and PGC-1β identified signalling pathways associated with OXPHOS in normal and disease states, and in the citrate cycle associated with glucose and fatty acid metabolism. Secondly, the non-biased GES identified the top regulated genes by PGC-1α and PGC-1β. In addition, highly regulated genes that may potentially be involved in muscle growth were biasedly selected and also explored. Thirdly, PGC-1α mRNA was increased and PGC-1β mRNA was decreased in human skeletal muscle following resistance exercise, while PGC-1α and PGC-1β were both decreased in skeletal muscle of ALS patients. Lastly, several of the differentially expressed genes identified from both the non-biased and biased selections were also differentially regulated in human skeletal muscle following resistance exercise and/or in skeletal muscle of ALS patients.

3.4.1 GSEA

GSEA is a popular method to identify differentially expressed genes and proteins that may commonly regulate biological functions and intracellular signalling pathways [265]. Many GO terms identified using GSEA were associated with mitochondrial biology and oxidative metabolism. GO terms associated with the

ribosome and ribonucleoprotein complex were also common, supporting the role of PGC-1α and PGC-1β in regulating protein synthesis. These findings are consistent with enriched GO terms in skeletal muscle of PGC-1α transgenic mice [280], and other cell culture models overexpressing PGC-1α [157]. Ribosomal biogenesis is decreased during denervation-induced atrophy, contributing to the decrease in protein synthesis [281]. Interestingly, this is paralleled with an increase in Akt/mTOR activity, showing that other mechanisms control ribosomal biogenesis/activity during inactivity. As PGC-1α and PGC-1β are also reduced in denervated muscle [65], and do not require Akt/mTOR to increase protein synthesis, it may be possible that PGC-1α and PGC-1β increase protein synthesis by increasing the transcription of these ribosomal genes. The effect of PGC-1α and PGC-1β on ribosomal biogenesis should be a future area of research.

Genes and proteins differentially expressed by PGC-1β (and proteins for PGC-1α) also clustered with muscle contractile and cytoskeletal related GO terms. In Chapter 2, it was established that PGC-1α and PGC-1β regulate protein synthesis via ERRα. Interestingly, gene expression profiling in ERRα-null cardiac muscle reveals down-regulation of genes that cluster with GO terms involved in heart and muscle development, muscle contraction, and protein metabolism and transcription [282]. Together these observations suggest that PGC-1α/ERRα and PGC-1β/ERRα may increase the synthesis of structural and contractile proteins in skeletal muscle. KEGG pathway mapping of the genes regulated by PGC-1α and PGC-1β was also associated with cardiac muscle contraction, as well as OXPHOS in normal and disease states, and in the citrate cycle associated with glucose and fatty acid metabolism. Again, similar KEGG pathways are enriched in PGC-1α transgenic skeletal muscle [280]. Interestingly, some of these disease states are associated with mitochondrial defects as well as muscle atrophy [152, 283-287].

3.4.2 GES

The GES created from the microarray data identified an increase in Ppp1R16a, MRPS9, TARBP2, and CDC14B, and a decrease in EXOC1, TRIM25 and TRIM32.

Genes up-regulated in the GES

The regulation and function of Ppp1R16a, MRPS9, TRBP2 and CDC14B have not previously been investigated in skeletal muscle. Ppp1R16a, also known as Myosin phosphatase-targeting subunit 3 (MYPT3), is part of the MYPT family, which specifically target protein phosphatase 1c (PP1c) [288]. While its role in skeletal muscle is unknown, it is known to target myosin light chain phosphatase and is involved in the regulation of smooth muscle contraction [288]. MRPS9 is involved in mitochondrial protein synthesis in a yeast cell line [289], however its role in mammalian cells is unknown. As PGC-1α and PGC-1β regulate many genes involved in mitochondrial biogenesis in skeletal muscle [162, 171, 172], this may be another gene by which PGC-1α and PGC-1β mediate their effects on mitochondria. CDC14B is known for its regulation of the cell cycle, particularly in the termination of cell mitosis [290], however its role in differentiated cells such as myotubes has not been investigated. TARBP2 inhibits the phosphorylation of the eukaryotic translation initiation factor eIF2A, by the dsRNA-regulated protein kinase (PKR) in murine embryo fibroblasts [291]. This removes the inhibition of translation initiation and likely increases protein synthesis in these cells [291].

Genes down-regulated in the GES

EXOC1 (also known as Sec3) is a protein of the exocyst complex; a multiple protein complex involved in targeting secretory vesicles to the cell membrane during exocytosis [292, 293]. Other members of the exocyst complex regulate exocytosis of the glucose transporter type 4 (GLUT4) in adipocytes in response to insulin [294, 295], although their role in skeletal muscle has not been identified. TRIM25 is a member of the RING-finger B-box coiled-coil (RBCC) motif family, and is involved in estrogen-dependent cell proliferation and organ development [296]. Its expression is lowest in skeletal muscle compared to other tissues [297], suggesting that it may play a minor role in skeletal muscle; although this has not been investigated. TRIM32 is an E3 ubiquitin ligase that degrades thin myofibrillar contractile proteins (i.e. actin, tropomyosin and troponin) during muscular atrophy [298]. Short-hairpin RNA (shRNA) down-regulation of TRIM32 attenuates the decrease in muscle fibre diameter and loss of thin myofibrillar proteins during fasting [298]. PGC-1α and PGC-1β attenuate skeletal muscle protein degradation by down-regulating other ubiquitin ligases, Atrogin-1 and Muscle Ring Finger-1 (MuRF1) [219]. The PGC-1α-

and PGC-1β-induced decrease in TRIM32 observed in the current study may also attenuate protein degradation in skeletal muscle.

3.4.3 Biasedly selected genes

In addition to the genes identified by the GES, the top regulated genes that may potentially be involved in skeletal muscle development and growth were explored. In response to PGC-1α and PGC-1β overexpression, eEF1A2, eIF2B4, eIF4E3, and VEGF-A mRNA was increased, while Caspase1, TCEAL7, TSC22D3, Asprv1, and Prnp mRNA was decreased.

Up-regulated genes

eEF1A2, eIF2B4, and eIF4E3 are all members of protein families known to positively regulate translation initiation and elongation [38, 299, 300]. The eukaryotic elongation factor, eEF1A2, is known for its role in muscle growth. Deletion of eEF1A2 results in severe muscle wasting, weakness, and degeneration of motor neurons in *wasted* mice [301, 302], while overexpression of eEF1A2 prevents apoptosis in myotubes *in vitro* [303]. However the role of eEF1A2 in skeletal muscle protein synthesis has not been defined. The translation initiation factor, eIF2B4 (also known as eIF2Bδ), is part of an eIF2B complex consisting of α-, β-, γ-, δ- and ε- sub-units [304]. While the role of eIF2B4/δ in skeletal muscle is not clear, the ε-sub-unit protects from the sepsis-induced decrease in protein synthesis in rat skeletal muscle [304]. eIF2B4/δ mRNA is increased in skeletal muscle after resistance exercise in rats [305], suggesting that it may also be involved in the exercise-induced increase in protein synthesis. Another translation initiation factor, eIF4E3, is part of the eIF4E family which consists of eIF4E1, eIF4E2 and eIF4E3 [306]. The role of eIF4E3 has not been investigated in skeletal muscle, although eIF4E1 increases protein synthesis in this tissue [38, 307]. However, eIF4E3 is thought to oppose the role of eIF4E1 in other tissues [308, 309], suggesting that it may decrease translation initiation.

Lastly, VEGF-A (also known as VEGF) is a major regulator of angiogenesis, and its expression is induced by both PGC-1α and PGC-1β in skeletal muscle [110, 170]. In the current experiment, VEGF-A mirrored PGC-1α expression very closely. VEGF-A expression is increased after acute resistance exercise [310], and recent studies

show that VEGF-A can improve muscle regeneration [311, 312]. VEGF-A has also been implicated in the pathogenesis of ALS. Reduced circulating levels of VEGF-A are thought to predispose mice and humans to ALS [313], while genetically increasing VEGF-A in rodent models of ALS prevents motor neuron degeneration and prolongs survival in rodents [314-316].

Down-regulated genes

The role of TSC22D3 in mammalian tissues is unknown, although other TSC22D family members negatively regulate cell proliferation and growth in salivary gland cancer cells [317], and cardiac myofibroblast differentiation [318]. Asprv1 is involved in proteolysis and regeneration in the skin [319], however its role in other tissues is unknown. In contrast, TCEAL7 [320], Prnp [321, 322], and Caspase 1 [323] may play a role in skeletal muscle growth and wasting. Overexpression of TCEAL7 in C2C12 myoblasts decreases proliferation and enhances differentiation [320], although its role in terminally differentiated myotubes is unknown. Caspase1 activity is increased in skeletal muscle undergoing cancer cachexia [324], and other caspase family members are known to contribute to protein degradation during muscle atrophy [325]. Lastly, Prnp expression is elevated in diseased skeletal muscle [326, 327], and skeletal muscle-specific overexpression of Prnp causes muscle atrophy and degeneration *in vivo* [328]. However, reducing Prnp levels decreases muscle weight and force production [329], and impairs skeletal muscle regeneration *in vivo* [321]. The role of Prnp in skeletal muscle therefore requires further investigation.

3.4.4 Human clinical models

To determine the clinical relevance of these observations, the expression of PGC-1α and PGC-1β, as well as the genes selected from the GES and biased approach, were measured in skeletal muscle before and after acute resistance exercise, and in muscle samples from ALS patients. Similar to previous studies [330], PGC-1α mRNA was increased transiently following resistance exercise, while both PGC-1α and PGC-1β were decreased in skeletal muscle of ALS patients [155]. Many genes that were up-regulated by PGC-1α and PGC-1β overexpression also followed this expression pattern. Of interest, Ppp1R16a, eEF1A2, eIF2B4, and VEGF-A, were increased in

skeletal muscle after resistance exercise, while eEF1A2 and VEGF-A were also decreased in skeletal muscle of ALS patients. These genes are potentially involved in skeletal muscle contraction, protein synthesis, and growth [288, 301, 302, 305, 311, 312], and therefore may be involved in the PGC-1α- and PGC-1β-induced increase in protein synthesis. Future studies are required to determine if these genes may play direct roles in regulating skeletal muscle protein synthesis under healthy and diseased conditions.

Of the genes that were down-regulated by PGC-1α and PGC-1β overexpression, TSC22D3 and TRIM32 were also decreased following acute resistance exercise, whereas TSC22D3, TRIM32 and Prnp were increased in atrophied skeletal muscle of ALS patients. While the role of TSC22D3 in skeletal muscle is unknown, TRIM32 is a known ubiquitin ligase in skeletal muscle [298], and overexpression if Prnp causes muscle atrophy and degeneration [328]. These observations suggest that TRIM32, Prnp, and potentially TSC22D3, may contribute to the PGC-1α- and PGC-1β-induced attenuation of skeletal muscle atrophy.

3.4.5 Summary and Conclusions

PGC-1α and PGC-1β positively regulate skeletal muscle mass by increasing protein synthesis and decreasing protein degradation, however the downstream molecular mechanisms mediating these responses are relatively unknown. The current study used GSEA to identify common biological functions and pathways that are regulated by PGC-1α and PGC-1β. Further analysis has identified novel gene targets that were up- or down-regulated in response to PGC-1α and PGC-1β overexpression in C2C12 myotubes. Many of the up-regulated genes were also increased in skeletal muscle following resistance exercise (a positive stimulator of protein synthesis [32, 34, 35]), and decreased in ALS skeletal muscle (a condition with reduced capacity for skeletal muscle protein synthesis [15]), suggesting that they may play a role in the PGC-1α- and PGC-1β-induced increase in protein synthesis. In contrast, genes that were down-regulated displayed inverse expression in these models, suggesting that their decreased expression by PGC-1α and PGC-1β may contribute to the attenuation of muscle atrophy. These findings provide novel avenues to investigate the effects of

PGC-1α and PGC-1β in skeletal muscle protein turnover, however further investigation into the role of these genes is required.

Chapter 4

PGC-1α and PGC-1β regulate creatine uptake via ERRα/CrT

4.1 Introduction

Creatine is found at high concentrations in highly metabolically active tissues such as skeletal muscle, heart and brain [230]. It plays an important role in maintaining cellular energy homeostasis by resynthesising ATP when in its phosphorylated form, phosphocreatine. Traditionally, creatine supplementation, in combination with resistance training, has been used to assist with skeletal muscle growth [231-233]. More recently, its use in the clinical setting has become of interest. Skeletal muscle creatine levels are reduced in many conditions associated with skeletal muscle atrophy, such as in patients with muscular dystrophy, and inflammatory, congenital and mitochondrial myopathies [229]. Supplementation with creatine monohydrate in these patients leads to gains in muscular strength and total body weight [234]. Creatine supplementation also stimulates muscle hypertrophy during rehabilitative strength training following limb immobilisation [235], attenuates corticosteroid-induced muscle wasting in rats [236], and reduces muscular degeneration in mdx mice [237]. Creatine therefore appears to be an effective strategy for improving skeletal muscle mass in such conditions. However, creatine supplementation does not always increase intracellular creatine content, which is controlled via the Na^+/Cl^- dependent Creatine transporter (CrT) [238]. Long-term creatine supplementation decreases CrT content in rat skeletal muscle [238], and may therefore not be effective for longer term use. Furthermore, CrT mRNA is significantly reduced in skeletal muscle of patients with various myopathies, suggesting that CrT levels may be the limiting factor to increase intracellular creatine content in response to creatine supplementation [239, 240]. Understanding the molecular mechanisms regulating the expression and/or activity of the CrT is therefore important to maximise the efficiency and benefits of creatine supplementation in skeletal muscle.

Currently, little is known about how the CrT is regulated. In healthy rodent skeletal muscle, high-dose creatine supplementation (initially increasing intracellular creatine) decreases CrT content [238], while depletion of intracellular creatine by β-Guanidinoproprionic acid (β-GPA), a competitive inhibitor of the CrT, increases sarcolemmal CrT expression [241, 242]. Furthermore, slow-twitch oxidative muscle fibres have increased CrT and rates of creatine uptake, but have a lower intracellular total creatine pool, when compared to fast-twitch glycolytic fibres [243, 244]. However the molecular mechanisms regulating these changes in CrT expression and therefore creatine uptake in skeletal muscle are unknown.

The transcriptional coactivators, peroxisome proliferator-activated receptor gamma coactivator-1α (PGC-1α) and PGC-1β, are also highly expressed in oxidative muscle fibres where they regulate many genes involved energy metabolism, substrate oxidation and growth [96, 219]. In particular, they regulate the uptake of two major fuel sources in skeletal muscle, glucose and fatty acids. Overexpression of PGC-1α or PGC-1β in rodent skeletal muscle or myotubes results in increased expression of the glucose transporter type 4 (GLUT4), with parallel increases in insulin-stimulated glucose transport [142, 167]. Similarly, PGC-1α and PGC-1β increase the expression of the fatty acid transporter, CD36, as well as many genes associated with fat oxidation in skeletal muscle [164, 167]. As creatine is also an important substrate for energy production, it is plausible that PGC-1α or PGC-1β may also regulate the CrT, and therefore creatine uptake, in skeletal muscle. Furthermore, as many of the metabolic effects that PGC-1α and/or PGC-1β have on skeletal muscle health involve the coactivation and regulation of ERRα, it is possible that PGC-1α and PGC-1β may regulate the CrT and creatine uptake in an ERRα-dependent manner.

In Chapter two, it was established that PGC-1α and PGC-1β can increase protein synthesis in mouse C2C12 myotubes. This effect was dependent on the coactivation of the transcription factor, estrogen-related receptor-alpha (ERRα), but the downstream targets regulating this increase in protein synthesis remain elusive. Creatine supplementation *in vivo* increases muscle growth, and although it remains controversial on whether this is a result of increased rates of protein synthesis [246, 247], creatine has been shown to increase the synthesis of contractile proteins in differentiating myotubes *in vitro* [248, 249]. It is also noteworthy that many

conditions associated with decreased CrT levels and reduced muscle mass [234, 239], also show reduced levels of PGC-1α or PGC-1β [65, 245]. Therefore it is possible that PGC-1α and PGC-1β may increase protein synthesis by regulating CrT levels and increasing intracellular creatine content.

The primary aim of this study was to determine if PGC-1α and/or PGC-1β can increase the expression of the CrT, and therefore regulate creatine uptake in L6 myotubes. If so, a secondary aim was to determine whether this effect was dependent on the transcription factor, ERRα, and whether ERRα can directly bind to the CrT promoter to increase its expression. Finally, it was of interest to determine if the PGC-1α- and PGC-1β-induced increase in protein synthesis takes places via their up-regulation of CrT mRNA and creatine uptake.

4.2 Methods

4.2.1 Cell culture

This study used L6 rat myoblasts (American type culture collection; ATCC, Manassas, VA) instead of C2C12 myotubes due to the siRNA sequences being specific to the rat. L6 myoblasts were incubated at 37°C with 5% CO_2, in high-glucose Dulbecco's Modified Eagle Medium (DMEM) supplemented with 10% foetal bovine serum (FBS) 100 U/ml penicillin and 100 µg/ml streptomycin (Invitrogen, Carlsbad, CA). Myoblasts were plated at a density of 2 x $10^4/cm^2$ in 12-well plates. Upon confluence (~48 hours), medium was changed to high-glucose DMEM supplemented with 2% horse serum (Invitrogen) 100 U/ml penicillin and 100 µg/ml streptomycin for 6-7 days until multinucleated myotubes had formed. For CrT siRNA experiments, medium without penicillin or streptomycin was used. Medium was changed every 48 hours.

4.2.2 CrT siRNA transfections

Myotubes were transfected with 60 pmol pre-designed Stealth RNAi^{TM} siRNA for the CrT gene (SLC6A8 solute carrier class 6, member 8) (cat no. RSS328932, RSS328933 and RSS328934) or the Stealth RNAi siRNA Negative Control Medium GC (scramble siRNA; Invitrogen). Transfections were performed using 2µL/well Lipofectamine 2000 Transfection Reagent diluted in Opti-MEM Reduced Serum Medium (Invitrogen). Medium was replaced after 24 hours. For optimisation of the different siRNA sequences, myotubes were harvested for RNA after 72 hours. For all other experiments, myotubes were infected with GFP, hPGC-1α or hPGC-1β for 48 hours following the transfection. Myotubes were harvested at 72 hours for RNA, protein and creatine uptake assays, and 96 hours for protein synthesis assays.

4.2.3 Adenoviral Infections

siERRa combined with PGC-1 experiments

To infect cells, the required amount of adenovirus was added to fresh cell culture medium and then added to each well. Myotubes were infected with an adenovirus expressing siRNA for ERRα (siERRα) or its control, siSUPER, using an MOI 200. After 24 hours, myotubes were infected with an additional dose of siERRα (or its

control vector), as well as GFP, hPGC-1α or hPGC-1β at an MOI of 100. Cells were harvested after 72 hours for RNA, protein and creatine uptake assays.

VP16-ERRα experiments

Myotubes were infected with an adenovirus expressing ERRα with a heterogeneous strong transcriptional activation domain, VP16-ERRα, or its control VP16-control, using an MOI of 100. Cells were harvested after 72 hours for RNA, protein, and creatine uptake assays.

4.2.4 Messenger RNA (mRNA) expression

RNA extraction

RNA was extracted using Tri-Reagent solution (Ambion Inc., Austin, TX) according to manufacturer's protocol. RNA concentrations were determined using the NanoDrop 2000 (NanoDrop products, Wilmington, DE). RNA (1 µg) was reverse transcribed to complementary DNA (cDNA) using a High Capacity cDNA reverse transcription kit (Applied Biosystems, Forster City, CA) according to manufacturer's protocol. cDNA was diluted to 5 ng/µl in nuclease free water (NFW).

Real-time polymerase chain reaction

Real-time quantitative polymerase chain reaction (qPCR) was performed using a Stratagene Mx3000P qPCR System and the MxPro qPCR software (Stratagene, La Jolla, CA). Cycling conditions for the PCR consisted of one denaturing cycle at 95°C for 2 minutes, followed by 40 cycles of denaturing at 95°C for 5 seconds and annealing at 60°C for 20 seconds, and elongation at 72°C for 60 seconds. A dissociation curve was generated to show that only one product had been amplified during the PCR. Each 20 µL reaction contained 0.5 x Power SYBR Green PCR Master Mix (Applied Biosystems), 25 ng of cDNA, and the forward and reverse primers for the gene of interest. Primers were designed to cross exons using Primer 3 (www.primer3.sourceforge.net) and the sequences cross checked for gene specificity using a BLAST search (www.ncbi.nlm.gov/BLAST). Primers were synthesised by Gene Works (Adelaide, SA). Genes amplified in the PCR are shown in Table 4.01. All samples were measured in triplicate. To compensate for variations in input RNA

amounts and efficiency of the reverse transcription, data was normalised ribosomal protein, 36B4 (also known as RPLPO) mRNA.

Table 4.01 Primers used in the real-time qPCR

Primer	GenBank accession no.	Forward Primer (5'-3')	Reverse Primer (5'-3')
Rat CrT	NM_017348.2	CTGTCTCCTCAGGGCAAAAG	CTAAAGCTGGGGCTGCTATG
Rat 36B4	NM_022402.2	CCAGAGGTGCTGGACATCACAGAG	TGGAGTGAGGCACTGAGGCAAC

4.2.5 Protein expression

Protein extraction

Myotubes were lysed in RIPA buffer (Merck-Millipore, Kilsyth, VIC) with 1 µL/mL protease inhibitor cocktail (Sigma-Aldrich, St Louis, MO) and 10 µL/mL Halt Phosphatase Inhibitor Single-Use Cocktail (Thermo scientific, Rockford, IL). Protein concentrations were determined using the bicinchoninic acid (BCA) Protein Assay Kit (Pierce Biotechnology, Rockford, IL) according to the manufacturer's protocol, and absorbance was measured on a Synergy 2 Microplate Reader (BioTek, Winooski, VT).

Western Blotting

Electrophoresis was performed using a 4-12% NuPAGE® Novex Bis-Tris Gel (Invitrogen) in NuPAGE® SDS MOPS Running Buffer (Invitrogen). Twenty micrograms of protein was loaded into each well of a 10-well gel. Protein transfer was performed in a Bjerrum buffer containing 50 mM Tris, 17 mM glycine and 10 % methanol using polyvinylidene difluoride (PVDF) membranes (Merck-Millipore). The membranes were blocked with 5 % bovine serum albumin (BSA; Sigma-Aldrich) in PBS for one hour, and incubated overnight at 4ºC with the following primary antibodies diluted in 5% BSA in PBS: PGC-1α (Merck-Millipore); PGC-1β (Novus Biologicals, Littleton, CO); ERRα (Epitomics, Burlingame, CA); and Glyceraldehyde 3-phosphate dehydrogenase (GAPDH; Sigma-Aldrich). All primary antibodies were diluted 1:1,000, except for GAPDH which was diluted 1:10,000). Following washing, the membranes were incubated for 1 hour with either IRDye® 800CW Goat Anti-Rabbit IgG (H+L) (LI-COR Biosciences, Lincoln NE), or Alexa Fluor® 680 Rabbit Anti-Mouse IgG (H+L) (Invitrogen), diluted 1:5,000 in PBS containing 50% Odyssey Blocking Buffer. Proteins were visualised on an Odyssey

Infrared Imaging System (LI-COR Biosciences) and densitometry was achieved using Odyssey Application Software 3.0 (LI-COR Biosciences). All blots were normalised to GAPDH protein.

4.2.6 Creatine Uptake Assay

Creatine uptake was determine by measuring the incorporation of radiolabelled [^{14}C]-creatine (American Radiolabeled Chemicals, St Louis, MO) into the myotubes. During the last hour of adenoviral infections, myotubes were incubated in creatine uptake buffer consisting of DMEM with 2% FBS (Invitrogen), 100 μM creatine (Sigma-Aldrich), and 1 μCi/mL [^{14}C]-Creatine. To stop the reaction, myotubes were washed in PBS and lysed in 500 μL 0.5 N NaOH/0.1% Triton X-100 (Sigma-Aldrich). Samples were mixed with Ultima Gold scintillation liquid (Perkin Elmer, Boston, MA) and the uptake of [^{14}C]-Creatine was measured using a Wallac 1409 DSA liquid scintillation counter (Perkin Elmer). Counts were normalised to protein content determined via the BCA Protein Assay Kit (Pierce Biotechnology).

4.2.7 Protein synthesis

Protein synthesis was determined by measuring the incorporation of radio-labelled [^{3}H]-tyrosine (Perkin Elmer) into the myotubes (modified from [254]). After adenoviral infections, myotubes were incubated in 1 μCi/ml of radio-labelled [^{3}H]-tyrosine and 2 mM L-tyrosine (Sigma-Aldrich). The use of excess non-radioactive tyrosine in the medium gives an accurate indication of protein synthesis rates without alterations in the free intracellular tyrosine pool [255]. The reaction was stopped by washing the cells with cold PBS, and then 0.5 ml of cold 10% trichloroacetic acid (TCA; Sigma-Aldrich) was added to each well. After scraping, myotubes sat on ice for 1 hour to precipitate the protein, followed by centrifugation at 20,000 x g for 10 minutes. The supernatant was removed, and the precipitates were dissolved in 0.1 M NaOH/1% Triton X-100 (Sigma-Aldrich) overnight at room temperature. The samples were mixed with Ultima Gold scintillation liquid (Perkin Elmer) and myotube protein radioactivity was measured using a Wallac 1409 DSA liquid scintillation counter (Perkin Elmer) and expressed as counts per minute (CPM). Counts were normalised to total genomic DNA which was extracted using the

Allprep DNA/RNA mini kit (Qiagen, Clifton Hill, VIC), as per the manufacturer's protocol. DNA was quantified using the NanoDrop 2000 (NanoDrop products).

4.2.8 Myotube Diameter

Myotubes were visualised using an Olympus IX70 microscope (Olympus, Mt Waverly, VIC), and digital images were obtained using a DS-U3 microscope camera and NIS-Elements imaging software (Nikon Instruments Inc., Melville, NY). Approximately 10 myotubes from 10 different fields of view were analysed for myotube diameter for each condition. Three measurements along each myotube were made to allow for differences in diameter across the length of the myotube

4.2.9 Chromatin immunoprecipitation (ChIP)

Cell culture and adenoviral infections

Adenoviruses expressing LacZ, FLAG-tagged PGC-1α, ERRα, and short hairpin RNA (shRNA) for GFP and ERRα were a gift from Natasha Kralli (Scripps Research Institute, La Jolla, CA) and have been described previously [212, 331]. C2C12 myoblasts were maintained in DMEM with 10% FBS (Invitrogen, Carlsbad, CA) at 37 °C with 5% CO2. Confluent myoblasts were differentiated into myotubes by the addition of DMEM with 2% horse serum (Invitrogen). Myotubes were infected on day 4 of differentiation with adenoviruses expressing shRNAs (at MOI 50), and on day 6 of differentiation with adenoviruses expressing LacZ (control) and FLAG-PGC-1α (at MOI 50), together with a second dose of shRNA-expressing adenoviruses (at MOI 25). The cells were harvested 24 h later.

ChIP assay

ChIP assays were performed with adenovirus-infected C2C12 myotubes as described previously [173]. C2C12 myotubes were cross-linked for 10 minutes at 37º in 1% formaldehyde in PBS. After quenching, sonication to ~500bp fragments, and pre-clearing by treatment with protein A/G sepharose, soluble chromatin was immunoprecipitated with the following antibodies: anti-GFP (control), anti-FLAG (clone M2) for the detection of FLAG-Tagged PGC-1α, or anti-ERRα (Epitomics, Burlingame, CA). Genomic DNA in the immunopurified complex was quantified by PCR using CrT primers: Forward: 5' GGATCCCATGGAATCAGGTCTT and

Reverse: 5’ GGCAACTGGGAAACAGAAATCA, which amplifies a region containing an ERRα response element (ERRE) upstream of the transcriptional start-site. Data were normalised to total genomic DNA input and expressed relative to the PCR values in the anti-GFP control samples.

4.2.10 Statistics

Statistical analyses were performed using either a t-test or a two-way analysis of variance (ANOVA) (Prism, GraphPad Software, La Jolla, CA). Multiple t-tests were used for post-hoc analysis to determine differences between groups if significant interactions were found. The level of significance was set at $P < 0.05$ for paired t-test analysis, while a Bonferroni adjustment was used for the two-way ANOVA reducing the level of significance to $P < 0.0125$. All data is presented as mean ± standard error of the mean (SEM) and as fold-change relative to GFP control, unless otherwise stated.

4.3 Results

4.3.1 PGC-1α and PGC-1β regulate CrT mRNA

Overexpression of PGC-1α and PGC-1β in L6 myotubes led to a 2.1-and 1.7-fold increase in CrT mRNA expression respectively (Figure 4.01).

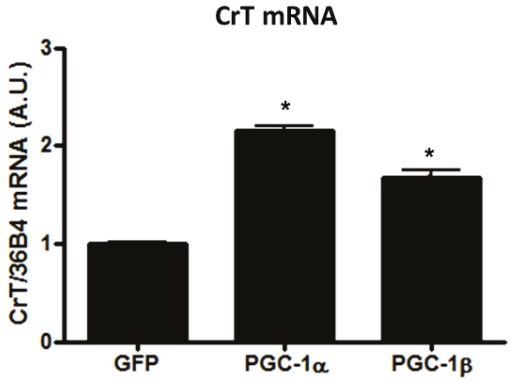

Figure 4.01 CrT mRNA expression in GFP, PGC-1α and PGC-1β infected L6 myotubes. Samples were harvested 48 hours after infection. Values were normalised to 36B4 mRNA expression. $n = 5$ per group. *$P < 0.01$ compared to GFP.

4.3.2 PGC-1α and PGC-1β regulate creatine uptake via the creatine transporter.

As PGC-1α and PGC-1β increase CrT mRNA expression, creatine uptake into the cells was also measured. To confirm that the effect of PGC-1α and PGC-1β on creatine uptake was via their increase in CrT levels, myotubes were co-transfected with siRNA for CrT. The efficiency of the CrT siRNA was determined by transfecting L6 myotubes with three different CrT sequences, cat no. RSS328932, RSS328933 and RSS328934 (hereon referred to as 932, 933 and 934, respectively), as well as the scramble siRNA control. Figure 4.02A shows that there was a 71%, 65% and 69% decrease in CrT mRNA expression with the 932, 933, and 934 siRNA sequences respectively. CrT protein expression was unable to be measured due to antibody unavailability [332, 333]. Sequences 932 and 934 were then used for future experiments to ensure optimal knockdown of CrT. Figure 4.02B shows CrT mRNA expression when myotubes were transfected with CrT siRNA and overexpressed with PGC-1α and PGC-1β. Transfection with CrT siRNA lead to a 52% decrease in CrT mRNA in the GFP group. PGC-1α and PGC-1β increased CrT mRNA by 2.1- and 1.7-fold respectively, however this was attenuated with the co-transfection of the CrT siRNA.

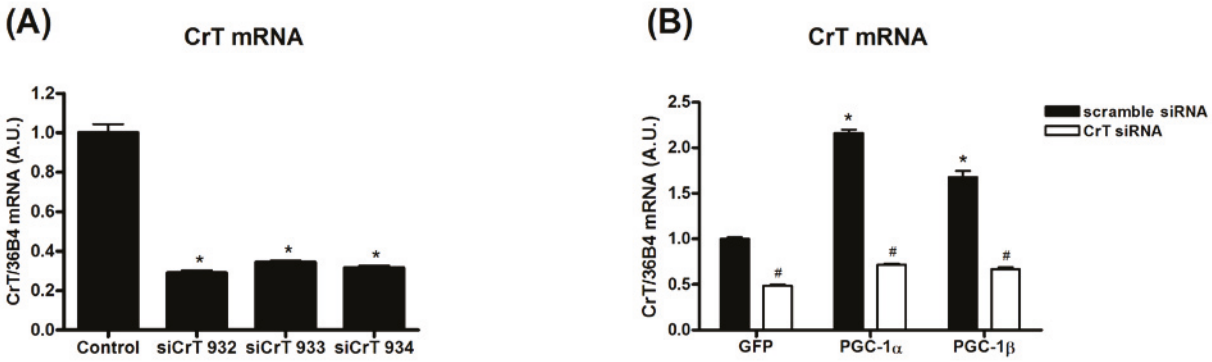

Figure 4.02 CrT mRNA expression in L6 myotubes. (A) CrT mRNA expression measured 72 hours after transfection with CrT siRNAs 932, 933 and 934, compared to the scramble siRNA control. Values were normalised to 36B4 mRNA. *P < 0.01 compared to scramble siRNA. (B) CrT mRNA expression in GFP, hPGC-1α- and hPGC-1β-infected L6 myotubes, co-transfected with either scramble or CrT siRNA. Values were normalised to 36B4 mRNA. n = 5 per group. *P < 0.0125 compared to GFP scramble siRNA; $^{\#}P$ < 0.0125 compared to scramble siRNA for each group.

Figure 4.03A and figure 4.03B show protein expression via western blot analysis for PGC-1α and PGC-1β respectively, to confirm their overexpression in these samples. No differences were seen in PGC-1α or PGC-1β protein levels between scramble and CrT siRNA.

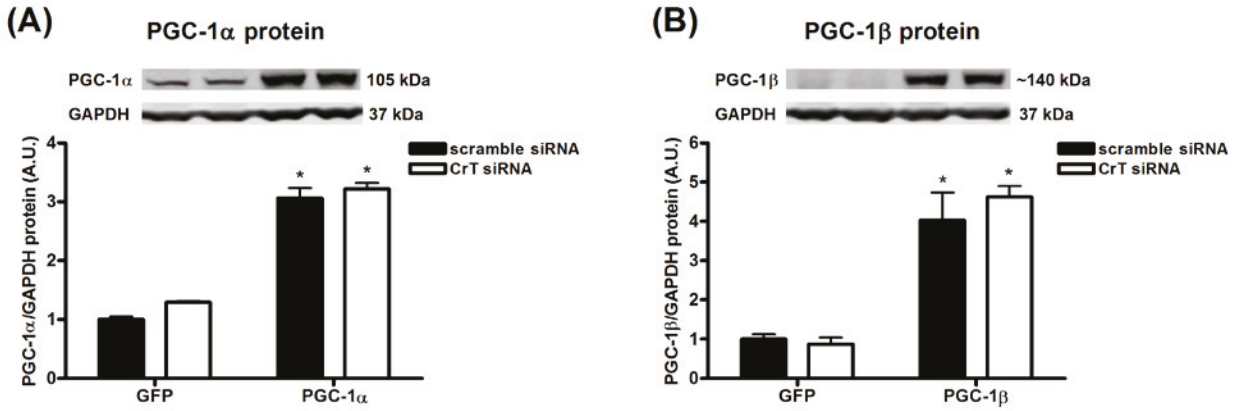

Figure 4.03 PGC-1α and PGC-1β protein expression GFP-, hPGC-1α- and hPGC-1β-infected L6 myotubes, co-transfected with either scramble or CrT siRNA. Samples were harvested after 72 hours. (A) PGC-1α protein, and (B) PGC-1β protein. Bands were normalised to GAPDH protein. n = 3 per group. *P < 0.0125 compared to GFP-scramble siRNA.

Figure 4.04 shows that PGC-1α and PGC-1β overexpression increased creatine uptake by 1.8- and 1.6-fold respectively, when compared to GFP. Similar to the expression of CrT mRNA, co-transfection with CrT siRNA reduced creatine uptake by 40% in the GFP samples and prevented the PGC-1α- and PGC-1β-induced increase in creatine uptake.

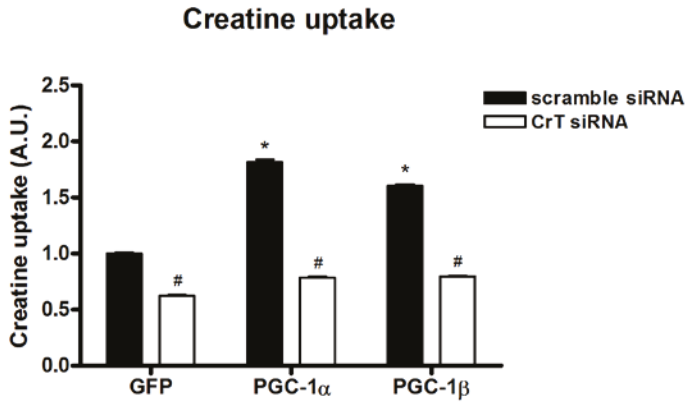

Figure 4.04 Creatine uptake in GFP, PGC-1α and PGC-1β infected L6 myotubes, co-transfected with either scramble or CrT siRNA. [^{14}C]-creatine incorporation was measured during the last hour of infection. $n = 6$ per group, repeated in 3 experiments. $^{*}P < 0.0125$ compared to GFP scramble siRNA; $^{\#}P < 0.0125$ compared to scramble siRNA for each group.

4.3.3 PGC-1α and PGC-1β regulate CrT and creatine uptake via ERRα

To determine if PGC-1α and PGC-1β regulate creatine transport via ERRα, L6 myotubes were co-infected with siERRα or its control vector siSUPER. Figure 4.05A shows protein expression for ERRα to confirm its knockdown in L6 myotubes. As expected [100, 190], PGC-1α and PGC-1β overexpression lead to a significant increase in ERRα protein. Infection with siERRα reduced ERRα protein in all groups when compared to siSUPER. However, when compared to GFP, ERRα protein was still higher in the PGC-1α and PGC-1β groups. Figure 4.05B and C show protein expression for PGC-1α and PGC-1β respectively, to confirm their overexpression in the samples. PGC-1α expression was increased in both the siSUPER and siERRα groups when compared to GFP (Figure 4.05B). PGC-1β expression was also increased in both groups; however it was lower in the PGC-1β-siERRα group when compared to the PGC-1β-siSUPER group (Figure 4.05C).

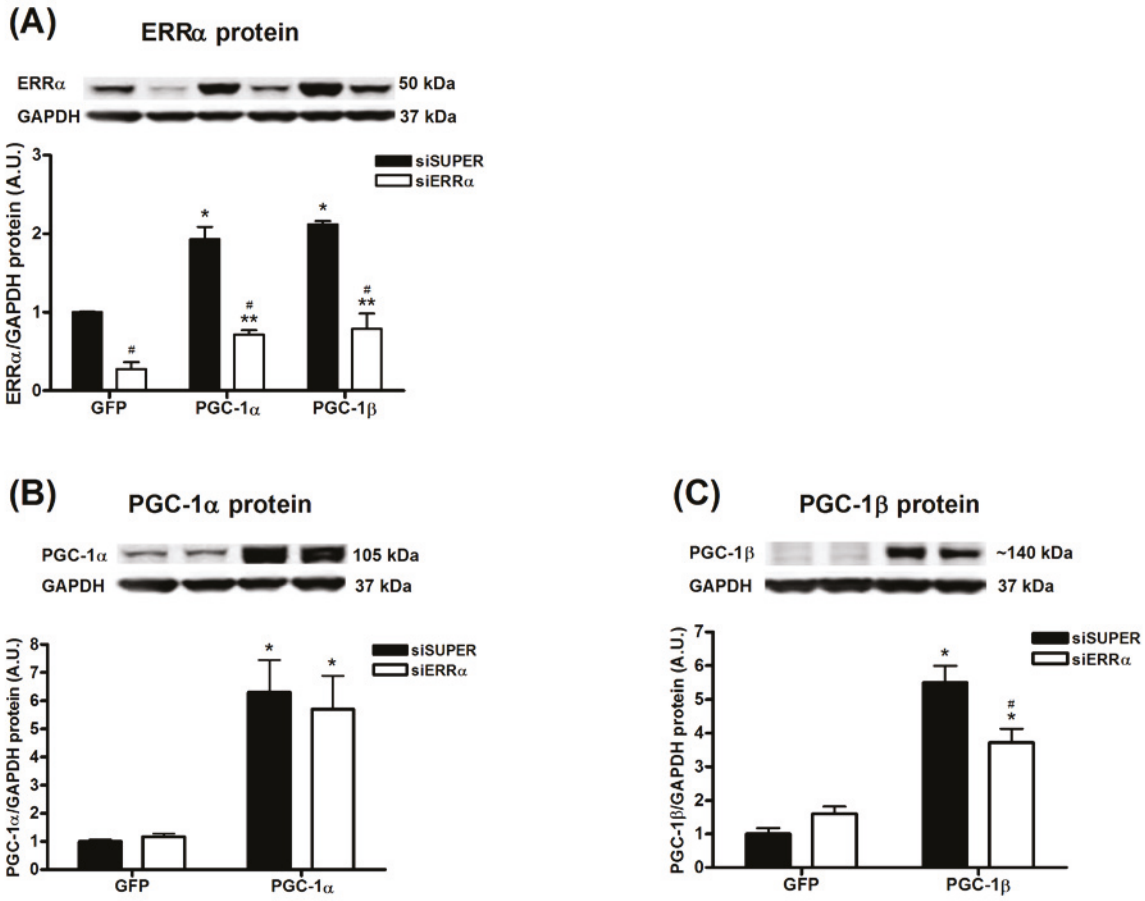

Figure 4.05 ERRα, PGC-1α and PGC-1β protein expression in L6 myotubes infected with siERRα and PGC-1 adenoviruses. Myotubes were infected with either siSUPER or siERRα, followed by infection with GFP, hPGC-1α or hPGC-1β. Samples were harvested after 72 hours. (A) ERRα protein, (B) PGC-1α protein, and (C) PGC-1β protein. Bands were normalised to GAPDH protein. $n = 4$ per group. $^{*}P < 0.0125$ compared to GFP-siSUPER; $^{**}P < 0.0125$ compared to GFP-siERRα; $^{\#}P < 0.0125$ compared to siSUPER for each group.

Knockdown of ERRα reduced CrT mRNA by 25% in the GFP infected samples, and also prevented the increase in CrT mRNA that was seen with PGC-1α and PGC-1β overexpression (Figure 4.06A). PGC-1α and PGC-1β overexpression increased creatine uptake in the siSUPER control samples (Figure 4.06B). Knockdown of ERRα inhibited this increase in creatine uptake, but had no effect on creatine uptake in the GFP samples.

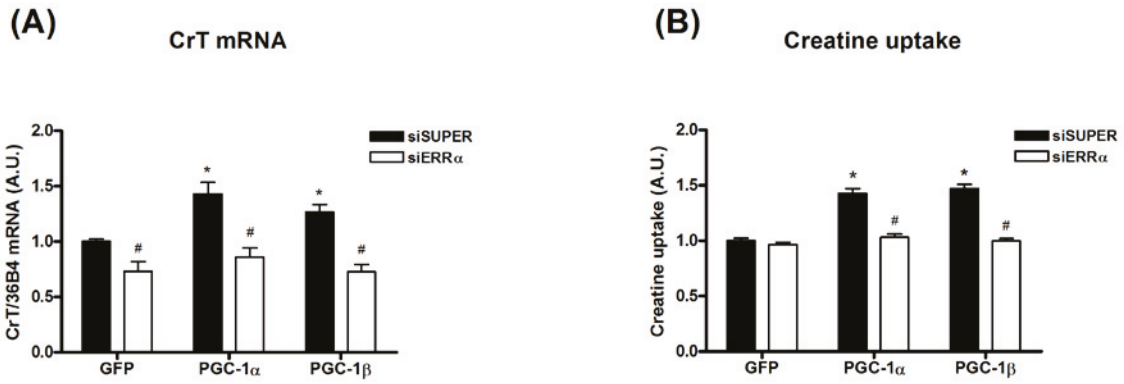

Figure 4.06 CrT mRNA and creatine uptake in L6 myotubes infected with siERRα and PGC-1 adenoviruses. Myotubes were infected with either siSUPER or siERRα, followed by infection with GFP, hPGC-1α or hPGC-1β. Samples were harvested after 72 hours. (A) CrT mRNA expression, normalised to 36B4 mRNA expression. (B) Creatine uptake, determined by [^{14}C]-creatine incorporation during the last hour of infection. n = 6 per group, repeated in 3 experiments. *P < 0.0125 compared to GFP siSUPER; $^{\#}P$ < 0.0125 compared to siSUPER for each virus.

4.3.4 Constitutively active ERRα increases CrT expression and creatine uptake.

The previous results show that ERRα may regulate creatine uptake when activated by PGC-1α or PGC-1β, but had no effect under basal conditions. To further support the role of ERRα in the regulation of creatine uptake, L6 myotubes were expressed with a constitutively active form of ERRα (VP16-ERRα) and its control (VP16-control). Figure 4.07 shows that infection with VP16-ERRα at an MOI of 100 lead to approximately a 4-fold increase in ERRα protein.

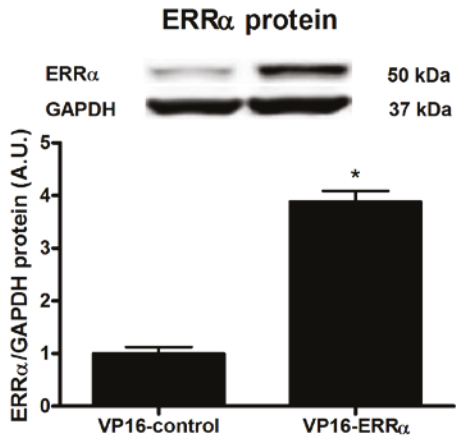

Figure 4.07 ERRα protein in L6 myotubes infected with VP16-ERRα. VP16-control was the control adenovirus. Samples were harvested after 48 hours. Bands were normalised to GAPDH protein. $n = 4$ per group. *$P < 0.01$ compared to VP16-control.

VP16-ERRα infection increased CrT mRNA by approximately 8-fold when compared to VP16-control (Figure 4.08A). Furthermore, creatine uptake was increased by roughly 2.2-fold when compared to the VP16-control group (Figure 4.08B).

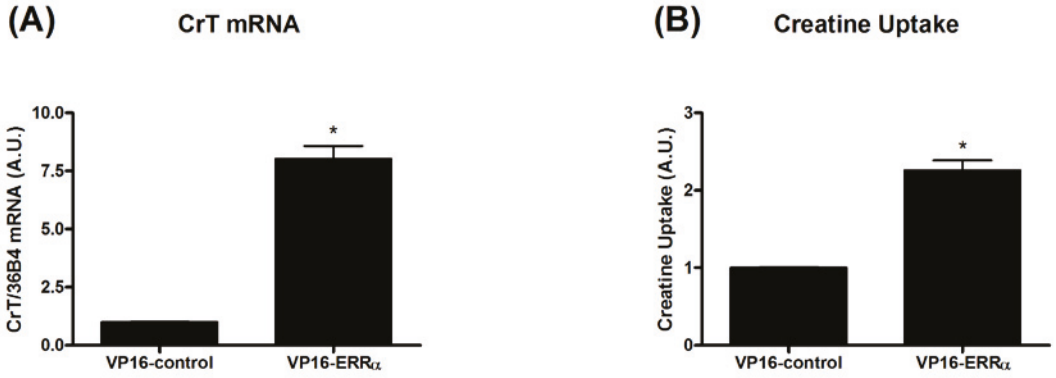

Figure 4.08 CrT mRNA and creatine uptake in L6 myotubes infected with VP16-ERRα. Samples were harvested after 72 hours of infection. (A) CrT mRNA expression, normalised to 36B4 mRNA. (B) Creatine uptake, determined by [^{14}C]-creatine incorporation during the last hour of infection. $n = 6$ per group, repeated in 3 experiments. *$P < 0.01$ compared to VP16-control.

4.3.5 ERRα is essential for recruitment of PGC-1α to the CrT promoter

To test if ERRα and PGC-1α act directly at the CrT gene to induce its expression, ChIP was performed to determine whether ERRα and PGC-1α interact physically with the CrT promoter. Analysis of the CrT genomic sequence indicated a putative ERRα binding site matching the known 9 bp ERRE consensus 5'-TNAAGGTCA-3' [244] and conserved across species (Figure 4.09A), suggesting that CrT is a direct target of PGC-1α and ERRα. To determine binding of endogenous ERRα and exogenous adenovirally-expressed PGC-1α at this region, crosslinked chromatin was immunoprecipitated with antibodies against either GFP (control antibody measuring background), FLAG-tagged PGC-1α, or ERRα, and the enrichment of the CrT locus DNA in the immunoprecipitated material was measured. Both PGC-1α and ERRα were detected at the CrT ERRE (Figure 4.09B). ERRα was detected at the CrT locus only when PGC-1α was expressed, i.e. when endogenous ERRα levels were induced [238]. Knockdown of endogenous ERRα expression by shRNA ablated binding of PGC-1α to the CrT ERRE (Figure 4.09B), demonstrating a critical role for ERRα in recruitment of the PGC-1α coactivator to the CrT promoter.

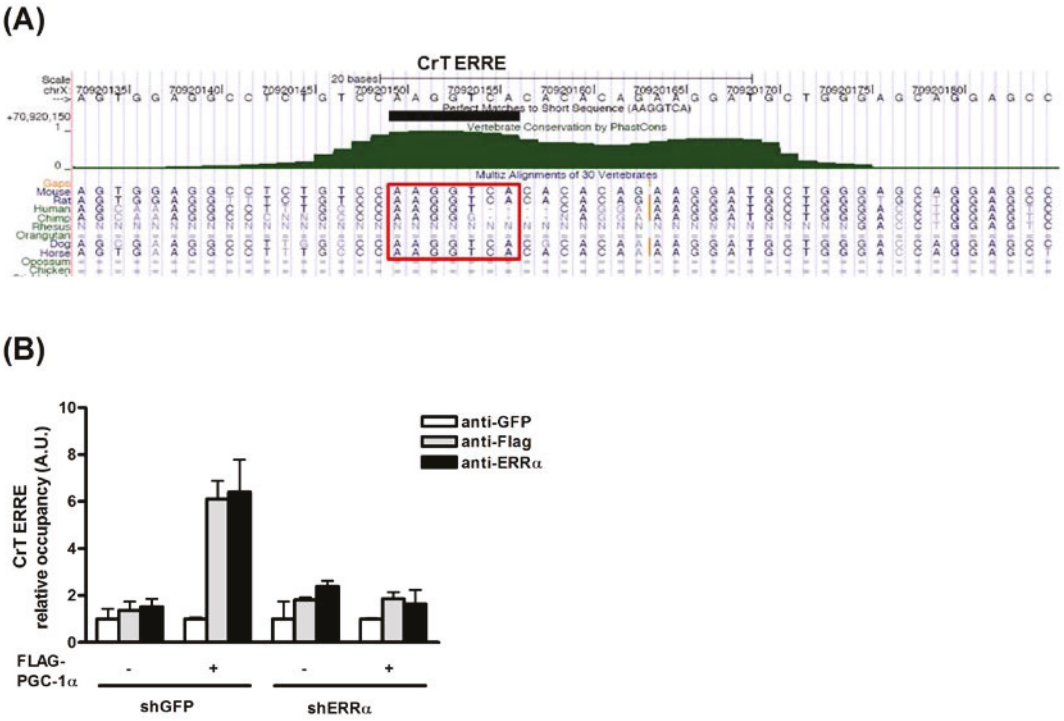

Figure 4.09 PGC-1α and ERRα bind an ERRE in the first intron of the CrT promoter. (A) Graphic representation of the ERRE located in the first intron of the CrT promoter across species (University of California, Santa Cruz, genome browser). (B) ChIPs were performed using antibodies against GFP (control), FLAG (PGC-1α) and ERRα, in C2C12 myotubes infected with adenoviruses expressing LacZ (control) or PGC-1α, in the absence (shGFP) or presence of shRNA for ERRα (shERRα). The abundance of CrT ERRE is expressed relative to each region in the control, GFP samples. Data are mean ± SD of two independent experiments (n = 5).

4.3.6 PGC-1α and PGC-1β increase protein synthesis and myotube diameter independently of CrT

To determine whether the PGC-1α-and PGC-1β-induced increase in protein synthesis was via their increase in CrT and creatine transport, [^{3}H]-tyrosine incorporation was measured in these samples. Figure 4.10A shows that PGC-1α and PGC-1β overexpression lead to a 19% and 23% increase in protein synthesis respectively, when compared to GFP. However this effect was not influenced by the knock-down of the CrT. Similarly, knockdown of CrT did not affect myotube diameter in L6 myotubes (Figure 4.10A & B).

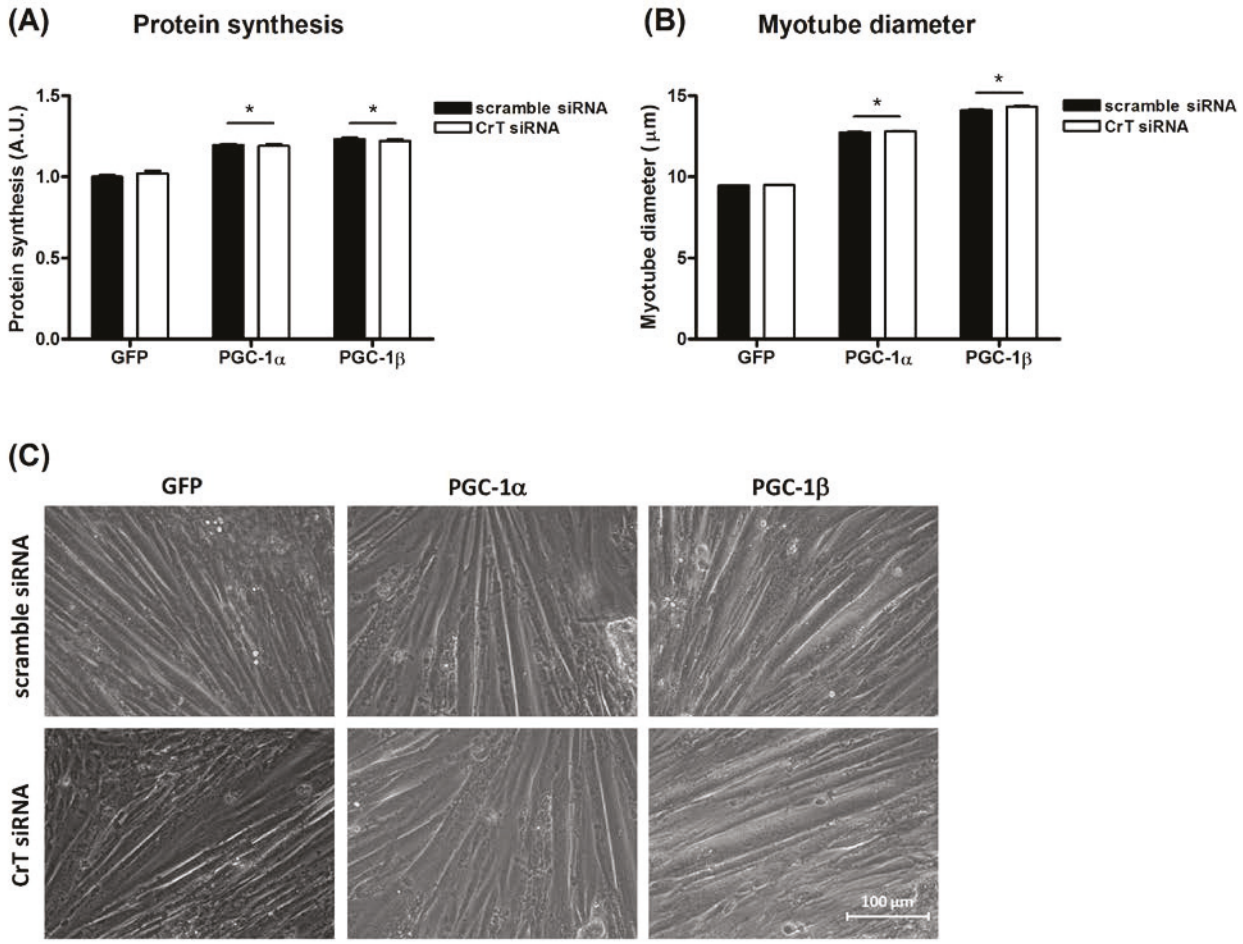

Figure 4.10 Protein synthesis and myotube diameter in GFP-, PGC-1α- and PGC-1β-infected L6 myotubes, co-transfected with either scramble or CrT siRNA. (A) Protein synthesis, measured via [^{3}H]-tyrosine incorporation for 24 hours following adenovirus infection. n = 6 per group, repeated in 3 experiments. (B) Average myotube diameter from 10 myotubes per visual field (10 visual fields for each group). (C) Representative images of GFP, PGC-1α and PGC-1β infected myotubes, with scramble or CrT siRNA. *P < 0.0125 compared to GFP-scramble siRNA.

4.4 Discussion

Skeletal muscle creatine levels are reduced in many conditions associated with skeletal muscle atrophy [229], and creatine supplementation increases muscular strength and mass under such conditions [234]. However, the ability for creatine to enter the cell is dependent on the CrT, and CrT levels are often reduced in diseased skeletal muscle [239]. As such, understanding the molecular mechanisms that regulate the CrT and creatine uptake into skeletal muscle is important for restoring or increasing intracellular creatine levels and improving skeletal muscle health. This study aimed to determine whether PGC-1α and PGC-1β can regulate the CrT and creatine uptake in rat L6 myotubes, and whether PGC-1α and PGC-1β increase protein synthesis by increasing the CrT and intracellular creatine uptake. Several novels observations were made. Firstly, overexpression of PGC-1α or PGC-1β increased CrT mRNA as well as creatine uptake into L6 myotubes. Secondly, these effects were dependent on the transcription factor, ERRα. Thirdly, PGC-1α and ERRα directly bind to the CrT promoter to induce its expression. And lastly, the PGC-1α- and PGC-1β-induced increase in protein synthesis and myotube diameter was not associated with CrT or intracellular creatine content.

In skeletal muscle, PGC-1α and PGC-1β are expressed in a similar manner to the CrT, as they are highly expressed in oxidative muscle fibres [163, 177] and down-regulated in many disease conditions associated with skeletal muscle atrophy [65, 155]. PGC-1α and PGC-1β regulate the expression of many genes involved in energy metabolism [96]. Therefore, it was of interest to determine whether they may regulate CrT expression and creatine uptake, which are critical to maintaining cellular energy homeostasis. For the first time, this study has shown that overexpression of PGC-1α or PGC-1β increase CrT mRNA and uptake of [^{14}C]-Creatine in L6 myotubes. It is important to note that CrT protein levels were unable to be measured due to a lack of specific antibodies [333]. However, the increased creatine uptake is a good indication of CrT function [334]. In addition, knockdown of the CrT using siRNA completely ablated this effect. As decreased intracellular creatine is thought to regulate CrT expression [241, 242], it is possible that under normal conditions, a decrease in creatine within the muscle may signal to PGC-1α

and PGC-1β to increase CrT expression. PGC-1α activity is induced in response to metabolic stress [94, 335], in particular, by activation from the energy sensor, 5' adenosine monophosphate-activated protein kinase (AMPK) [134, 136]. Increased levels of phosphocreatine down-regulate AMPK in mouse myotubes *in vitro* [336], while treatment with β-GPA, a competitive inhibitor of the CrT, increases AMPK expression in the soleus muscle of mice [152]. Interestingly, PGC-1α and PGC-1β mRNA are also slightly increased after β-GPA treatment [152]. Furthermore, activation of AMPK by 5-aminoimidazole-4-carboxamide-1-β-D-ribonucleoside (AICAR) increases creatine transport and CrT content in rodent cardiomyocytes [337]; whether this is directly via PGC-1α or PGC-1β however, has not been investigated. Moreover, it is unknown whether PGC-1β can be regulated by AMPK, and therefore further investigation is required into signalling mechanisms that may be responsible for the induction of PGC-1β, as well as PGC-1α, to increase CrT expression and creatine uptake in skeletal muscle.

In skeletal muscle, PGC-1α and PGC-1β induce the expression of many genes involved in energy metabolism and mitochondrial function via their co-activation of ERRα [160, 190]. In chapter 2, it was established that PGC-1α and PGC-1β increase protein synthesis in C2C12 myotubes, and that this effect is also dependent on ERRα. It was therefore of interest to determine whether PGC-1α and PGC-1β increase CrT mRNA expression and creatine uptake via ERRα. Knockdown of ERRα using siRNA inhibited the PGC-1α- and PGC-1β-induced increase in CrT mRNA and creatine uptake in L6 myotubes. However, knockdown of ERRα did not affect creatine uptake under basal conditions (i.e. in the GFP-infected cells), despite a 25% decrease in CrT mRNA. The lack of effect on basal creatine uptake is in line with other studies that suggest ERRα is active only when coactivated by PGC-1α or PGC-1β [212]. It was interesting that CrT mRNA was decreased, showing that ERRα may have been partially active under basal conditions. However additional studies are required to determine this. Further supporting the role of ERRα in creatine uptake, overexpression of a constitutively active ERRα increased CrT mRNA and creatine uptake by 8- and 2.2-fold respectively. Lastly, ChIP assays revealed that PGC-1α and ERRα directly interact with the CrT promoter. These findings, together with the

ERRα knockdown experiments, suggest that ERRα is crucial for the PGC-1α- and PGC-1β-induced increase in CrT mRNA and creatine uptake.

Creatine supplementation increases strength, fat-free mass, and muscle fibre size when used in combination with resistance training [231-233], or in the treatment of myopathies presenting with muscle atrophy [234-236]. Whether this is due to an increase in protein synthesis is debateable [246, 247], although early studies show that creatine increases the synthesis of contractile proteins in differentiating myotubes *in vitro* [248, 249]. The current study has observed that the PGC-1α/ERRα and PGC-1β/ERRα transcriptional pathways result in increased CrT mRNA expression and creatine uptake in L6 myotubes. It is therefore plausible that PGC-1α and PGC-1β may increase protein synthesis by increasing CrT mRNA in myotubes. However, knockdown of CrT mRNA and inhibiting creatine uptake did not affect the PGC-1α- or PGC-1β-induced increase in protein synthesis or myotube diameter in L6 myotubes. This is the first study to measure protein synthesis in myotubes after decreasing CrT mRNA and intracellular creatine levels, however these findings are in line with studies that have shown that creatine supplementation does not increase protein synthesis *in vivo* [246, 247]. These studies also show that creatine supplementation increases muscle fibre size, however knocking down the CrT and decreasing creatine uptake in the current study did not effect myotube size *in vitro.*

In summary, this study has shown for the first time that overexpression of the transcriptional coactivators, PGC-1α and PGC-1β, can increase CrT mRNA and creatine uptake in L6 myotubes in an ERRα-dependent manner. These novel findings provide insight into how the CrT and creatine uptake are regulated in skeletal muscle, which may assist in the treatment of patients suffering from myopathies characterised by decreased CrT and intracellular creatine levels. Finally, knockdown of the CrT and decreased creatine uptake does not affect protein synthesis or myotube diameter in L6 myotubes.

Chapter 5

General Discussion, Conclusions and Future Directions

5.1 Summary of Major Findings

Skeletal muscle mass is regulated by a fine balance between protein synthesis and protein degradation [31]. Decreased rates of protein synthesis in combination with increased rates of protein degradation result in skeletal muscle atrophy, a devastating condition contributing to increased morbidity and mortality. Understanding the molecular and physiological mechanisms involved in the regulation of muscle mass is therefore a prerequisite for developing therapeutic interventions to improve clinical outcomes. The transcriptional coactivators, PGC-1α and PGC-1β, positively regulate skeletal muscle mass via their attenuation of protein degradation. However, their effect on protein synthesis is unknown. The general aim of this thesis was to investigate the roles of PGC-1α and PGC-1β in the regulation of protein synthesis in C2C12 myotubes, a rodent skeletal muscle cell line.

In Chapter 2, it was shown for the first time that overexpression of PGC-1α and PGC-1β increased protein synthesis and myotube diameter in C2C12 myotubes. This effect on protein synthesis also occurred in myotubes treated with dexamethasone, suggesting that PGC-1α and PGC-1β may have the potential to increase protein synthesis *in vivo* during systemic wasting diseases. Secondly, this increase in protein synthesis was independent of Akt and mTOR signalling, as this effect was not prevented after treatment with inhibitors of these pathways. Interestingly, the phosphorylation of Akt and p70S6k was suppressed after PGC-1α and PGC-1β overexpression, although the functional significance of these findings is unknown. Lastly, knockdown of the transcription factor, estrogen-related receptor alpha (ERRα) using siRNA prevented the PGC-1α- and PGC-1β-induced increase in protein synthesis and myotube diameter, while expression of a constitutively active ERRα exacerbated this effect. Like many other important PGC-1α- or PGC-1β-mediated processes in skeletal muscle, ERRα is therefore required for PGC-1α and

PGC-1β to increase protein synthesis in C2C12 myotubes. In addition to their already known effect on the attenuation of myotube protein degradation, these findings show that PGC-1α and PGC-1β can also increase protein synthesis, and therefore present as attractive targets for the development of treatment strategies to alleviate the debilitating effects of muscle atrophy. However, further investigation into the downstream targets regulated by PGC-1α and PGC-1β is required.

In Chapter 3, global gene and protein expression profiling was undertaken to investigate potential downstream targets that PGC-1α and PGC-1β may regulate to positively influence muscle mass. Gene set enrichment analysis (GSEA) identified several Gene Ontology (GO) terms and Kyoto Encyclopedia of Genes and Genomes (KEGG) pathways differentially regulated in response to PGC-1α or PGC-1β overexpression in C2C12 myotubes. Common GO terms were related to mitochondrial biology, energy metabolism, nucleotide binding, and the ribosome. Genes and proteins differentially expressed, specifically by PGC-1β, also clustered significantly with muscle contractile and cytoskeletal related GO terms. Similar to the GO terms, KEGG pathway mapping identified pathways associated with oxidative phosphorylation in both normal and disease states, and carbohydrate and fatty acid metabolism.

Further analysis of the genes differentially regulated in the microarray led to the identification of a non-biased gene expression signature (GES) which revealed the top regulated genes by PGC-1α and PGC-1β. In addition, highly regulated genes that may potentially be involved in muscle growth were biasedly selected and also explored. Of the up-regulated genes identified in the non-biased and biased approaches, protein phosphatase 1, regulatory subunit 16A (Ppp1R16a), eukaryotic translation elongation factor 1 alpha 2 (eEF1A2), eukaryotic translation initiation factor 2B, subunit 4 (eIF2B4), and vascular endothelial growth factor-A (VEGF-A) were of interest. Similar to PGC-1α expression, all of these genes were also significantly elevated in skeletal muscle after resistance exercise. Furthermore, eEF1A2 and VEGF-A mRNA were decreased in skeletal muscle of amyotrophic lateral sclerosis (ALS) patients, which corresponded with decreases in both PGC-1α and PGC-1β mRNA. These observations provide potential downstream targets that

PGC-1α and PGC-1β may regulate to increase protein synthesis for future investigation.

In contrast, of the genes that were down-regulated by PGC-1α and PGC-1β, Tripartite motif-containing protein 32 (TRIM32) and TSC22 domain family protein 3 (TSC22D3) were also decreased after resistance exercise and increased in skeletal muscle of ALS patients. TRIM32 is a ubiquitin ligase known to induce protein degradation in skeletal muscle [298], and its down-regulation by PGC-1α and PGC-1β suggests a new, additional mechanism by which PGC-1α and PGC-1β attenuate protein degradation. Lastly, Prion protein (Prnp) mRNA was also increased in skeletal muscle of ALS patients. This protein is increased in skeletal muscle during other myopathies [326, 327], and skeletal muscle-specific overexpression if Prnp causes muscle atrophy and degeneration *in vivo* [328]. It would be interesting to determine the effects of the PGC-1α- and PGC-1β-induced down-regulation of Prnp on skeletal muscle growth. Overall, the genes identified in Chapter 3 present as interesting new potential targets that may be involved in the regulation of skeletal muscle mass by PGC-1α or PGC-1β.

Lastly, Chapter 4 established that overexpression of PGC-1α and PGC-1β increased Creatine transporter (CrT) mRNA expression and creatine uptake in L6 myotubes. This effect was again dependent on the transcription factor ERRα, and it was shown that PGC-1α and ERRα directly bind to the CrT promoter to induce its expression. In skeletal muscle, PGC-1α/ERRα or PGC-1β/ERRα are known to increase mitochondrial biogenesis, the expression of OXPHOS genes, mitochondrial fusion, fatty acid oxidation, oxidative muscle fibre phenotype, and angiogenesis. Creatine uptake, as well as protein synthesis, can now be added to this list. These findings provide a commonality between muscle atrophy, mitochondrial impairments, and reduced intracellular creatine and CrT expression that is often observed during myopathies. This may provide a basis for a treatment strategy aimed at improving various aspects of skeletal muscle diseases. Lastly, the PGC-1α- and PGC-1β-induced increase in protein synthesis was not dependent on the CrT, and therefore other mechanisms may be responsible for the increase in muscle mass seen in response to increasing intracellular creatine.

5.2 Future directions

5.2.1 The effect of PGC-1α and PGC-1β on protein synthesis in vivo.

Rationale

In Chapter 2, it was shown that overexpression of PGC-1α and PGC-1β increases protein synthesis in C2C12 myotubes *in vitro*. This effect was dependent on ERRα. These studies suggest that PGC-1α and PGC-1β may increase protein synthesis *in vivo* via ERRα, however this has not been investigated.

Aims

To investigate the effect of PGC-1α/ERRα and PGC-1β/ERRα on protein synthesis *in vivo*.

Key methods

PGC-1α and PGC-1β overexpression *in vivo* can be achieved using recombinant adeno-associated viruses (rAAV) to infect mature skeletal muscle in mice. rAAVs are small single-stranded DNA viruses that are currently seen as attractive gene therapy tools to induce long-term gene expression changes without any associated pathological effects [338]. This technique also allows gene expression to be induced (i.e. after a catabolic stimulus), rather than using transgenic expression tools that require the target of interest to be overexpressed from the embryo. Currently, rAAVs are being used in several clinical trials for the treatment of muscular dystrophies [339]. rAAVs overexpressing PGC-1α or PGC-1β could be infected into ERRα knockout mice [340], and appropriate wild-type controls. In addition to basal conditions, these infections would also be carried out in different models known to decrease skeletal muscle protein synthesis, such as hindlimb immobilisation [341] and dexamethasone treatment [224, 342]. Outcome measures include measurement of protein synthesis, muscle fibre diameter and contractile function *in vivo*, as well as gene and protein expression analyses of potential downstream targets. The assessment of protein synthesis *in vivo* can be determined as described previously [343]. Briefly, following optimisation of the infection and treatment conditions, mice are injected intravenously with [^{13}C] leucine. Hindlimb muscles are extracted for the isolation of mixed, mitochondrial, and sarcoplasmic muscle proteins. Muscle

samples are then homogenized, hydrolysed, and the protein-derived amino acids purified by cation exchange chromatography. Measurement of [^{13}C]-leucine enrichment in muscle proteins is performed using a gas chromatography–isotope ratio mass spectrometer. Contractile function can be measured as described previously [344]. In brief, mice are anesthetized and the *tibialis anterior* (TA) muscle is exposed by a single incision. The TA muscle is stimulated by supramaximal (10 V) 0.2 ms square-wave pulses for 300 ms in duration, delivered via two wire electrodes adjacent to the femoral nerve. Muscle length (L_o) can be determined from maximal twitch force (P_t) and maximum tetanic force production (P_o) recorded from the plateau of a full frequency-force curve. Optimum fibre length (L_f) can be determined by multiplying L_o by the TA L_f/L_o ratio of 0.6 [345]. An isometric contraction will be initiated and held for 100 ms to allow a plateau in maximal force. Muscle lengthening occurs at a velocity of 2 L_f/s at progressively increasing magnitudes of stretch at 5, 10, 20, 30 and 40% of L_f with P_o determined prior to each lengthening contraction. This protocol examines the functional deficits following successive lengthening contractions of increasing magnitude. Muscle fibre diameter can be measured by microscopic examination of muscle sections, while gene and protein expression analyses can be performed using real-time qPCR and western blotting respectively.

Significance

PGC-1α and PGC-1β increase protein synthesis *in vitro*, and this is dependent on the transcription factor ERRα. The proposed study is required to determine whether this observation can be extended to *in vivo* models. An additional benefit of this model is the use of rAAVs to overexpress the gene of interest. Previous *in vivo* models investigating the effects of PGC-1α or PGC-1β on skeletal muscle mass have used transgenic models to investigate their effects [153, 191, 219]. Therefore, the gene of interest is overexpressed before the onset of a catabolic stimulus. Using an rAAV, it can be determined if PGC-1α and PGC-1β can increase protein synthesis after the onset of certain catabolic stimuli. This is more relevant to a human clinical setting, whereby treatment is usually given after a disease or condition has presented with symptoms. Results from the proposed study would be useful to identify possible molecular targets to therapeutically stimulate protein synthesis during catabolic conditions *in vivo*.

5.2.2 Identifying the molecular mechanisms required for the PGC-1α- and PGC-1β-induced increase in protein synthesis

Rationale

In Chapter 3, bioinformatic analysis identified several genes that were differentially expressed in response to PGC-1α or PGC-1β overexpression, in which their functions in skeletal muscle have not been well characterised. Of interest, Ppp1R16a, eEF1A2, eIF2B4, and VEGF-A, were increased in skeletal muscle after resistance exercise, while eEF1A2 and VEGF-A were also decreased in skeletal muscle of ALS patients. These are known conditions of increased and decreased muscle protein synthesis respectively. However, whether these genes are involved in the regulation of protein synthesis by PGC-1α and PGC-1β is unknown.

Aims

To determine if Ppp1R16a, eEF1A2, eIF2B4, and VEGF-A are required for the PGC-1α and PGC-1β-induced increase in protein synthesis in C2C12 myotubes *in vitro*.

Key Methods

To determine if Ppp1R16a, eEF1A2, eIF2B4, and VEGF-A are involved in regulating protein synthesis, siRNAs can be designed to knockdown their expression *in vitro.* Experiments can then be carried out using similar methods as in Chapters 2 and 4. Briefly, C2C12 myoblasts are grown and differentiated into myotubes. After optimisation conditions for each specific siRNA sequence, myotubes are transfected with siRNA for 24 hours to knockdown the gene of interest. Myotubes are then infected with adenoviruses expressing GFP, hPGC-1α, or hPGC-1β for 48 hours. Protein synthesis is determined by [^{3}H]-tyrosine incorporation over 24 hours into the myotubes, while myotube diameter is measured via microscopic examination.

Significance

The proposed study is required to determine if the differentially regulated genes identified in Chapter 3 may be involved in the PGC-1α- and PGC-1β-induced increase in protein synthesis *in vitro*. Identifying new targets that are regulated by

PGC-1α/ERRα and PGC-1β/ERRα transcriptional activity that are involved in protein synthesis will help elucidate the mechanisms by which PGC-1α and PGC-1β increase protein synthesis in skeletal muscle. Following on from this, further *in vivo* studies can be undertaken to confirm findings from these cell culture models.

5.2.3 Identifying the role of novel genes down-regulated by PGC-1α and PGC-1β in C2C12 myotubes.

Rationale

PGC-1α and PGC-1β are known to attenuate protein degradation in skeletal muscle via their down-regulation of genes involved in proteasomal and lysosomal proteolysis [219]. In Chapter 3, several novel genes were identified that were down-regulated by PGC-1α and PGC-1β overexpression. Of these, TRIM32 and Prnp were also increased in atrophied skeletal muscle of ALS patients. TRIM32 is a known ubiquitin ligase in skeletal muscle [298], suggesting another gene that PGC-1α and PGC-1β may regulate to inhibit protein degradation. Overexpression if Prnp causes muscle atrophy and degeneration *in vivo* [328], although its effects on protein degradation are unknown.

Aims

To determine if TRIM32 and/or Prnp are involved in the PGC-1α- and PGC-1β-induced attenuation of protein degradation in C2C12 myotubes *in vitro*.

Key Methods

To determine if TRIM32 or Prnp are involved in protein degradation regulated by PGC-1α and PGC-1β, siRNAs can be designed to knockdown their expression *in vitro.* Cell culture experiments can then be carried out using similar methods as in Chapters 2 and 4. Briefly, C2C12 myoblasts are grown and differentiated into myotubes. After optimisation conditions for each specific siRNA sequence, myotubes are transfected with siRNA for 24 hours to knockdown the gene of interest. Myotubes are then infected with adenoviruses expressing GFP, hPGC-1α, or hPGC-1β for 48 hours. Protein degradation *in vitro* is measured as described previously [40]. Briefly, after the desired changes in gene expression are induced, myotubes are labelled with [^{3}H]-tyrosine for 24 hours. Myotubes are then washed

and incubated in serum free medium for a further 24 hours, and the [^{3}H]-tyrosine (radioactivity) released into the media during this time is measured. Myotube diameter would also be assessed by microscopic examination.

Significance

The proposed study is required to determine the functional significance of the PGC-1α- and PGC-1β-induced down-regulation of TRIM32 and Prnp in C2C12 myotubes. Identifying new targets regulated by PGC-1α and PGC-1β that are involved in muscle growth or wasting will assist in identifying therapeutic strategies to prevent or lessen the debilitating effects of muscle atrophy.

5.2.4 Interaction of PGC-1β and ERRα with the CrT promoter

Rationale

In skeletal muscle, PGC-1α/ERRα and PGC-1β/ERRα are known to increase the transcription of genes involved in mitochondrial biogenesis, oxidative phosphorylation, mitochondrial fusion, fatty acid oxidation, oxidative muscle fibre phenotype, and angiogenesis. In Chapter 4, it was shown that PGC-1α and PGC-1β increase CrT mRNA and creatine uptake in L6 myotubes; an effect was dependent on ERRα. Furthermore, ChIP assays revealed that PGC-1α and ERRα interact directly with the CrT promoter to increase CrT expression. However, it is unknown if PGC-1β can also directly interact with ERRα on the CrT promoter.

Aim

To identify if PGC-1β interacts directly with ERRα on the CrT promoter.

Key methods

ChIP assays can be performed with adenovirus-infected C2C12 myotubes as described previously in Chapter 4, but with the use of PGC-1β adenovirus instead of PGC-1α. Briefly, myotubes are infected on day 4 of differentiation with adenoviruses expressing shRNAs for ERRα or GFP, and on day 6 of differentiation with adenoviruses expressing LacZ and FLAG-PGC-1β, together with a second dose of shRNA-expressing adenoviruses. The cells are harvested 24 h later, and chromatin is immunoprecipitated with the following antibodies: anti-GFP, anti-FLAG for the

detection of FLAG-Tagged PGC-1β, or anti-ERRα. Genomic DNA present in the immunopurified complex is quantified by real-time qPCR using mouse CrT primers: Forward: 5' GGATCCCATGGAATCAGGTCTT and Reverse: 5' GGCAACTGGGAAACAGAAATCA, which amplifies a region containing an ERRα response element (ERRE) upstream of the transcriptional start-site.

Significance

The proposed study will confirm whether PGC-1β can directly interact with ERRα and bind to the CrT to increase its gene expression. These findings will add to the list of gene targets that PGC-1α/ERRα and PGC-1β/ERRα are known to regulate in skeletal muscle, and further increase the understanding of how CrT expression and creatine transport are regulated in skeletal muscle.

5.2.5 The effect of PGC-1α and PGC-1β on creatine uptake *in vivo*

Rationale

Decreased intracellular creatine and CrT levels are characteristic of many myopathies [229, 239]. In Chapter 4, it was shown that overexpression of PGC-1α and PGC-1β increases CrT mRNA and creatine uptake in L6 myotubes *in vitro*. This effect was dependent on ERRα. Whether PGC-1α and PGC-1β can increase CrT mRNA and creatine uptake *in vivo* has not been investigated.

Aims

To investigate the effect of PGC-1α/ERRα and PGC-1β/ERRα on CrT mRNA expression and creatine uptake in skeletal muscle *in vivo*.

Key methods

PGC-1α and PGC-1β overexpression *in vivo* can be achieved using rAAVs as described in section 5.2.1 above. rAAVs overexpressing PGC-1α or PGC-1β could be infected into ERRα knockout mice [340], and appropriate wild-type controls. Creatine uptake *in vivo* can be measured by using hindlimb perfusion of [^{14}C]-Creatine in into skeletal muscle, as described previously [242]. Briefly, after perfusion of [^{14}C]-Creatine for the desired time period, metabolites from the muscle sections are extracted using perchloric acid. Radioactivity present in the

Phosphocreatine (PCr) and creatine pools can be measured in a similar manner to *in vitro* studies, using liquid scintillation counter. The net amount of radiolabel found within the muscle represents the creatine uptake rate for that period

Significance

PGC-1α and PGC-1β increase CrT mRNA and creatine uptake *in vitro*, and this is dependent on the transcription factor ERRα. The proposed study is required to determine whether this observation can be extended to *in vivo* models. Identifying the molecular mechanisms regulating creatine transport in skeletal muscle is essential for developing therapeutic strategies to increase intracellular creatine in myopathies associated with decreased creatine levels.

References

1. Rasmussen, B.B. and S.M. Phillips, *Contractile and nutritional regulation of human muscle growth.* Exerc Sport Sci Rev, 2003. **31**(3): p. 127-31.

2. Bassel-Duby, R. and E.N. Olson, *Signaling pathways in skeletal muscle remodeling.* Annu Rev Biochem, 2006. **75**: p. 19-37.

3. Frost, R.A. and C.H. Lang, *Protein kinase B/Akt: a nexus of growth factor and cytokine signaling in determining muscle mass.* J Appl Physiol, 2007. **103**(1): p. 378-87.

4. Zanchi, N. and A. Lancha, *Mechanical stimuli of skeletal muscle: implications on mTOR/p70s6k and protein synthesis.* European Journal of Applied Physiology, 2008. **102**(3): p. 253-263.

5. Coffey, V.G., et al., *Early signaling responses to divergent exercise stimuli in skeletal muscle from well-trained humans.* Faseb J, 2006. **20**(1): p. 190-2.

6. Hawley, J.A., *Adaptations of skeletal muscle to prolonged, intense endurance training.* Clin Exp Pharmacol Physiol, 2002. **29**(3): p. 218-22.

7. Holloszy, J.O. and E.F. Coyle, *Adaptations of skeletal muscle to endurance exercise and their metabolic consequences.* J Appl Physiol, 1984. **56**(4): p. 831-8.

8. Hickson, R.C., *Interference of strength development by simultaneously training for strength and endurance.* Eur J Appl Physiol Occup Physiol, 1980. **45**(2-3): p. 255-63.

9. Nader, G.A. and K.A. Esser, *Intracellular signaling specificity in skeletal muscle in response to different modes of exercise.* J Appl Physiol, 2001. **90**(5): p. 1936-42.

10. Rennie, M.J., et al., *Control of the size of the human muscle mass.* Annu Rev Physiol, 2004. **66**: p. 799-828.

11. Lynch, G.S., J.D. Schertzer, and J.G. Ryall, *Therapeutic approaches for muscle wasting disorders.* Pharmacol Ther, 2007. **113**(3): p. 461-87.

12. Paddon-Jones, D., et al., *Atrophy and impaired muscle protein synthesis during prolonged inactivity and stress.* J Clin Endocrinol Metab, 2006. **91**(12): p. 4836-41.

13. Tisdale, M.J., *Cancer cachexia.* Langenbecks Arch Surg, 2004. **389**(4): p. 299-305.

14. Welle, S., et al., *Myofibrillar protein synthesis in young and old men.* Am J Physiol, 1993. **264**(5 Pt 1): p. E693-8.

15. Leger, B., et al., *Human skeletal muscle atrophy in amyotrophic lateral sclerosis reveals a reduction in Akt and an increase in atrogin-1.* Faseb J, 2006. **20**(3): p. 583-5.

16. Lynch, G.S., *Therapies for improving muscle function in neuromuscular disorders.* Exerc Sport Sci Rev, 2001. **29**(4): p. 141-8.

17. Di Giovanni, S., et al., *Constitutive activation of MAPK cascade in acute quadriplegic myopathy.* Ann Neurol, 2004. **55**(2): p. 195-206.

18. Jagoe, R.T., et al., *Patterns of gene expression in atrophying skeletal muscles: response to food deprivation.* FASEB J, 2002. **16**(13): p. 1697-712.

19. Latronico, N., E. Peli, and M. Botteri, *Critical illness myopathy and neuropathy.* Curr Opin Crit Care, 2005. **11**(2): p. 126-32.

20. Leger, B., et al., *Human sarcopenia reveals an increase in SOCS-3 and myostatin and a reduced efficiency of Akt phosphorylation.* Rejuvenation Res, 2008. **11**(1): p. 163-175B.

21. Frontera, W.R., et al., *Aging of skeletal muscle: a 12-yr longitudinal study.* J Appl Physiol, 2000. **88**(4): p. 1321-6.

22. Doucet, M., et al., *Muscle atrophy and hypertrophy signaling in patients with chronic obstructive pulmonary disease.* Am J Respir Crit Care Med, 2007. **176**(3): p. 261-9.

23. Metter, E.J., et al., *Skeletal muscle strength as a predictor of all-cause mortality in healthy men.* J Gerontol A Biol Sci Med Sci, 2002. **57**(10): p. B359-65.

24. Zinna, E.M. and K.E. Yarasheski, *Exercise treatment to counteract protein wasting of chronic diseases.* Curr Opin Clin Nutr Metab Care, 2003. **6**(1): p. 87-93.

25. Gosker, H.R., et al., *Muscle fiber type IIX atrophy is involved in the loss of fat-free mass in chronic obstructive pulmonary disease.* Am J Clin Nutr, 2002. **76**(1): p. 113-9.

26. Roberts-Wilson, T.K., et al., *Calcineurin signaling and PGC-1alpha expression are suppressed during muscle atrophy due to diabetes.* Biochim Biophys Acta, 2010. **1803**(8): p. 960-7.

27. Tseng, B.S., et al., *Strength and aerobic training attenuate muscle wasting and improve resistance to the development of disability with aging.* J Gerontol A Biol Sci Med Sci, 1995. **50 Spec No**: p. 113-9.

28. Raue, U., et al., *Transcriptome signature of resistance exercise adaptations: mixed muscle and fiber type specific profiles in young and old adults.* J Appl Physiol, 2012. **112**(10): p. 1625-36.

29. Slivka, D., et al., *Single muscle fiber adaptations to resistance training in old (>80 yr) men: evidence for limited skeletal muscle plasticity.* Am J Physiol Regul Integr Comp Physiol, 2008. **295**(1): p. R273-80.

30. Derbre, F., et al., *Age associated low mitochondrial biogenesis may be explained by lack of response of PGC-1alpha to exercise training.* Age (Dordr), 2012. **34**(3): p. 669-79.

31. Glass, D.J., *Skeletal muscle hypertrophy and atrophy signaling pathways.* Int J Biochem Cell Biol, 2005. **37**(10): p. 1974-84.

32. D'Antona, G., et al., *Skeletal muscle hypertrophy and structure and function of skeletal muscle fibres in male body builders.* J Physiol, 2006. **570**(Pt 3): p. 611-27.

33. Baar, K., *Training for endurance and strength: lessons from cell signaling.* Med Sci Sports Exerc, 2006. **38**(11): p. 1939-44.

34. MacDougall, J.D., et al., *The time course for elevated muscle protein synthesis following heavy resistance exercise.* Can J Appl Physiol, 1995. **20**(4): p. 480-6.

35. Dreyer, H.C., et al., *Resistance exercise increases AMPK activity and reduces 4E-BP1 phosphorylation and protein synthesis in human skeletal muscle.* J Physiol, 2006. **576**(Pt 2): p. 613-24.

36. Dreyer, H.C., et al., *Leucine-enriched essential amino acid and carbohydrate ingestion following resistance exercise enhances mTOR signaling and protein synthesis in human muscle.* Am J Physiol Endocrinol Metab, 2008. **294**(2): p. E392-400.

37. Liu, Z., et al., *Branched chain amino acids activate messenger ribonucleic acid translation regulatory proteins in human skeletal muscle, and glucocorticoids blunt this action.* J Clin Endocrinol Metab, 2001. **86**(5): p. 2136-43.

38. Kimball, S.R., et al., *Insulin stimulates protein synthesis in skeletal muscle by enhancing the association of eIF-4E and eIF-4G.* Am J Physiol, 1997. **272**(2 Pt 1): p. C754-9.

39. Rommel, C., et al., *Mediation of IGF-1-induced skeletal myotube hypertrophy by PI(3)K/Akt/mTOR and PI(3)K/Akt/GSK3 pathways.* Nat Cell Biol, 2001. **3**(11): p. 1009-13.

40. Sacheck, J.M., et al., *IGF-I stimulates muscle growth by suppressing protein breakdown and expression of atrophy-related ubiquitin ligases, atrogin-1 and MuRF1.* Am J Physiol Endocrinol Metab, 2004. **287**(4): p. E591-601.

41. Vandenburgh, H.H., et al., *Insulin and IGF-I induce pronounced hypertrophy of skeletal myofibers in tissue culture.* Am J Physiol, 1991. **260**(3 Pt 1): p. C475-84.

42. Griggs, R.C., et al., *Effect of testosterone on muscle mass and muscle protein synthesis.* J Appl Physiol, 1989. **66**(1): p. 498-503.

43. Dunn, S.E., J.L. Burns, and R.N. Michel, *Calcineurin is required for skeletal muscle hypertrophy.* J Biol Chem, 1999. **274**(31): p. 21908-12.

44. Semsarian, C., et al., *Skeletal muscle hypertrophy is mediated by a Ca2+-dependent calcineurin signalling pathway.* Nature, 1999. **400**(6744): p. 576-81.

45. Deldicque, L., et al., *Decrease in Akt/PKB signalling in human skeletal muscle by resistance exercise.* Eur J Appl Physiol, 2008. **104**(1): p. 57-65.

46. Karlsson, H.K., et al., *Branched-chain amino acids increase p70S6k phosphorylation in human skeletal muscle after resistance exercise.* Am J Physiol Endocrinol Metab, 2004. **287**(1): p. E1-7.

47. Bodine, S.C., et al., *Akt/mTOR pathway is a crucial regulator of skeletal muscle hypertrophy and can prevent muscle atrophy in vivo.* Nat Cell Biol, 2001. **3**(11): p. 1014-9.

48. Al-Shanti, N. and C.E. Stewart, *Ca2+/calmodulin-dependent transcriptional pathways: potential mediators of skeletal muscle growth and development.* Biol Rev Camb Philos Soc, 2009. **84**(4): p. 637-52.

49. Pallafacchina, G., et al., *A protein kinase B-dependent and rapamycin-sensitive pathway controls skeletal muscle growth but not fiber type specification.* Proc Natl Acad Sci U S A, 2002. **99**(14): p. 9213-8.

50. Latres, E., et al., *Insulin-like growth factor-1 (IGF-1) inversely regulates atrophy-induced genes via the phosphatidylinositol 3-kinase/Akt/mammalian target of rapamycin (PI3K/Akt/mTOR) pathway.* J Biol Chem, 2005. **280**(4): p. 2737-44.

51. Stitt, T.N., et al., *The IGF-1/PI3K/Akt pathway prevents expression of muscle atrophy-induced ubiquitin ligases by inhibiting FOXO transcription factors.* Mol Cell, 2004. **14**(3): p. 395-403.

52. Nave, B.T., et al., *Mammalian target of rapamycin is a direct target for protein kinase B: identification of a convergence point for opposing effects of insulin and amino-acid deficiency on protein translation.* Biochem J, 1999. **344 Pt 2**: p. 427-31.

53. Tee, A.R., et al., *Tuberous sclerosis complex-1 and -2 gene products function together to inhibit mammalian target of rapamycin (mTOR)-mediated downstream signaling.* Proc Natl Acad Sci U S A, 2002. **99**(21): p. 13571-6.

54. Inoki, K., et al., *TSC2 is phosphorylated and inhibited by Akt and suppresses mTOR signalling.* Nat Cell Biol, 2002. **4**(9): p. 648-57.

55. Glass, D.J., *Signalling pathways that mediate skeletal muscle hypertrophy and atrophy.* Nat Cell Biol, 2003. **5**(2): p. 87-90.

56. Hara, K., et al., *Regulation of eIF-4E BP1 phosphorylation by mTOR.* J Biol Chem, 1997. **272**(42): p. 26457-63.

57. Pap, M. and G.M. Cooper, *Role of translation initiation factor 2B in control of cell survival by the phosphatidylinositol 3-kinase/Akt/glycogen synthase kinase 3beta signaling pathway.* Mol Cell Biol, 2002. **22**(2): p. 578-86.

58. Pap, M. and G.M. Cooper, *Role of glycogen synthase kinase-3 in the phosphatidylinositol 3-Kinase/Akt cell survival pathway.* J Biol Chem, 1998. **273**(32): p. 19929-32.

59. Jefferson, L.S., J.R. Fabian, and S.R. Kimball, *Glycogen synthase kinase-3 is the predominant insulin-regulated eukaryotic initiation factor 2B kinase in skeletal muscle.* Int J Biochem Cell Biol, 1999. **31**(1): p. 191-200.

60. Leger, B., et al., *Akt signalling through GSK-3beta, mTOR and Foxo1 is involved in human skeletal muscle hypertrophy and atrophy.* J Physiol, 2006. **576**(Pt 3): p. 923-33.

61. Mammucari, C., et al., *FoxO3 controls autophagy in skeletal muscle in vivo.* Cell Metab, 2007. **6**(6): p. 458-71.

62. Zhao, J., et al., *FoxO3 coordinately activates protein degradation by the autophagic/lysosomal and proteasomal pathways in atrophying muscle cells.* Cell Metab, 2007. **6**(6): p. 472-83.

63. Lecker, S.H., A.L. Goldberg, and W.E. Mitch, *Protein degradation by the ubiquitin-proteasome pathway in normal and disease states.* J Am Soc Nephrol, 2006. **17**(7): p. 1807-19.

64. Lecker, S.H., et al., *Multiple types of skeletal muscle atrophy involve a common program of changes in gene expression.* FASEB J, 2004. **18**(1): p. 39-51.

65. Sacheck, J.M., et al., *Rapid disuse and denervation atrophy involve transcriptional changes similar to those of muscle wasting during systemic diseases.* FASEB J, 2007. **21**(1): p. 140-55.

66. Bodine, S.C., et al., *Identification of ubiquitin ligases required for skeletal muscle atrophy.* Science, 2001. **294**(5547): p. 1704-8.

67. Bechet, D., et al., *Lysosomal proteolysis in skeletal muscle.* Int J Biochem Cell Biol, 2005. **37**(10): p. 2098-114.

68. Sandri, M., *Autophagy in skeletal muscle.* FEBS Lett. **584**(7): p. 1411-6.

69. Sandri, M., et al., *Foxo transcription factors induce the atrophy-related ubiquitin ligase atrogin-1 and cause skeletal muscle atrophy.* Cell, 2004. **117**(3): p. 399-412.

70. Lee, S.W., et al., *Regulation of muscle protein degradation: coordinated control of apoptotic and ubiquitin-proteasome systems by phosphatidylinositol 3 kinase.* J Am Soc Nephrol, 2004. **15**(6): p. 1537-45.

71. Smerdu, V., et al., *Type IIx myosin heavy chain transcripts are expressed in type IIb fibers of human skeletal muscle.* Am J Physiol, 1994. **267**(6 Pt 1): p. C1723-8.

72. Schiaffino, S. and C. Reggiani, *Myosin isoforms in mammalian skeletal muscle.* J Appl Physiol, 1994. **77**(2): p. 493-501.

73. Huey, K.A., et al., *Temporal effects of inactivty on myosin heavy chain gene expression in rat slow muscle.* Muscle Nerve, 2001. **24**(4): p. 517-26.

74. Roy, R.R., et al., *Mechanical properties of the electrically silent adult rat soleus muscle.* Muscle Nerve, 2002. **26**(3): p. 404-12.

75. Trappe, S., et al., *Human soleus single muscle fiber function with exercise or nutrition countermeasures during 60 days of bed rest.* Am J Physiol Regul Integr Comp Physiol, 2008. **294**(3): p. R939-47.

76. Borina, E., et al., *Myosin and actin content of human skeletal muscle fibers following 35 days bed rest.* Scand J Med Sci Sports, 2010. **20**(1): p. 65-73.

77. Holloszy, J.O., et al., *Skeletal muscle atrophy in old rats: differential changes in the three fiber types.* Mech Ageing Dev, 1991. **60**(2): p. 199-213.

78. Picard, M., et al., *Alterations in intrinsic mitochondrial function with aging are fiber type-specific and do not explain differential atrophy between muscles.* Aging Cell, 2011. **10**(6): p. 1047-55.

79. Carvalho, R.F., et al., *Heart failure increases atrogin-1 and MuRF1 gene expression in skeletal muscle with fiber type-specific atrophy.* J Mol Histol, 2010. **41**(1): p. 81-7.

80. Vescovo, G., et al., *Skeletal muscle fibres synthesis in heart failure: role of PGC-1alpha, calcineurin and GH.* Int J Cardiol, 2005. **104**(3): p. 298-306.

81. Tiao, G., et al., *Intracellular regulation of protein degradation during sepsis is different in fast- and slow-twitch muscle.* Am J Physiol, 1997. **272**(3 Pt 2): p. R849-56.

82. Fischer, D., et al., *The gene expression of ubiquitin ligase E3alpha is upregulated in skeletal muscle during sepsis in rats-potential role of glucocorticoids.* Biochem Biophys Res Commun, 2000. **267**(2): p. 504-8.

83. Marzetti, E., et al., *Sarcopenia of aging: underlying cellular mechanisms and protection by calorie restriction.* Biofactors, 2009. **35**(1): p. 28-35.

84. Marzetti, E., et al., *Mitochondrial death effectors: relevance to sarcopenia and disuse muscle atrophy.* Biochim Biophys Acta, 2010. **1800**(3): p. 235-44.

85. Ibebunjo, C., et al., *Genomic and proteomic profiling reveals reduced mitochondrial function and disruption of the neuromuscular junction driving rat sarcopenia.* Mol Cell Biol, 2013. **33**(2): p. 194-212.

86. Adhihetty, P.J., et al., *Effect of denervation on mitochondrially mediated apoptosis in skeletal muscle.* J Appl Physiol, 2007. **102**(3): p. 1143-51.

87. Kawamata, H. and G. Manfredi, *Mitochondrial dysfunction and intracellular calcium dysregulation in ALS.* Mech Ageing Dev, 2010. **131**(7-8): p. 517-26.

88. Chen, Y.W., et al., *Expression profiling in the muscular dystrophies: identification of novel aspects of molecular pathophysiology.* J Cell Biol, 2000. **151**(6): p. 1321-36.

89. Kuznetsov, A.V., et al., *Impaired mitochondrial oxidative phosphorylation in skeletal muscle of the dystrophin-deficient mdx mouse.* Mol Cell Biochem, 1998. **183**(1-2): p. 87-96.

90. Powers, S.K., et al., *Mitochondrial signaling contributes to disuse muscle atrophy.* Am J Physiol Endocrinol Metab, 2012. **303**(1): p. E31-9.

91. Romanello, V., et al., *Mitochondrial fission and remodelling contributes to muscle atrophy.* EMBO J, 2010. **29**(10): p. 1774-85.

92. Andersson, U. and R.C. Scarpulla, *Pgc-1-related coactivator, a novel, serum-inducible coactivator of nuclear respiratory factor 1-dependent transcription in mammalian cells.* Mol Cell Biol, 2001. **21**(11): p. 3738-49.

93. Lin, J., et al., *Peroxisome proliferator-activated receptor gamma coactivator 1beta (PGC-1beta), a novel PGC-1-related transcription coactivator associated with host cell factor.* J Biol Chem, 2002. **277**(3): p. 1645-8.

94. Puigserver, P., et al., *A cold-inducible coactivator of nuclear receptors linked to adaptive thermogenesis.* Cell, 1998. **92**(6): p. 829-39.

95. Kressler, D., et al., *The PGC-1-related protein PERC is a selective coactivator of estrogen receptor alpha.* J Biol Chem, 2002. **277**(16): p. 13918-25.

96. Handschin, C. and B.M. Spiegelman, *Peroxisome proliferator-activated receptor gamma coactivator 1 coactivators, energy homeostasis, and metabolism.* Endocr Rev, 2006. **27**(7): p. 728-35.

97. Esterbauer, H., et al., *Human peroxisome proliferator activated receptor gamma coactivator 1 (PPARGC1) gene: cDNA sequence, genomic organization, chromosomal localization, and tissue expression.* Genomics, 1999. **62**(1): p. 98-102.

98. Lin, J., C. Handschin, and B.M. Spiegelman, *Metabolic control through the PGC-1 family of transcription coactivators.* Cell Metab, 2005. **1**(6): p. 361-70.

99. Meirhaeghe, A., et al., *Characterization of the human, mouse and rat PGC1 beta (peroxisome-proliferator-activated receptor-gamma co-activator 1 beta) gene in vitro and in vivo.* Biochem J, 2003. **373**(Pt 1): p. 155-65.

100. Kamei, Y., et al., *PPARgamma coactivator 1beta/ERR ligand 1 is an ERR protein ligand, whose expression induces a high-energy expenditure and antagonizes obesity.* Proc Natl Acad Sci U S A, 2003. **100**(21): p. 12378-83.

101. Hock, M.B. and A. Kralli, *Transcriptional control of mitochondrial biogenesis and function.* Annu Rev Physiol, 2009. **71**: p. 177-203.

102. Puigserver, P., et al., *Insulin-regulated hepatic gluconeogenesis through FOXO1-PGC-1alpha interaction.* Nature, 2003. **423**(6939): p. 550-5.

103. Rhee, J., et al., *Regulation of hepatic fasting response by PPARgamma coactivator-1alpha (PGC-1): requirement for hepatocyte nuclear factor 4alpha in gluconeogenesis.* Proc Natl Acad Sci U S A, 2003. **100**(7): p. 4012-7.

104. Herzig, S., et al., *CREB regulates hepatic gluconeogenesis through the coactivator PGC-1.* Nature, 2001. **413**(6852): p. 179-83.

105. Yoon, J.C., et al., *Control of hepatic gluconeogenesis through the transcriptional coactivator PGC-1.* Nature, 2001. **413**(6852): p. 131-8.

106. Lin, J., et al., *Hyperlipidemic effects of dietary saturated fats mediated through PGC-1beta coactivation of SREBP.* Cell, 2005. **120**(2): p. 261-73.

107. Nagai, Y., et al., *The role of peroxisome proliferator-activated receptor gamma coactivator-1 beta in the pathogenesis of fructose-induced insulin resistance.* Cell Metab, 2009. **9**(3): p. 252-64.

108. Liang, H., et al., *Whole body overexpression of PGC-1alpha has opposite effects on hepatic and muscle insulin sensitivity.* Am J Physiol Endocrinol Metab, 2009. **296**(4): p. E945-54.

109. Pearen, M.A., et al., *Expression profiling of skeletal muscle following acute and chronic beta2-adrenergic stimulation: implications for hypertrophy, metabolism and circadian rhythm.* BMC Genomics, 2009. **10**: p. 448.

110. Chinsomboon, J., et al., *The transcriptional coactivator PGC-1alpha mediates exercise-induced angiogenesis in skeletal muscle.* Proc Natl Acad Sci U S A, 2009. **106**(50): p. 21401-6.

111. Ijiri, D., Y. Kanai, and M. Hirabayashi, *Possible roles of myostatin and PGC-1alpha in the increase of skeletal muscle and transformation of fiber type in*

cold-exposed chicks: expression of myostatin and PGC-1alpha in chicks exposed to cold. Domest Anim Endocrinol, 2009. **37**(1): p. 12-22.

112. Gerhart-Hines, Z., et al., *Metabolic control of muscle mitochondrial function and fatty acid oxidation through SIRT1/PGC-1alpha.* EMBO J, 2007. **26**(7): p. 1913-23.

113. Baar, K., et al., *Adaptations of skeletal muscle to exercise: rapid increase in the transcriptional coactivator PGC-1.* FASEB J, 2002. **16**(14): p. 1879-86.

114. Russell, A.P., et al., *Regulation of metabolic transcriptional co-activators and transcription factors with acute exercise.* FASEB J, 2005. **19**(8): p. 986-8.

115. Terada, S., et al., *Effects of low-intensity prolonged exercise on PGC-1 mRNA expression in rat epitrochlearis muscle.* Biochem Biophys Res Commun, 2002. **296**(2): p. 350-4.

116. Henriksen, E.J., *Invited review: Effects of acute exercise and exercise training on insulin resistance.* J Appl Physiol, 2002. **93**(2): p. 788-96.

117. Hood, D.A., *Invited Review: contractile activity-induced mitochondrial biogenesis in skeletal muscle.* J Appl Physiol, 2001. **90**(3): p. 1137-57.

118. Russell, A.P., *PGC-1alpha and exercise: important partners in combating insulin resistance.* Curr Diabetes Rev, 2005. **1**(2): p. 175-81.

119. Mathai, A.S., et al., *Rapid exercise-induced changes in PGC-1alpha mRNA and protein in human skeletal muscle.* J Appl Physiol, 2008. **105**(4): p. 1098-105.

120. Russell, A.P., et al., *Endurance Training in Humans Leads to Fiber Type-Specific Increases in Levels of Peroxisome Proliferator-Activated Receptor-Î³ Coactivator-1 and Peroxisome Proliferator-Activated Receptor-Îµ in Skeletal Muscle.* Diabetes, 2003. **52**(12): p. 2874-2881.

121. Pilegaard, H., B. Saltin, and P.D. Neufer, *Exercise induces transient transcriptional activation of the PGC-1alpha gene in human skeletal muscle.* J Physiol, 2003. **546**(Pt 3): p. 851-8.

122. Akimoto, T., et al., *Exercise stimulates Pgc-1alpha transcription in skeletal muscle through activation of the p38 MAPK pathway.* J Biol Chem, 2005. **280**(20): p. 19587-93.

123. Gibala, M.J., et al., *Brief intense interval exercise activates AMPK and p38 MAPK signaling and increases the expression of PGC-1alpha in human skeletal muscle.* J Appl Physiol, 2009. **106**(3): p. 929-34.

124. Coffey, V.G., et al., *Effect of consecutive repeated sprint and resistance exercise bouts on acute adaptive responses in human skeletal muscle.* Am J Physiol Regul Integr Comp Physiol, 2009. **297**(5): p. R1441-51.

125. Yan, Z., P. Li, and T. Akimoto, *Transcriptional control of the Pgc-1alpha gene in skeletal muscle in vivo.* Exerc Sport Sci Rev, 2007. **35**(3): p. 97-101.

126. Koves, T.R., et al., *Peroxisome proliferator-activated receptor-gamma co-activator 1alpha-mediated metabolic remodeling of skeletal myocytes mimics exercise training and reverses lipid-induced mitochondrial inefficiency.* J Biol Chem, 2005. **280**(39): p. 33588-98.

127. Berchtold, M.W., H. Brinkmeier, and M. Muntener, *Calcium ion in skeletal muscle: its crucial role for muscle function, plasticity, and disease.* Physiol Rev, 2000. **80**(3): p. 1215-65.

128. Olson, E.N. and R.S. Williams, *Calcineurin signaling and muscle remodeling.* Cell, 2000. **101**(7): p. 689-92.

129. Guerfali, I., et al., *Calcineurin A and CaMKIV transactivate PGC-1alpha promoter, but differentially regulate cytochrome c promoter in rat skeletal muscle.* Pflugers Arch, 2007. **454**(2): p. 297-305.

130. Long, Y.C., et al., *Calcineurin regulates skeletal muscle metabolism via coordinated changes in gene expression.* J Biol Chem, 2007. **282**(3): p. 1607-14.

131. Ryder, J.W., et al., *Skeletal muscle reprogramming by activation of calcineurin improves insulin action on metabolic pathways.* J Biol Chem, 2003. **278**(45): p. 44298-304.

132. Wu, H., et al., *Regulation of mitochondrial biogenesis in skeletal muscle by CaMK.* Science, 2002. **296**(5566): p. 349-52.

133. Hardie, D.G. and K. Sakamoto, *AMPK: a key sensor of fuel and energy status in skeletal muscle.* Physiology (Bethesda), 2006. **21**: p. 48-60.

134. Lee, W.J., et al., *AMPK activation increases fatty acid oxidation in skeletal muscle by activating PPARalpha and PGC-1.* Biochem Biophys Res Commun, 2006. **340**(1): p. 291-5.

135. Zong, H., et al., *AMP kinase is required for mitochondrial biogenesis in skeletal muscle in response to chronic energy deprivation.* Proc Natl Acad Sci U S A, 2002. **99**(25): p. 15983-7.

136. Jager, S., et al., *AMP-activated protein kinase (AMPK) action in skeletal muscle via direct phosphorylation of PGC-1alpha.* Proc Natl Acad Sci U S A, 2007. **104**(29): p. 12017-22.

137. Goodyear, L.J., et al., *Effects of exercise and insulin on mitogen-activated protein kinase signaling pathways in rat skeletal muscle.* Am J Physiol, 1996. **271**(2 Pt 1): p. E403-8.

138. Amat, R., et al., *SIRT1 controls the transcription of the peroxisome proliferator-activated receptor-gamma Co-activator-1alpha (PGC-1alpha) gene in skeletal muscle through the PGC-1alpha autoregulatory loop and interaction with MyoD.* J Biol Chem, 2009. **284**(33): p. 21872-80.

139. Rodgers, J.T., et al., *Metabolic adaptations through the PGC-1 alpha and SIRT1 pathways.* FEBS Lett, 2008. **582**(1): p. 46-53.

140. Suwa, M., et al., *Endurance exercise increases the SIRT1 and peroxisome proliferator-activated receptor gamma coactivator-1alpha protein expressions in rat skeletal muscle.* Metabolism, 2008. **57**(7): p. 986-98.

141. Mortensen, O.H., et al., *PGC-1beta is downregulated by training in human skeletal muscle: no effect of training twice every second day vs. once daily on expression of the PGC-1 family.* J Appl Physiol, 2007. **103**(5): p. 1536-42.

142. Kelly, T.J., et al., *GCN5-mediated transcriptional control of the metabolic coactivator PGC-1beta through lysine acetylation.* J Biol Chem, 2009. **284**(30): p. 19945-52.

143. Lelliott, C.J. and A. Vidal-Puig, *PGC-1beta: a co-activator that sets the tone for both basal and stress-stimulated mitochondrial activity.* Adv Exp Med Biol, 2009. **646**: p. 133-9.

144. Sonoda, J., et al., *PGC-1beta controls mitochondrial metabolism to modulate circadian activity, adaptive thermogenesis, and hepatic steatosis.* Proc Natl Acad Sci U S A, 2007. **104**(12): p. 5223-8.

145. Handschin, C., et al., *Skeletal muscle fiber-type switching, exercise intolerance, and myopathy in PGC-1alpha muscle-specific knock-out animals.* J Biol Chem, 2007. **282**(41): p. 30014-21.

146. Handschin, C., et al., *Abnormal glucose homeostasis in skeletal muscle-specific PGC-1alpha knockout mice reveals skeletal muscle-pancreatic beta cell crosstalk.* J Clin Invest, 2007. **117**(11): p. 3463-74.

147. Rodriguez-Calvo, R., et al., *PGC-1beta down-regulation is associated with reduced ERRalpha activity and MCAD expression in skeletal muscle of senescence-accelerated mice.* J Gerontol A Biol Sci Med Sci, 2006. **61**(8): p. 773-80.

148. Wenz, T., et al., *Increased muscle PGC-1alpha expression protects from sarcopenia and metabolic disease during aging.* Proc Natl Acad Sci U S A, 2009. **106**(48): p. 20405-10.

149. Garnier, A., et al., *Depressed mitochondrial transcription factors and oxidative capacity in rat failing cardiac and skeletal muscles.* J Physiol, 2003. **551**(Pt 2): p. 491-501.

150. Menconi, M.J., et al., *Sepsis and glucocorticoids downregulate the expression of the nuclear cofactor PGC-1beta in skeletal muscle.* Am J Physiol Endocrinol Metab, 2010. **299**(4): p. E533-43.

151. Crunkhorn, S., et al., *Peroxisome proliferator activator receptor gamma coactivator-1 expression is reduced in obesity: potential pathogenic role of saturated fatty acids and p38 mitogen-activated protein kinase activation.* J Biol Chem, 2007. **282**(21): p. 15439-50.

152. Chaturvedi, R.K., et al., *Impaired PGC-1alpha function in muscle in Huntington's disease.* Hum Mol Genet, 2009. **18**(16): p. 3048-65.

153. Sandri, M., et al., *PGC-1alpha protects skeletal muscle from atrophy by suppressing FoxO3 action and atrophy-specific gene transcription.* Proc Natl Acad Sci U S A, 2006. **103**(44): p. 16260-5.

154. Remels, A.H., et al., *Peroxisome proliferator-activated receptor expression is reduced in skeletal muscle in COPD.* Eur Respir J, 2007. **30**(2): p. 245-52.

155. Russell, A.P., et al., *Disruption of skeletal muscle mitochondrial network genes and miRNAs in amyotrophic lateral sclerosis.* Neurobiol Dis, 2012. **49C**: p. 107-117.

156. Ling, C., et al., *Multiple environmental and genetic factors influence skeletal muscle PGC-1alpha and PGC-1beta gene expression in twins.* J Clin Invest, 2004. **114**(10): p. 1518-26.

157. Mootha, V.K., et al., *PGC-1alpha-responsive genes involved in oxidative phosphorylation are coordinately downregulated in human diabetes.* Nat Genet, 2003. **34**(3): p. 267-73.

158. Patti, M.E., et al., *Coordinated reduction of genes of oxidative metabolism in humans with insulin resistance and diabetes: Potential role of PGC1 and NRF1.* Proc Natl Acad Sci U S A, 2003. **100**(14): p. 8466-71.

159. Liesa, M., et al., *Mitochondrial fusion is increased by the nuclear coactivator PGC-1beta.* PLoS One, 2008. **3**(10): p. e3613.

160. Schreiber, S.N., et al., *The estrogen-related receptor alpha (ERRalpha) functions in PPARgamma coactivator 1alpha (PGC-1alpha)-induced mitochondrial biogenesis.* Proc Natl Acad Sci U S A, 2004. **101**(17): p. 6472-7.

161. Soriano, F.X., et al., *Evidence for a mitochondrial regulatory pathway defined by peroxisome proliferator-activated receptor-gamma coactivator-1 alpha, estrogen-related receptor-alpha, and mitofusin 2.* Diabetes, 2006. **55**(6): p. 1783-91.

162. St-Pierre, J., et al., *Bioenergetic analysis of peroxisome proliferator-activated receptor gamma coactivators 1alpha and 1beta (PGC-1alpha and PGC-1beta) in muscle cells.* J Biol Chem, 2003. **278**(29): p. 26597-603.

163. Lin, J., et al., *Transcriptional co-activator PGC-1 alpha drives the formation of slow-twitch muscle fibres.* Nature, 2002. **418**(6899): p. 797-801.

164. Arany, Z., et al., *The transcriptional coactivator PGC-1beta drives the formation of oxidative type IIX fibers in skeletal muscle.* Cell Metab, 2007. **5**(1): p. 35-46.

165. Rasbach, K.A., et al., *PGC-1alpha regulates a HIF2alpha-dependent switch in skeletal muscle fiber types.* Proc Natl Acad Sci U S A, 2010. **107**(50): p. 21866-71.

166. Michael, L.F., et al., *Restoration of insulin-sensitive glucose transporter (GLUT4) gene expression in muscle cells by the transcriptional coactivator PGC-1.* Proc Natl Acad Sci U S A, 2001. **98**(7): p. 3820-5.

167. Benton, C.R., et al., *Modest PGC-1alpha overexpression in muscle in vivo is sufficient to increase insulin sensitivity and palmitate oxidation in subsarcolemmal, not intermyofibrillar, mitochondria.* J Biol Chem, 2008. **283**(7): p. 4228-40.

168. Espinoza, D.O., et al., *Dual modulation of both lipid oxidation and synthesis by peroxisome proliferator-activated receptor-gamma coactivator-1alpha and -1beta in cultured myotubes.* FASEB J. **24**(4): p. 1003-14.

169. Rowe, G.C., et al., *PGC-1beta regulates angiogenesis in skeletal muscle.* Am J Physiol Endocrinol Metab, 2011. **301**(1): p. E155-63.

170. Arany, Z., et al., *HIF-independent regulation of VEGF and angiogenesis by the transcriptional coactivator PGC-1alpha.* Nature, 2008. **451**(7181): p. 1008-12.

171. Wu, Z., et al., *Mechanisms controlling mitochondrial biogenesis and respiration through the thermogenic coactivator PGC-1.* Cell, 1999. **98**(1): p. 115-24.

172. Shao, D., et al., *PGC-1 beta-regulated mitochondrial biogenesis and function in myotubes is mediated by NRF-1 and ERR alpha.* Mitochondrion, 2010. **10**(5): p. 516-27.

173. Cartoni, R., et al., *Mitofusins 1/2 and ERRalpha expression are increased in human skeletal muscle after physical exercise.* J Physiol, 2005. **567**(Pt 1): p. 349-58.

174. Chen, H., et al., *Mitochondrial fusion is required for mtDNA stability in skeletal muscle and tolerance of mtDNA mutations.* Cell, 2010. **141**(2): p. 280-9.

175. Lelliott, C.J., et al., *Ablation of PGC-1beta results in defective mitochondrial activity, thermogenesis, hepatic function, and cardiac performance.* PLoS Biol, 2006. **4**(11): p. e369.

176. Vianna, C.R., et al., *Hypomorphic mutation of PGC-1beta causes mitochondrial dysfunction and liver insulin resistance.* Cell Metab, 2006. **4**(6): p. 453-64.

177. Ling, C., et al., *Impact of the peroxisome proliferator activated receptor-gamma coactivator-1beta (PGC-1beta) Ala203Pro polymorphism on in vivo metabolism, PGC-1beta expression and fibre type composition in human skeletal muscle.* Diabetologia, 2007. **50**(8): p. 1615-20.

178. Schiaffino, S. and C. Reggiani, *Myosin Isoforms in Mammalian Skeletal-Muscle.* Journal of Applied Physiology, 1994. **77**(2): p. 493-501.

179. Larsson, L., et al., *Mhc Composition and Enzyme-Histochemical and Physiological-Properties of a Novel Fast-Twitch Motor Unit Type.* American Journal of Physiology, 1991. **261**(1): p. C93-C101.

180. Mortensen, O.H., et al., *PGC-1alpha and PGC-1beta have both similar and distinct effects on myofiber switching toward an oxidative phenotype.* Am J Physiol Endocrinol Metab, 2006. **291**(4): p. E807-16.

181. Wende, A.R., et al., *PGC-1alpha coactivates PDK4 gene expression via the orphan nuclear receptor ERRalpha: a mechanism for transcriptional control of muscle glucose metabolism.* Mol Cell Biol, 2005. **25**(24): p. 10684-94.

182. Wright, L.E., et al., *Amelioration of lipid-induced insulin resistance in rat skeletal muscle by overexpression of Pgc-1beta involves reductions in long-chain acyl-CoA levels and oxidative stress.* Diabetologia, 2011. **54**(6): p. 1417-26.

183. Cha, S.H., et al., *Hypothalamic malonyl-CoA triggers mitochondrial biogenesis and oxidative gene expression in skeletal muscle: Role of PGC-1alpha.* Proc Natl Acad Sci U S A, 2006. **103**(42): p. 15410-5.

184. Mensink, M., et al., *Improved skeletal muscle oxidative enzyme activity and restoration of PGC-1 alpha and PPAR beta/delta gene expression upon rosiglitazone treatment in obese patients with type 2 diabetes mellitus.* Int J Obes (Lond), 2007. **31**(8): p. 1302-10.

185. Ek, J., et al., *Mutation analysis of peroxisome proliferator-activated receptor-gamma coactivator-1 (PGC-1) and relationships of identified amino acid polymorphisms to Type II diabetes mellitus.* Diabetologia, 2001. **44**(12): p. 2220-6.

186. Hara, K., et al., *A genetic variation in the PGC-1 gene could confer insulin resistance and susceptibility to Type II diabetes.* Diabetologia, 2002. **45**(5): p. 740-3.

187. Muller, Y.L., et al., *A Gly482Ser missense mutation in the peroxisome proliferator-activated receptor gamma coactivator-1 is associated with altered lipid oxidation and early insulin secretion in Pima Indians.* Diabetes, 2003. **52**(3): p. 895-8.

188. Fanelli, M., et al., *The Gly482Ser missense mutation of the peroxisome proliferator-activated receptor gamma coactivator-1 alpha (PGC-1 alpha) gene associates with reduced insulin sensitivity in normal and glucose-intolerant obese subjects.* Dis Markers, 2005. **21**(4): p. 175-80.

189. Sugden, M.C., P.W. Caton, and M.J. Holness, *PPAR control: it's SIRTainly as easy as PGC.* J Endocrinol. **204**(2): p. 93-104.

190. Mootha, V.K., et al., *Erralpha and Gabpa/b specify PGC-1alpha-dependent oxidative phosphorylation gene expression that is altered in diabetic muscle.* Proc Natl Acad Sci U S A, 2004. **101**(17): p. 6570-5.

191. Handschin, C., et al., *PGC-1alpha regulates the neuromuscular junction program and ameliorates Duchenne muscular dystrophy.* Genes Dev, 2007. **21**(7): p. 770-83.

192. Ye, J.M., et al., *Peroxisome proliferator-activated receptor (PPAR)-alpha activation lowers muscle lipids and improves insulin sensitivity in high fat-fed rats: comparison with PPAR-gamma activation.* Diabetes, 2001. **50**(2): p. 411-7.

193. Wang, Y.X., et al., *Peroxisome-proliferator-activated receptor delta activates fat metabolism to prevent obesity.* Cell, 2003. **113**(2): p. 159-70.

194. Gilde, A.J. and M. Van Bilsen, *Peroxisome proliferator-activated receptors (PPARS): regulators of gene expression in heart and skeletal muscle.* Acta Physiol Scand, 2003. **178**(4): p. 425-34.

195. Vega, R.B., J.M. Huss, and D.P. Kelly, *The coactivator PGC-1 cooperates with peroxisome proliferator-activated receptor alpha in transcriptional control of nuclear genes encoding mitochondrial fatty acid oxidation enzymes.* Mol Cell Biol, 2000. **20**(5): p. 1868-76.

196. Guerre-Millo, M., et al., *Peroxisome proliferator-activated receptor alpha activators improve insulin sensitivity and reduce adiposity.* J Biol Chem, 2000. **275**(22): p. 16638-42.

197. Amin, R.H., et al., *Selective Activation of PPAR{gamma} in Skeletal Muscle * Induces Endogenous Production of Adiponectin and Protects Mice From Diet-Induced Insulin Resistance.* Am J Physiol Endocrinol Metab, 2009.

198. Loviscach, M., et al., *Distribution of peroxisome proliferator-activated receptors (PPARs) in human skeletal muscle and adipose tissue: relation to insulin action.* Diabetologia, 2000. **43**(3): p. 304-11.

199. Braissant, O., et al., *Differential expression of peroxisome proliferator-activated receptors (PPARs): tissue distribution of PPAR-alpha, -beta, and -gamma in the adult rat.* Endocrinology, 1996. **137**(1): p. 354-66.

200. Hondares, E., et al., *PPARdelta, but not PPARalpha, activates PGC-1alpha gene transcription in muscle.* Biochem Biophys Res Commun, 2007. **354**(4): p. 1021-7.

201. Tanaka, T., et al., *Activation of peroxisome proliferator-activated receptor delta induces fatty acid beta-oxidation in skeletal muscle and attenuates metabolic syndrome.* Proc Natl Acad Sci U S A, 2003. **100**(26): p. 15924-9.

202. Luquet, S., et al., *Peroxisome proliferator-activated receptor delta controls muscle development and oxidative capability.* FASEB J, 2003. **17**(15): p. 2299-301.

203. Wang, Y.X., et al., *Regulation of muscle fiber type and running endurance by PPARdelta.* PLoS Biol, 2004. **2**(10): p. e294.

204. Potthoff, M.J., et al., *Histone deacetylase degradation and MEF2 activation promote the formation of slow-twitch myofibers.* J Clin Invest, 2007. **117**(9): p. 2459-67.

205. Wu, H., et al., *MEF2 responds to multiple calcium-regulated signals in the control of skeletal muscle fiber type.* EMBO J, 2000. **19**(9): p. 1963-73.

206. Czubryt, M.P., et al., *Regulation of peroxisome proliferator-activated receptor gamma coactivator 1 alpha (PGC-1 alpha) and mitochondrial function by MEF2 and HDAC5.* Proc Natl Acad Sci U S A, 2003. **100**(4): p. 1711-6.

207. Holmes, B.F., et al., *Regulation of muscle GLUT4 enhancer factor and myocyte enhancer factor 2 by AMP-activated protein kinase.* Am J Physiol Endocrinol Metab, 2005. **289**(6): p. E1071-6.

208. Thai, M.V., et al., *Myocyte enhancer factor 2 (MEF2)-binding site is required for GLUT4 gene expression in transgenic mice. Regulation of MEF2 DNA binding activity in insulin-deficient diabetes.* J Biol Chem, 1998. **273**(23): p. 14285-92.

209. Handschin, C., et al., *An autoregulatory loop controls peroxisome proliferator-activated receptor gamma coactivator 1alpha expression in muscle.* Proc Natl Acad Sci U S A, 2003. **100**(12): p. 7111-6.

210. Cunningham, J.T., et al., *mTOR controls mitochondrial oxidative function through a YY1-PGC-1alpha transcriptional complex.* Nature, 2007. **450**(7170): p. 736-40.

211. Giguere, V., *Transcriptional control of energy homeostasis by the estrogen-related receptors.* Endocr Rev, 2008. **29**(6): p. 677-96.

212. Schreiber, S.N., et al., *The transcriptional coactivator PGC-1 regulates the expression and activity of the orphan nuclear receptor estrogen-related receptor alpha (ERRalpha).* J Biol Chem, 2003. **278**(11): p. 9013-8.

213. Chen, L. and C. Wong, *Estrogen-related receptor alpha inverse agonist enhances basal glucose uptake in myotubes through reactive oxygen species.* Biol Pharm Bull, 2009. **32**(7): p. 1199-203.

214. Gacias, M., et al., *PGC-1beta regulates mouse carnitine-acylcarnitine translocase through estrogen-related receptor alpha.* Biochem Biophys Res Commun, 2012. **423**(4): p. 838-43.

215. Vega, R.B. and D.P. Kelly, *A role for estrogen-related receptor alpha in the control of mitochondrial fatty acid beta-oxidation during brown adipocyte differentiation.* J Biol Chem, 1997. **272**(50): p. 31693-9.

216. Wagatsuma, A., et al., *Expression of nuclear-encoded genes involved in mitochondrial biogenesis and dynamics in experimentally denervated muscle.* J Physiol Biochem, 2011. **67**(3): p. 359-70.

217. Qin, W., et al., *Protection against dexamethasone-induced muscle atrophy is related to modulation by testosterone of FOXO1 and PGC-1alpha.* Biochem Biophys Res Commun, 2010. **403**(3-4): p. 473-8.

218. Oishi, Y., et al., *Cellular adaptations in soleus muscle during recovery after hindlimb unloading.* Acta Physiol (Oxf), 2008. **192**(3): p. 381-95.

219. Brault, J.J., J.G. Jespersen, and A.L. Goldberg, *Peroxisome proliferator-activated receptor gamma coactivator 1alpha or 1beta overexpression inhibits muscle protein degradation, induction of ubiquitin ligases, and disuse atrophy.* J Biol Chem, 2010. **285**(25): p. 19460-71.

220. Hanai, J., et al., *The muscle-specific ubiquitin ligase atrogin-1/MAFbx mediates statin-induced muscle toxicity.* J Clin Invest, 2007. **117**(12): p. 3940-51.

221. Acharyya, S., et al., *Cancer cachexia is regulated by selective targeting of skeletal muscle gene products.* J Clin Invest, 2004. **114**(3): p. 370-8.

222. Roy, R.R., et al., *Persistence of myosin heavy chain-based fiber types in innervated but silenced rat fast muscle.* Muscle Nerve, 2000. **23**(5): p. 735-47.

223. Da Cruz, S., et al., *Elevated PGC-1alpha activity sustains mitochondrial biogenesis and muscle function without extending survival in a mouse model of inherited ALS.* Cell Metab, 2012. **15**(5): p. 778-86.

224. Long, W., L. Wei, and E.J. Barrett, *Dexamethasone inhibits the stimulation of muscle protein synthesis and PHAS-I and p70 S6-kinase phosphorylation.* Am J Physiol Endocrinol Metab, 2001. **280**(4): p. E570-5.

225. Smith, K.L. and M.J. Tisdale, *Increased protein degradation and decreased protein synthesis in skeletal muscle during cancer cachexia.* Br J Cancer, 1993. **67**(4): p. 680-5.

226. Eley, H.L. and M.J. Tisdale, *Skeletal muscle atrophy, a link between depression of protein synthesis and increase in degradation.* J Biol Chem, 2007. **282**(10): p. 7087-97.

227. Emery, P.W., et al., *Protein synthesis in muscle measured in vivo in cachectic patients with cancer.* Br Med J (Clin Res Ed), 1984. **289**(6445): p. 584-6.

228. Fry, C.S., et al., *Skeletal muscle autophagy and protein breakdown following resistance exercise are similar in younger and older adults.* J Gerontol A Biol Sci Med Sci, 2013. **68**(5): p. 599-607.

229. Tarnopolsky, M.A. and G. Parise, *Direct measurement of high-energy phosphate compounds in patients with neuromuscular disease.* Muscle Nerve, 1999. **22**(9): p. 1228-33.

230. Wyss, M. and R. Kaddurah-Daouk, *Creatine and creatinine metabolism.* Physiol Rev, 2000. **80**(3): p. 1107-213.

231. Becque, M.D., J.D. Lochmann, and D.R. Melrose, *Effects of oral creatine supplementation on muscular strength and body composition.* Med Sci Sports Exerc, 2000. **32**(3): p. 654-8.

232. Candow, D.G., et al., *Effect of different frequencies of creatine supplementation on muscle size and strength in young adults.* J Strength Cond Res, 2011. **25**(7): p. 1831-8.

233. Kreider, R.B., et al., *Effects of creatine supplementation on body composition, strength, and sprint performance.* Med Sci Sports Exerc, 1998. **30**(1): p. 73-82.

234. Tarnopolsky, M. and J. Martin, *Creatine monohydrate increases strength in patients with neuromuscular disease.* Neurology, 1999. **52**(4): p. 854-7.

235. Hespel, P., et al., *Oral creatine supplementation facilitates the rehabilitation of disuse atrophy and alters the expression of muscle myogenic factors in humans.* J Physiol, 2001. **536**(Pt 2): p. 625-33.

236. Menezes, L.G., et al., *Creatine supplementation attenuates corticosteroid-induced muscle wasting and impairment of exercise performance in rats.* J Appl Physiol, 2007. **102**(2): p. 698-703.

237. Passaquin, A.C., et al., *Creatine supplementation reduces skeletal muscle degeneration and enhances mitochondrial function in mdx mice.* Neuromuscul Disord, 2002. **12**(2): p. 174-82.

238. Guerrero-Ontiveros, M.L. and T. Wallimann, *Creatine supplementation in health and disease. Effects of chronic creatine ingestion in vivo: down-regulation of the expression of creatine transporter isoforms in skeletal muscle.* Mol Cell Biochem, 1998. **184**(1-2): p. 427-37.

239. Tarnopolsky, M.A., et al., *Creatine transporter and mitochondrial creatine kinase protein content in myopathies.* Muscle Nerve, 2001. **24**(5): p. 682-8.

240. Tarnopolsky, M.A., *Creatine as a therapeutic strategy for myopathies.* Amino Acids, 2011. **40**(5): p. 1397-407.

241. Derave, W., et al., *Electrolysis stimulates creatine transport and transporter cell surface expression in incubated mouse skeletal muscle: potential role of ROS.* Am J Physiol Endocrinol Metab, 2006. **291**(6): p. E1250-7.

242. Brault, J.J., K.A. Abraham, and R.L. Terjung, *Muscle creatine uptake and creatine transporter expression in response to creatine supplementation and depletion.* J Appl Physiol, 2003. **94**(6): p. 2173-80.

243. Brault, J.J. and R.L. Terjung, *Creatine uptake and creatine transporter expression among rat skeletal muscle fiber types.* Am J Physiol Cell Physiol, 2003. **284**(6): p. C1481-9.

244. Murphy, R., et al., *Creatine transporter protein content, localization, and gene expression in rat skeletal muscle.* Am J Physiol Cell Physiol, 2001. **280**(3): p. C415-22.

245. Wenz, T., et al., *Activation of the PPAR/PGC-1alpha pathway prevents a bioenergetic deficit and effectively improves a mitochondrial myopathy phenotype.* Cell Metab, 2008. **8**(3): p. 249-56.

246. Louis, M., et al., *No effect of creatine supplementation on human myofibrillar and sarcoplasmic protein synthesis after resistance exercise.* Am J Physiol Endocrinol Metab, 2003. **285**(5): p. E1089-94.

247. Parise, G., et al., *Effects of acute creatine monohydrate supplementation on leucine kinetics and mixed-muscle protein synthesis.* J Appl Physiol, 2001. **91**(3): p. 1041-7.

248. Ingwall, J.S., et al., *Specificity of creatine in the control of muscle protein synthesis.* J Cell Biol, 1974. **62**(1): p. 145-51.

249. Ingwall, J.S., M.F. Morales, and F.E. Stockdale, *Creatine and the control of myosin synthesis in differentiating skeletal muscle.* Proc Natl Acad Sci U S A, 1972. **69**(8): p. 2250-3.

250. Hornberger, T.A., et al., *Mechanical stimuli regulate rapamycin-sensitive signalling by a phosphoinositide 3-kinase-, protein kinase B- and growth factor-independent mechanism.* Biochem J, 2004. **380**(Pt 3): p. 795-804.

251. Han, S., et al., *Activation of peroxisome proliferator-activated receptor beta/delta induces lung cancer growth via peroxisome proliferator-activated receptor coactivator gamma-1alpha.* Am J Respir Cell Mol Biol, 2009. **40**(3): p. 325-31.

252. Kressler, D., M.B. Hock, and A. Kralli, *Coactivators PGC-1beta and SRC-1 interact functionally to promote the agonist activity of the selective estrogen receptor modulator tamoxifen.* J Biol Chem, 2007. **282**(37): p. 26897-907.

253. Foletta, V.C., et al., *Ndrg2 is a PGC-1alpha/ERRalpha target gene that controls protein synthesis and expression of contractile-type genes in C2C12 myotubes.* Biochim Biophys Acta, 2013. **1833**(12): p. 3112-3123.

254. Plaisance, I., et al., *TNF-alpha increases protein content in C2C12 and primary myotubes by enhancing protein translation via the TNF-R1, PI3K, and MEK.* Am J Physiol Endocrinol Metab, 2008. **294**(2): p. E241-50.

255. Vandenburgh, H.H., et al., *Skeletal muscle growth is stimulated by intermittent stretch-relaxation in tissue culture.* Am J Physiol, 1989. **256**(3 Pt 1): p. C674-82.

256. Selsby, J.T., et al., *Rescue of dystrophic skeletal muscle by PGC-1alpha involves a fast to slow fiber type shift in the mdx mouse.* PLoS One, 2012. **7**(1): p. e30063.

257. Quinn, L.S., et al., *Overexpression of interleukin-15 induces skeletal muscle hypertrophy in vitro: implications for treatment of muscle wasting disorders.* Exp Cell Res, 2002. **280**(1): p. 55-63.

258. Wilkinson, S.B., et al., *Differential effects of resistance and endurance exercise in the fed state on signalling molecule phosphorylation and protein synthesis in human muscle.* J Physiol, 2008. **586**(Pt 15): p. 3701-17.

259. Ruas, J.L., et al., *A PGC-1alpha isoform induced by resistance training regulates skeletal muscle hypertrophy.* Cell, 2012. **151**(6): p. 1319-31.

260. Quinn, L.S., B.G. Anderson, and S.R. Plymate, *Muscle-specific overexpression of the type 1 IGF receptor results in myoblast-independent muscle hypertrophy via PI3K, and not calcineurin, signaling.* Am J Physiol Endocrinol Metab, 2007. **293**(6): p. E1538-51.

261. Taylor, W.E., et al., *Myostatin inhibits cell proliferation and protein synthesis in C2C12 muscle cells.* Am J Physiol Endocrinol Metab, 2001. **280**(2): p. E221-8.

262. Agley, C.C., et al., *An image analysis method for the precise selection and quantitation of fluorescently labeled cellular constituents: application to the measurement of human muscle cells in culture.* J Histochem Cytochem, 2012. **60**(6): p. 428-38.

263. Lu, H., et al., *The identification of potential factors associated with the development of type 2 diabetes: a quantitative proteomics approach.* Mol Cell Proteomics, 2008. **7**(8): p. 1434-51.

264. van de Vijver, M.J., et al., *A gene-expression signature as a predictor of survival in breast cancer.* N Engl J Med, 2002. **347**(25): p. 1999-2009.

265. Subramanian, A., et al., *Gene set enrichment analysis: a knowledge-based approach for interpreting genome-wide expression profiles.* Proc Natl Acad Sci U S A, 2005. **102**(43): p. 15545-50.

266. Wrzodek, C., et al., *Precise generation of systems biology models from KEGG pathways.* BMC Syst Biol, 2013. **7**: p. 15.

267. Du, P., W.A. Kibbe, and S.M. Lin, *lumi: a pipeline for processing Illumina microarray.* Bioinformatics, 2008. **24**(13): p. 1547-8.

268. Lin, S.M., et al., *Model-based variance-stabilizing transformation for Illumina microarray data.* Nucleic Acids Res, 2008. **36**(2): p. e11.

269. Casey, T., et al., *Quantitative proteomic analysis of G-protein signalling in Stagonospora nodorum using isobaric tags for relative and absolute quantification.* Proteomics, 2010. **10**(1): p. 38-47.

270. Huang da, W., B.T. Sherman, and R.A. Lempicki, *Systematic and integrative analysis of large gene lists using DAVID bioinformatics resources.* Nat Protoc, 2009. **4**(1): p. 44-57.

271. Huang da, W., B.T. Sherman, and R.A. Lempicki, *Bioinformatics enrichment tools: paths toward the comprehensive functional analysis of large gene lists.* Nucleic Acids Res, 2009. **37**(1): p. 1-13.

272. Stegmaier, K., et al., *Gene expression-based high-throughput screening(GE-HTS) and application to leukemia differentiation.* Nat Genet, 2004. **36**(3): p. 257-63.

273. Buford, T.W., M.B. Cooke, and D.S. Willoughby, *Resistance exercise-induced changes of inflammatory gene expression within human skeletal muscle.* Eur J Appl Physiol, 2009. **107**(4): p. 463-71.

274. Louis, E., et al., *Time course of proteolytic, cytokine, and myostatin gene expression after acute exercise in human skeletal muscle.* J Appl Physiol, 2007. **103**(5): p. 1744-51.

275. Vella, L.D., et al., *Resistance exercise increases nuclear factor-kappa B activity in human skeletal muscle.* Am J Physiol Regul Integr Comp Physiol, 2011. **302**: p. R667-673.

276. McKay, B.R., et al., *Association of interleukin-6 signalling with the muscle stem cell response following muscle-lengthening contractions in humans.* PLoS One, 2009. **4**(6): p. e6027.

277. Hubal, M.J., et al., *Inflammatory gene changes associated with the repeated-bout effect.* Am J Physiol Regul Integr Comp Physiol, 2008. **294**(5): p. R1628-37.

278. Brooks, B.R., *El Escorial World Federation of Neurology criteria for the diagnosis of amyotrophic lateral sclerosis. Subcommittee on Motor Neuron Diseases/Amyotrophic Lateral Sclerosis of the World Federation of Neurology Research Group on Neuromuscular Diseases and the El Escorial "Clinical limits of amyotrophic lateral sclerosis" workshop contributors.* J Neurol Sci, 1994. **124 Suppl**: p. 96-107.

279. *Declaration of Helsinki.* Law Med Health Care, 1991. **19**(3-4): p. 264-5.

280. Perez-Schindler, J., et al., *The corepressor NCoR1 antagonizes PGC-1alpha and estrogen-related receptor alpha in the regulation of skeletal muscle function and oxidative metabolism.* Mol Cell Biol, 2012. **32**(24): p. 4913-24.

281. Machida, M., et al., *Reduction of ribosome biogenesis with activation of the mTOR pathway in denervated atrophic muscle.* J Cell Physiol, 2012. **227**(4): p. 1569-76.

282. Dufour, C.R., et al., *Genome-wide orchestration of cardiac functions by the orphan nuclear receptors ERRalpha and gamma.* Cell Metab, 2007. **5**(5): p. 345-56.

283. Blin, O., et al., *Mitochondrial respiratory failure in skeletal muscle from patients with Parkinson's disease and multiple system atrophy.* J Neurol Sci, 1994. **125**(1): p. 95-101.

284. Zheng, B., et al., *PGC-1alpha, a potential therapeutic target for early intervention in Parkinson's disease.* Sci Transl Med, 2010. **2**(52): p. 52ra73.

285. Wrede, A., et al., *Myofibrillar disorganization characterizes myopathy of camptocormia in Parkinson's disease.* Acta Neuropathol, 2012. **123**(3): p. 419-32.

286. Choe, M.A., et al., *Effect of DHEA on recovery of muscle atrophy induced by Parkinson's disease.* J Korean Acad Nurs, 2011. **41**(6): p. 834-42.

287. She, P., et al., *Molecular characterization of skeletal muscle atrophy in the R6/2 mouse model of Huntington's disease.* Am J Physiol Endocrinol Metab, 2011. **301**(1): p. E49-61.

288. Grassie, M.E., et al., *The myosin phosphatase targeting protein (MYPT) family: a regulated mechanism for achieving substrate specificity of the catalytic subunit of protein phosphatase type 1delta.* Arch Biochem Biophys, 2011. **510**(2): p. 147-59.

289. Kotter, P. and K.D. Entian, *Cloning and analysis of the nuclear gene MRP-S9 encoding mitochondrial ribosomal protein S9 of Saccharomyces cerevisiae.* Curr Genet, 1995. **28**(1): p. 26-31.

290. Cho, H.P., et al., *The dual-specificity phosphatase CDC14B bundles and stabilizes microtubules.* Mol Cell Biol, 2005. **25**(11): p. 4541-51.

291. Dorin, D., et al., *The TAR RNA-binding protein, TRBP, stimulates the expression of TAR-containing RNAs in vitro and in vivo independently of its ability to inhibit the dsRNA-dependent kinase PKR.* J Biol Chem, 2003. **278**(7): p. 4440-8.

292. He, B. and W. Guo, *The exocyst complex in polarized exocytosis.* Curr Opin Cell Biol, 2009. **21**(4): p. 537-42.

293. Liu, J. and W. Guo, *The exocyst complex in exocytosis and cell migration.* Protoplasma, 2012. **249**(3): p. 587-97.

294. Lyons, P.D., et al., *Insulin stimulates the phosphorylation of the exocyst protein Sec8 in adipocytes.* Biosci Rep, 2009. **29**(4): p. 229-35.

295. Inoue, M., et al., *The exocyst complex is required for targeting of Glut4 to the plasma membrane by insulin.* Nature, 2003. **422**(6932): p. 629-33.

296. Urano, T., et al., *Efp targets 14-3-3 sigma for proteolysis and promotes breast tumour growth.* Nature, 2002. **417**(6891): p. 871-5.

297. Kong, H.J., et al., *Molecular characterization of tripartite motif protein 25 (TRIM25) involved in ERalpha-mediated transcription in the Korean rose*

bitterling Rhodeus uyekii. Comp Biochem Physiol B Biochem Mol Biol, 2012. **163**(1): p. 147-53.

298. Cohen, S., et al., *Ubiquitylation by Trim32 causes coupled loss of desmin, Z-bands, and thin filaments in muscle atrophy.* J Cell Biol, 2012. **198**(4): p. 575-89.

299. Khalyfa, A., et al., *Characterization of elongation factor-1A (eEF1A-1) and eEF1A-2/S1 protein expression in normal and wasted mice.* J Biol Chem, 2001. **276**(25): p. 22915-22.

300. Tohyama, D., A. Yamaguchi, and T. Yamashita, *Inhibition of a eukaryotic initiation factor (eIF2Bdelta/F11A3.2) during adulthood extends lifespan in Caenorhabditis elegans.* FASEB J, 2008. **22**(12): p. 4327-37.

301. Chambers, D.M., J. Peters, and C.M. Abbott, *The lethal mutation of the mouse wasted (wst) is a deletion that abolishes expression of a tissue-specific isoform of translation elongation factor 1alpha, encoded by the Eef1a2 gene.* Proc Natl Acad Sci U S A, 1998. **95**(8): p. 4463-8.

302. Newbery, H.J., et al., *Progressive loss of motor neuron function in wasted mice: effects of a spontaneous null mutation in the gene for the eEF1 A2 translation factor.* J Neuropathol Exp Neurol, 2005. **64**(4): p. 295-303.

303. Ruest, L.B., R. Marcotte, and E. Wang, *Peptide elongation factor eEF1A-2/S1 expression in cultured differentiated myotubes and its protective effect against caspase-3-mediated apoptosis.* J Biol Chem, 2002. **277**(7): p. 5418-25.

304. Tuckow, A.P., et al., *Ectopic expression of eIF2Bepsilon in rat skeletal muscle rescues the sepsis-induced reduction in guanine nucleotide exchange activity and protein synthesis.* Am J Physiol Endocrinol Metab, 2010. **299**(2): p. E241-8.

305. Kubica, N., et al., *Alterations in the expression of mRNAs and proteins that code for species relevant to eIF2B activity after an acute bout of resistance exercise.* J Appl Physiol, 2004. **96**(2): p. 679-87.

306. Joshi, B., A. Cameron, and R. Jagus, *Characterization of mammalian eIF4E-family members.* Eur J Biochem, 2004. **271**(11): p. 2189-203.

307. Vary, T.C., *IGF-I stimulates protein synthesis in skeletal muscle through multiple signaling pathways during sepsis.* Am J Physiol Regul Integr Comp Physiol, 2006. **290**(2): p. R313-21.

308. Volpon, L., et al., *eIF4E3, a new actor in mRNA metabolism and tumor suppression.* Cell Cycle, 2013. **12**(8): p. 1159-60.

309. Osborne, M.J., et al., *eIF4E3 acts as a tumor suppressor by utilizing an atypical mode of methyl-7-guanosine cap recognition.* Proc Natl Acad Sci U S A, 2013. **110**(10): p. 3877-82.

310. Gavin, T.P., et al., *Acute resistance exercise increases skeletal muscle angiogenic growth factor expression.* Acta Physiol (Oxf), 2007. **191**(2): p. 139-46.

311. Frey, S.P., et al., *VEGF improves skeletal muscle regeneration after acute trauma and reconstruction of the limb in a rabbit model.* Clin Orthop Relat Res, 2012. **470**(12): p. 3607-14.

312. Deasy, B.M., et al., *Effect of VEGF on the regenerative capacity of muscle stem cells in dystrophic skeletal muscle.* Mol Ther, 2009. **17**(10): p. 1788-98.

313. Lambrechts, D., et al., *VEGF is a modifier of amyotrophic lateral sclerosis in mice and humans and protects motoneurons against ischemic death.* Nat Genet, 2003. **34**(4): p. 383-94.

314. Dewil, M., et al., *Vascular endothelial growth factor counteracts the loss of phospho-Akt preceding motor neurone degeneration in amyotrophic lateral sclerosis.* Neuropathol Appl Neurobiol, 2007. **33**(5): p. 499-509.

315. Sakowski, S.A., et al., *Neuroprotection using gene therapy to induce vascular endothelial growth factor-A expression.* Gene Ther, 2009. **16**(11): p. 1292-9.

316. Lunn, J.S., et al., *Vascular endothelial growth factor prevents G93A-SOD1-induced motor neuron degeneration.* Dev Neurobiol, 2009. **69**(13): p. 871-84.

317. Nakashiro, K., et al., *Down-regulation of TSC-22 (transforming growth factor beta-stimulated clone 22) markedly enhances the growth of a human salivary gland cancer cell line in vitro and in vivo.* Cancer Res, 1998. **58**(3): p. 549-55.

318. Yan, X., et al., *TSC-22 promotes transforming growth factor beta-mediated cardiac myofibroblast differentiation by antagonizing Smad7 activity.* Mol Cell Biol, 2011. **31**(18): p. 3700-9.

319. Hildenbrand, M., et al., *Impaired skin regeneration and remodeling after cutaneous injury and chemically induced hyperplasia in taps-transgenic mice.* J Invest Dermatol, 2010. **130**(7): p. 1922-30.

320. Shi, X. and D.J. Garry, *Myogenic regulatory factors transactivate the Tceal7 gene and modulate muscle differentiation.* Biochem J, 2010. **428**(2): p. 213-21.

321. Stella, R., et al., *Cellular prion protein promotes regeneration of adult muscle tissue.* Mol Cell Biol, 2010. **30**(20): p. 4864-76.

322. Furukawa, H., et al., *Accumulation of prion protein in muscle fibers of experimental chloroquine myopathy: in vivo model for deposition of prion protein in non-neuronal tissues.* Lab Invest, 2004. **84**(7): p. 828-35.

323. Powers, S.K., A.N. Kavazis, and J.M. McClung, *Oxidative stress and disuse muscle atrophy.* J Appl Physiol, 2007. **102**(6): p. 2389-97.

324. Belizario, J.E., M.J. Lorite, and M.J. Tisdale, *Cleavage of caspases-1, -3, -6, -8 and -9 substrates by proteases in skeletal muscles from mice undergoing cancer cachexia.* Br J Cancer, 2001. **84**(8): p. 1135-40.

325. Du, J., et al., *Activation of caspase-3 is an initial step triggering accelerated muscle proteolysis in catabolic conditions.* J Clin Invest, 2004. **113**(1): p. 115-23.

326. Askanas, V., et al., *Prion protein is abnormally accumulated in inclusion-body myositis.* Neuroreport, 1993. **5**(1): p. 25-8.

327. Sarkozi, E., V. Askanas, and W.K. Engel, *Abnormal accumulation of prion protein mRNA in muscle fibers of patients with sporadic inclusion-body myositis and hereditary inclusion-body myopathy.* Am J Pathol, 1994. **145**(6): p. 1280-4.

328. Huang, S., et al., *Inducible overexpression of wild-type prion protein in the muscles leads to a primary myopathy in transgenic mice.* Proc Natl Acad Sci U S A, 2007. **104**(16): p. 6800-5.

329. Smith, J.D., et al., *Prion protein expression and functional importance in skeletal muscle.* Antioxid Redox Signal, 2011. **15**(9): p. 2465-75.

330. Deldicque, L., et al., *Effects of resistance exercise with and without creatine supplementation on gene expression and cell signaling in human skeletal muscle.* J Appl Physiol, 2008. **104**(2): p. 371-8.

331. Tiraby, C., et al., *Estrogen-related receptor gamma promotes mesenchymal-to-epithelial transition and suppresses breast tumor growth.* Cancer Res, 2011. **71**(7): p. 2518-28.

332. Christie, D.L., *Functional insights into the creatine transporter.* Subcell Biochem, 2007. **46**: p. 99-118.

333. Speer, O., et al., *Creatine transporters: a reappraisal.* Mol Cell Biochem, 2004. **256-257**(1-2): p. 407-24.

334. Fischer, A., et al., *Changes in creatine transporter function during cardiac maturation in the rat.* BMC Dev Biol, 2010. **10**: p. 70.

335. Puigserver, P. and B.M. Spiegelman, *Peroxisome proliferator-activated receptor-gamma coactivator 1 alpha (PGC-1 alpha): transcriptional coactivator and metabolic regulator.* Endocr Rev, 2003. **24**(1): p. 78-90.

336. Ponticos, M., et al., *Dual regulation of the AMP-activated protein kinase provides a novel mechanism for the control of creatine kinase in skeletal muscle.* EMBO J, 1998. **17**(6): p. 1688-99.

337. Darrabie, M.D., et al., *AMPK and substrate availability regulate creatine transport in cultured cardiomyocytes.* Am J Physiol Endocrinol Metab, 2011. **300**(5): p. E870-6.

338. Lai, C.M., Y.K. Lai, and P.E. Rakoczy, *Adenovirus and adeno-associated virus vectors.* DNA Cell Biol, 2002. **21**(12): p. 895-913.

339. Tang, Y., et al., *AAV-directed muscular dystrophy gene therapy.* Expert Opin Biol Ther, 2010. **10**(3): p. 395-408.

340. Villena, J.A., et al., *Orphan nuclear receptor estrogen-related receptor alpha is essential for adaptive thermogenesis.* Proc Natl Acad Sci U S A, 2007. **104**(4): p. 1418-23.

341. Linderman, J.K., et al., *Stimulation of myofibrillar protein synthesis in hindlimb suspended rats by resistance exercise and growth hormone.* Life Sci, 1995. **57**(8): p. 755-62.

342. Shah, O.J., S.R. Kimball, and L.S. Jefferson, *Acute attenuation of translation initiation and protein synthesis by glucocorticoids in skeletal muscle.* Am J Physiol Endocrinol Metab, 2000. **278**(1): p. E76-82.

343. Guillet, C., et al., *Mitochondrial and sarcoplasmic proteins, but not myosin heavy chain, are sensitive to leucine supplementation in old rat skeletal muscle.* Exp Gerontol, 2004. **39**(5): p. 745-51.

344. Harcourt, L.J., et al., *Low dose formoterol administration improves muscle function in dystrophic mdx mice without increasing fatigue.* Neuromuscul Disord, 2007. **17**(1): p. 47-55.

345. Burkholder, T.J., et al., *Relationship between muscle fiber types and sizes and muscle architectural properties in the mouse hindlimb.* J Morphol, 1994. **221**(2): p. 177-90.

Appendices

Appendix 1.

Complete list of Gene Ontology (GO) terms identified from the up- and down- regulated genes and proteins by PGC-1α and PGC-1β.

Table S1 Complete list of GO terms identified by analysis of PGC-1α-differentially expressed genes.

GO Term	Category	Count (No. of genes)	Fold Enrichment	P-Value
GO:0005739~mitochondrion	CC	361	4.8	2.36E-169
GO:0044429~mitochondrial part	CC	187	6.2	6.29E-100
GO:0031966~mitochondrial membrane	CC	136	6.4	1.44E-72
GO:0005740~mitochondrial envelope	CC	139	6.2	9.32E-72
GO:0005743~mitochondrial inner membrane	CC	115	6.8	3.20E-63
GO:0019866~organelle inner membrane	CC	117	6.5	2.05E-62
GO:0031967~organelle envelope	CC	144	4.6	3.80E-56
GO:0031975~envelope	CC	144	4.6	6.36E-56
GO:0006091~generation of precursor metabolites and energy	BP	91	7.1	2.47E-49
GO:0031090~organelle membrane	CC	161	3.5	7.89E-45
GO:0022900~electron transport chain	BP	55	7.8	1.55E-38
GO:0070469~respiratory chain	CC	43	11.5	5.09E-34
GO:0055114~oxidation reduction	BP	114	3.5	4.39E-29
GO:0005759~mitochondrial matrix	CC	59	6.3	9.52E-29
GO:0031980~mitochondrial lumen	CC	59	6.3	9.52E-29
GO:0045333~cellular respiration	BP	29	10.0	3.50E-18
GO:0015980~energy derivation by oxidation of organic compounds	BP	33	6.8	3.81E-15
GO:0051186~cofactor metabolic process	BP	43	4.8	2.98E-14
GO:0044455~mitochondrial membrane part	CC	23	8.2	1.47E-12
GO:0006732~coenzyme metabolic process	BP	35	2.7	6.94E-12
GO:0007005~mitochondrion organization	BP	28	9.7	2.05E-11
GO:0048037~cofactor binding	MF	43	5.9	1.70E-10
GO:0006084~acetyl-CoA metabolic process	BP	17	11.2	3.16E-10
GO:0009060~aerobic respiration	BP	16	12.1	4.38E-10
GO:0003954~NADH dehydrogenase activity	MF	15	12.4	6.35E-10
GO:0008137~NADH dehydrogenase (ubiquinone) activity	MF	15	12.4	6.35E-10
GO:0050136~NADH dehydrogenase (quinone) activity	MF	15	12.4	6.35E-10
GO:0015077~monovalent inorganic cation transmembrane transporter activity	MF	25	5.4	1.20E-09
GO:0006099~tricarboxylic acid cycle	BP	14	5.7	3.59E-09
GO:0016655~oxidoreductase activity, acting on NADH or NADPH, quinone or similar compound as acceptor	MF	15	3.9	4.70E-09

GO:0051188~cofactor biosynthetic process	BP	25	11.0	5.64E-09
GO:0015078~hydrogen ion transmembrane transporter activity	MF	24	12.4	1.37E-08
GO:0046356~acetyl-CoA catabolic process	BP	14	11.9	2.85E-08
GO:0006119~oxidative phosphorylation	BP	19	12.6	1.07E-07
GO:0051187~cofactor catabolic process	BP	15	4.4	1.21E-07
GO:0022890~inorganic cation transmembrane transporter activity	MF	28	6.9	1.76E-07
GO:0016651~oxidoreductase activity, acting on NADH or NADPH	MF	18	7.0	1.84E-07
GO:0009109~coenzyme catabolic process	BP	14	6.8	5.17E-07
GO:0031968~organelle outer membrane	CC	23	4.6	8.33E-07
GO:0022904~respiratory electron transport chain	BP	13	3.2	1.17E-06
GO:0005840~ribosome	CC	35	4.5	1.66E-06
GO:0019867~outer membrane	CC	23	3.5	2.39E-06
GO:0050662~coenzyme binding	MF	29	9.4	5.75E-06
GO:0009108~coenzyme biosynthetic process	BP	18	3.6	5.93E-06
GO:0005741~mitochondrial outer membrane	CC	21	6.4	1.09E-05
GO:0005761~mitochondrial ribosome	CC	15	6.4	1.09E-05
GO:0000313~organellar ribosome	CC	15	4.3	1.41E-05
GO:0015002~heme-copper terminal oxidase activity	MF	11	4.0	3.95E-05
GO:0016676~oxidoreductase activity, acting on heme group of donors, oxygen as acceptor	MF	11	9.5	5.35E-05
GO:0004129~cytochrome-c oxidase activity	MF	11	9.5	5.35E-05
GO:0016675~oxidoreductase activity, acting on heme group of donors	MF	11	9.5	5.35E-05
GO:0006631~fatty acid metabolic process	BP	29	9.5	5.35E-05
GO:0051540~metal cluster binding	MF	15	5.9	8.92E-05
GO:0051536~iron-sulfur cluster binding	MF	15	5.2	9.90E-05
GO:0009055~electron carrier activity	MF	30	3.3	1.89E-04
GO:0000166~nucleotide binding	MF	160	3.2	1.93E-04
GO:0006626~protein targeting to mitochondrion	BP	10	1.4	3.39E-04
GO:0070585~protein localization in mitochondrion	BP	10	8.7	3.62E-04
GO:0005746~mitochondrial respiratory chain	CC	9	8.6	7.37E-04
GO:0051539~4 iron, 4 sulfur cluster binding	MF	10	9.2	9.63E-04
GO:0017076~purine nucleotide binding	MF	139	1.5	1.27E-03
GO:0019842~vitamin binding	MF	21	3.4	2.13E-03
GO:0055085~transmembrane transport	BP	47	4.9	2.97E-03
GO:0009144~purine nucleoside triphosphate metabolic process	BP	19	4.1	4.30E-03
GO:0006839~mitochondrial transport	BP	12	1.5	0.01
GO:0045259~proton-transporting ATP synthase complex	CC	9	1.5	0.01
GO:0009150~purine ribonucleotide metabolic process	BP	20	1.5	0.01
GO:0019725~cellular homeostasis	BP	38	1.5	0.01
GO:0001883~purine nucleoside binding	MF	117	2.1	0.01
GO:0030554~adenyl nucleotide binding	MF	116	3.6	0.01
GO:0046034~ATP metabolic process	BP	17	5.8	0.01
GO:0009205~purine ribonucleoside triphosphate metabolic process	BP	18	3.4	0.01

GO:0045454~cell redox homeostasis	BP	14	2.3	0.01
GO:0001882~nucleoside binding	MF	117	4.8	0.01
GO:0009199~ribonucleoside triphosphate metabolic process	BP	18	2.2	0.01
GO:0009259~ribonucleotide metabolic process	BP	20	13.3	0.01
GO:0009141~nucleoside triphosphate metabolic process	BP	19	3.8	0.01
GO:0009145~purine nucleoside triphosphate biosynthetic process	BP	17	3.6	0.02
GO:0042773~ATP synthesis coupled electron transport	BP	8	4.6	0.02
GO:0009142~nucleoside triphosphate biosynthetic process	BP	17	3.6	0.02
GO:0009152~purine ribonucleotide biosynthetic process	BP	18	2.9	0.02
GO:0015405~P-P-bond-hydrolysis-driven transmembrane transporter activity	MF	18	3.3	0.02
GO:0019318~hexose metabolic process	BP	23	3.4	0.03
GO:0015399~primary active transmembrane transporter activity	MF	18	3.7	0.03
GO:0009260~ribonucleotide biosynthetic process	BP	18	9.0	0.03
GO:0044275~cellular carbohydrate catabolic process	BP	13	3.6	0.03
GO:0042775~mitochondrial ATP synthesis coupled electron transport	BP	7	3.4	0.04
GO:0006744~ubiquinone biosynthetic process	BP	6	4.1	0.04
GO:0006743~ubiquinone metabolic process	BP	6	5.0	0.04

CC = cellular component, MF = molecular function, BP = biological process.

Table S2 Complete list of GO terms identified by analysis of PGC-1β-differentially expressed genes.

GO Term	Category	Count (No. of genes)	Fold Enrichment	P-Value
GO:0005739~mitochondrion	CC	536	2.7	1.79E-124
GO:0044429~mitochondrial part	CC	253	3.2	5.43E-72
GO:0005740~mitochondrial envelope	CC	188	3.2	7.18E-52
GO:0031966~mitochondrial membrane	CC	180	3.2	6.88E-51
GO:0005743~mitochondrial inner membrane	CC	151	3.4	4.80E-45
GO:0019866~organelle inner membrane	CC	155	3.3	2.02E-44
GO:0031967~organelle envelope	CC	214	2.6	2.02E-42
GO:0031975~envelope	CC	214	2.6	4.06E-42
GO:0031090~organelle membrane	CC	266	2.2	3.50E-36
GO:0006091~generation of precursor metabolites and energy	BP	111	3.0	5.16E-25
GO:0031980~mitochondrial lumen	CC	81	3.3	5.50E-22
GO:0005759~mitochondrial matrix	CC	81	3.3	5.50E-22
GO:0070469~respiratory chain	CC	46	4.7	5.79E-20
GO:0022900~electron transport chain	BP	60	3.7	2.95E-18
GO:0055114~oxidation reduction	BP	179	1.9	2.97E-14
GO:0043292~contractile fiber	CC	49	3.4	3.25E-13
GO:0005840~ribosome	CC	74	2.5	3.18E-12
GO:0030016~myofibril	CC	46	3.3	7.73E-12
GO:0051186~cofactor metabolic process	BP	68	2.6	9.70E-11
GO:0007005~mitochondrion organization	BP	44	3.2	2.87E-09
GO:0044449~contractile fiber part	CC	42	3.2	5.43E-10
GO:0045333~cellular respiration	BP	32	3.8	1.79E-08
GO:0006732~coenzyme metabolic process	BP	53	2.6	1.30E-07
GO:0030017~sarcomere	CC	38	3.1	2.16E-08
GO:0044455~mitochondrial membrane part	CC	28	3.8	6.14E-08
GO:0005761~mitochondrial ribosome	CC	25	4.0	1.22E-07
GO:0000313~organellar ribosome	CC	25	4.0	1.22E-07
GO:0015980~energy derivation by oxidation of organic compounds	BP	40	2.9	1.72E-06
GO:0003735~structural constituent of ribosome	MF	52	2.4	8.95E-07
GO:0008092~cytoskeletal protein binding	MF	105	1.8	1.42E-06
GO:0005829~cytosol	CC	136	1.6	1.41E-06
GO:0006412~translation	BP	86	1.9	1.44E-05
GO:0000166~nucleotide binding	MF	396	1.3	8.17E-06
GO:0017076~purine nucleotide binding	MF	346	1.3	1.21E-05
GO:0003779~actin binding	MF	78	1.9	1.24E-05
GO:0031968~organelle outer membrane	CC	36	2.7	7.05E-06
GO:0005741~mitochondrial outer membrane	CC	34	2.8	8.78E-06
GO:0006084~acetyl-CoA metabolic process	BP	19	4.3	6.83E-05
GO:0031974~membrane-enclosed lumen	CC	246	1.4	1.34E-05
GO:0019867~outer membrane	CC	36	2.6	1.98E-05
GO:0031674~I band	CC	26	3.2	1.98E-05
GO:0051187~cofactor catabolic process	BP	19	4.1	1.35E-04
GO:0030554~adenyl nucleotide binding	MF	289	1.3	5.24E-05
GO:0001883~purine nucleoside binding	MF	291	1.3	5.29E-05
GO:0050136~NADH dehydrogenase (quinone) activity	MF	16	4.7	8.37E-05
GO:0008137~NADH dehydrogenase	MF	16	4.7	8.37E-05

(ubiquinone) activity				
GO:0003954~NADH dehydrogenase activity	MF	16	4.7	8.37E-05
GO:0001882~nucleoside binding	MF	291	1.3	9.93E-05
GO:0015078~hydrogen ion transmembrane transporter activity	MF	32	2.8	1.10E-04
GO:0009060~aerobic respiration	BP	17	4.4	2.88E-04
GO:0033279~ribosomal subunit	CC	29	2.9	5.24E-05
GO:0032553~ribonucleotide binding	MF	327	1.3	1.88E-04
GO:0032555~purine ribonucleotide binding	MF	327	1.3	1.88E-04
GO:0016528~sarcoplasm	CC	20	3.7	9.31E-05
GO:0043232~intracellular non-membrane-bounded organelle	CC	367	1.3	1.44E-04
GO:0043228~non-membrane-bounded organelle	CC	367	1.3	1.44E-04
GO:0016529~sarcoplasmic reticulum	CC	19	3.7	1.86E-04
GO:0006099~tricarboxylic acid cycle	BP	15	4.6	0.0012025
GO:0015077~monovalent inorganic cation transmembrane transporter activity	MF	32	2.6	5.20E-04
GO:0055002~striated muscle cell development	BP	24	3.1	0.0014828
GO:0016651~oxidoreductase activity, acting on NADH or NADPH	MF	23	3.2	5.85E-04
GO:0051188~cofactor biosynthetic process	BP	33	2.5	0.0018064
GO:0016655~oxidoreductase activity, acting on NADH or NADPH, quinone or similar compound as acceptor	MF	16	4.2	7.31E-04
GO:0032559~adenyl ribonucleotide binding	MF	270	1.3	7.61E-04
GO:0046356~acetyl-CoA catabolic process	BP	15	4.4	0.0025037
GO:0006119~oxidative phosphorylation	BP	24	3.0	0.0032361
GO:0005524~ATP binding	MF	266	1.3	0.0012749
GO:0051146~striated muscle cell differentiation	BP	32	2.5	0.0034395
GO:0070013~intracellular organelle lumen	CC	230	1.3	5.80E-04
GO:0048037~cofactor binding	MF	60	1.9	0.0015812
GO:0043233~organelle lumen	CC	230	1.3	7.11E-04
GO:0055001~muscle cell development	BP	25	2.9	0.0047741
GO:0030529~ribonucleoprotein complex	CC	109	1.6	8.38E-04
GO:0009109~coenzyme catabolic process	BP	16	3.9	0.0079039
GO:0005198~structural molecule activity	MF	100	1.6	0.0034305
GO:0042692~muscle cell differentiation	BP	37	2.2	0.0137265
GO:0030018~Z disc	CC	21	3.0	0.0022827
GO:0005996~monosaccharide metabolic process	BP	52	1.9	0.0169813
GO:0060537~muscle tissue development	BP	40	1.9	0.0170800
GO:0016044~membrane organization	BP	67	1.7	0.0264807
GO:0022890~inorganic cation transmembrane transporter activity	MF	38	2.1	0.0108924
GO:0060537~muscle tissue development	BP	40	2.1	0.0360468
GO:0004129~cytochrome-c oxidase activity	MF	13	4.0	0.0241856
GO:0016676~oxidoreductase activity, acting on heme group of donors, oxygen as acceptor	MF	13	4.0	0.0241856
GO:0015002~heme-copper terminal oxidase activity	MF	13	4.0	0.0241856
GO:0016675~oxidoreductase activity, acting on heme group of donors	MF	13	4.0	0.0241856
GO:0030029~actin filament-based process	BP	47	1.9	0.0852432

GO:0019725~cellular homeostasis	BP	78	1.6	0.0935832
GO:0014706~striated muscle tissue development	BP	37	2.0	0.0992478
GO:0031970~organelle envelope lumen	CC	18	3.0	0.0172322
GO:0006399~tRNA metabolic process	BP	34	2.1	0.1084652
GO:0050662~coenzyme binding	MF	43	1.9	0.0452314
GO:0005625~soluble fraction	CC	32	2.1	0.0217746
GO:0005758~mitochondrial intermembrane space	CC	15	3.3	0.0245880
GO:0009108~coenzyme biosynthetic process	BP	23	2.5	0.1483761
GO:0022904~respiratory electron transport chain	BP	14	3.5	0.1548241
GO:0009260~ribonucleotide biosynthetic process	BP	33	2.1	0.1802321
GO:0060538~skeletal muscle organ development	BP	25	2.4	0.1944596
GO:0008104~protein localization	BP	146	1.4	0.2396605
GO:0070585~protein localization in mitochondrion	BP	12	3.8	0.2443469
GO:0006626~protein targeting to mitochondrion	BP	12	3.8	0.2443469
GO:0005746~mitochondrial respiratory chain	CC	10	4.4	0.0497257

CC = cellular component, MF = molecular function, BP = biological process.

Table S3 Complete list of GO terms identified by analysis of PGC-1α-differentially expressed proteins.

GO Term	Category	Count (No. of proteins)	Fold Enrichment	P-Value
GO:0006091~generation of precursor metabolites and energy	BP	28	11	3.77E-17
GO:0005739~mitochondrion	CC	52	4	3.35E-15
GO:0019866~organelle inner membrane	CC	27	8	2.64E-14
GO:0044429~mitochondrial part	CC	31	6	3.99E-12
GO:0005743~mitochondrial inner membrane	CC	24	8	1.21E-11
GO:0031966~mitochondrial membrane	CC	26	7	1.85E-11
GO:0005740~mitochondrial envelope	CC	26	6	7.29E-11
GO:0031967~organelle envelope	CC	29	5	3.92E-10
GO:0031975~envelope	CC	29	5	4.29E-10
GO:0031090~organelle membrane	CC	33	4	1.06E-08
GO:0005829~cytosol	CC	24	4	3.06E-06
GO:0033279~ribosomal subunit	CC	10	14	6.56E-06
GO:0003735~structural constituent of ribosome	MF	13	8	1.99E-05
GO:0005840~ribosome	CC	14	7	2.73E-05
GO:0006007~glucose catabolic process	BP	9	17	4.03E-05
GO:0019320~hexose catabolic process	BP	9	17	4.03E-05
GO:0046365~monosaccharide catabolic process	BP	9	17	5.48E-05
GO:0006412~translation	BP	17	5	1.14E-04
GO:0015935~small ribosomal subunit	CC	7	23	1.14E-04
GO:0044275~cellular carbohydrate catabolic process	BP	9	15	1.28E-04
GO:0006006~glucose metabolic process	BP	12	9	1.44E-04
GO:0000166~nucleotide binding	MF	48	2	1.50E-04
GO:0055114~oxidation reduction	BP	24	4	1.95E-04
GO:0006096~glycolysis	BP	8	18	2.30E-04
GO:0046164~alcohol catabolic process	BP	9	14	2.42E-04
GO:0030529~ribonucleoprotein complex	CC	19	4	3.95E-04
GO:0019318~hexose metabolic process	BP	12	7	0.001
GO:0015077~monovalent inorganic cation transmembrane transporter activity	MF	9	10	0.001
GO:0016052~carbohydrate catabolic process	BP	9	11	0.001
GO:0005198~structural molecule activity	MF	18	4	0.002
GO:0022900~electron transport chain	BP	10	9	0.002
GO:0045333~cellular respiration	BP	8	13	0.002
GO:0022890~inorganic cation transmembrane transporter activity	MF	10	7	0.002
GO:0042625~ATPase activity, coupled to transmembrane movement of ions	MF	8	11	0.002
GO:0006099~tricarboxylic acid cycle	BP	6	26	0.003
GO:0005996~monosaccharide metabolic process	BP	12	6	0.003
GO:0046356~acetyl-CoA catabolic process	BP	6	25	0.003
GO:0003988~acetyl-CoA C-acyltransferase activity	MF	4	75	0.004
GO:0015980~energy derivation by oxidation of organic compounds	BP	9	9	0.006
GO:0009060~aerobic respiration	BP	6	22	0.006

GO:0009109~coenzyme catabolic process	BP	6	21	0.009
GO:0017076~purine nucleotide binding	MF	39	2	0.011
GO:0006084~acetyl-CoA metabolic process	BP	6	19	0.012
GO:0043232~intracellular non-membrane-bounded organelle	CC	39	2	0.014
GO:0043228~non-membrane-bounded organelle	CC	39	2	0.014
GO:0051187~cofactor catabolic process	BP	6	19	0.014
GO:0070469~respiratory chain	CC	7	10	0.014
GO:0006754~ATP biosynthetic process	BP	8	10	0.016
GO:0003779~actin binding	MF	13	4	0.017
GO:0042626~ATPase activity, coupled to transmembrane movement of substances	MF	8	8	0.023
GO:0016820~hydrolase activity, acting on acid anhydrides, catalyzing transmembrane movement of substances	MF	8	8	0.023
GO:0043492~ATPase activity, coupled to movement of substances	MF	8	8	0.023
GO:0046034~ATP metabolic process	BP	8	9	0.030
GO:0030554~adenyl nucleotide binding	MF	33	2	0.033
GO:0009201~ribonucleoside triphosphate biosynthetic process	BP	8	9	0.037
GO:0009206~purine ribonucleoside triphosphate biosynthetic process	BP	8	9	0.037
GO:0008092~cytoskeletal protein binding	MF	15	3	0.037
GO:0042623~ATPase activity, coupled	MF	11	5	0.039
GO:0001883~purine nucleoside binding	MF	33	2	0.039
GO:0019829~cation-transporting ATPase activity	MF	5	19	0.039
GO:0009145~purine nucleoside triphosphate biosynthetic process	BP	8	8	0.040
GO:0015405~P-P-bond-hydrolysis-driven transmembrane transporter activity	MF	8	7	0.042
GO:0009142~nucleoside triphosphate biosynthetic process	BP	8	8	0.042
GO:0001882~nucleoside binding	MF	33	2	0.044
GO:0015399~primary active transmembrane transporter activity	MF	8	7	0.044

CC = cellular component, MF = molecular function, BP = biological process.

Table S4 Complete list of GO terms identified by analysis of PGC-1β-differentially expressed proteins.

GO Term	Category	Count (No. of proteins)	Fold Enrichment	P-Value
GO:0006091~generation of precursor metabolites and energy	BP	13	10	1.54E-06
GO:0006096~glycolysis	BP	7	5	5.57E-06
GO:0031090~organelle membrane	CC	18	4	1.10E-05
GO:0005739~mitochondrion	CC	22	33	3.06E-05
GO:0006007~glucose catabolic process	BP	7	6	7.02E-05
GO:0019320~hexose catabolic process	BP	7	6	7.32E-05
GO:0044275~cellular carbohydrate catabolic process	BP	7	28	8.56E-05
GO:0031967~organelle envelope	CC	14	28	8.56E-05
GO:0046365~monosaccharide catabolic process	BP	7	27	1.08E-04
GO:0031975~envelope	CC	14	8	1.43E-04
GO:0046164~alcohol catabolic process	BP	7	24	2.05E-04
GO:0019866~organelle inner membrane	CC	11	23	3.31E-04
GO:0016052~carbohydrate catabolic process	BP	7	6	3.56E-04
GO:0044429~mitochondrial part	CC	13	7	0.001
GO:0031966~mitochondrial membrane	CC	11	6	0.001
GO:0005743~mitochondrial inner membrane	CC	9	7	0.001
GO:0003779~actin binding	MF	10	18	0.001
GO:0051494~negative regulation of cytoskeleton organization	BP	5	6	0.003
GO:0005740~mitochondrial envelope	CC	11	7	0.007
GO:0008092~cytoskeletal protein binding	MF	11	14	0.010
GO:0006006~glucose metabolic process	BP	7	21	0.014
GO:0043292~contractile fiber	CC	6	4	0.019
GO:0031674~I band	CC	5	10	0.028
GO:0051129~negative regulation of cellular component organization	BP	6	3	0.042
GO:0030029~actin filament-based process	BP	7	22	0.042
GO:0006099~tricarboxylic acid cycle	BP	4	13	0.042

CC = cellular component, MF = molecular function, BP = biological process.

Appendix 2.

Table S5 The top 33 genes identified in the Gene Expression Signature (GES).

GFP vs. PGC-1α		GFP vs. PGC-1β	
Gene Symbol	**GenBank Accession no.**	**Gene Symbol**	**GenBank Accession no.**
0610042C05Rik	NM_025343.2	LOC100048313	XM_001480281.1
LOC100046395	XR_032392.1	LOC100047963	XM_001479238.1
Tmem14c	NM_025387.2	Mrps9	NM_023514.3
1300001I01Rik	NM_001081158.2	Tarbp2	NM_009319.1
Brd7	NM_012047.1	Cdc14b	NM_172587.2
Exoc1	NM_027270.1	Ppp1r16a	NM_033371.2
9430038I01Rik	XM_925223.2	Pgbpll	NM_145147.5
Poli	NM_011972.1	LOC100044363	XM_001471994.1
LOC100048313	XM_001480281.1	C78339	NM_001033192.2
LOC100047963	XM_001479238.1	LOC100046741	XM_001476728.1
Tarbp2	NM_009319.1	Xpnpep3	NM_177310.2
Rpl26	NM_009080.2	0610042C05Rik	NM_025343.2
Acp6	NM_019800.3	9430038I01Rik	XM_925223.2
Trim32	NM_053084.1	Rccd1	NM_173445.1
Gm889	NM_001033437.1	Trim25	NM_009546.2
Ppp1r16a	NM_033371.2	Ints1	NM_026748.1
Ssbp4	XM_356132.1	Eif2a	NM_001005509.1
LOC100046741	XM_001476728.1	Ankmy2	NM_146033.2
Cuedc1	NM_198013.1	Tmem14c	NM_025387.2
Atp5c1	NM_020615.3	AI314976	NM_207219.2
Rapgefl1	NM_001080925.1	LOC100047126	XM_001477492.1
C78339	NM_001033192.2	Asnsd1	NM_133728.2
Ppap2a	NM_008903.1	Ifngr1	NM_010511.2
Cdc14b	NM_172587.2	Snrpd3	NM_026095.4
Daam2	NM_001008231.2	Ssbp4	XM_356132.1
Abhd1	NR_003522.1	Hcfc1r1	NM_181821.1
4930455C21Rik	XM_148429.1	LOC381398	XM_355356.1
Mnat1	NM_008612.1	scl0003651.1_17	XM_356680.1
Nef3	NM_008691.2	Prpsap1	XM_181343.5
Mrps9	NM_023514.3	7030401E22Rik	
Aifm1	NM_012019.2	Lyrm1	NM_029610.1
Tlr6	NM_011604.2	Hnrpm	NM_029804.1
Smpd1	*NM_011421.1*	Plscr4	NM_178711.2